Mathematisches Forschungsinstitut Oberwolfach

Interfaces, Free Boundaries and Geometric Partial Differential Equations

Organized by
Charles M. Elliott, Coventry
Harald Garcke, Regensburg
Barbara Niethammer, Bonn
Gieri Simonett, Nashville

11 February – 16 February 2024

ABSTRACT. Partial differential equations arising in the context of interfaces and free boundaries encompass a flourishing area of research. The workshop focused on new developments and emerging new themes. At the same time also new interesting results on more traditional areas like, e.g. regularity theory and classical numerical approaches have been addressed. By convening experts from various disciplines related to modeling, analysis, and numerical methods concerning interfaces and free boundaries, the workshop facilitated progress on longstanding open questions and paved the way for novel research directions.

Introduction by the Organizers

Interfaces and free boundaries appear in numerous applications, ranging from tumor growth, finance, biological membranes, porous media, two-phase flows, fluid structure interaction to shape optimisation problems. Often, geometric partial differential equations have to be solved on a surface in order to determine the evolution of interfaces and free boundaries. Besides classical methods from the existence, uniqueness and regularity analysis of partial differential equations new approaches involving a close interaction between modeling, analysis and numerical methods have been proven to be successful. The workshop brought together researchers working on aspects of geometry, the theory of partial differential equations, classical analysis, asymptotic analysis, and novel numerical methods. Thus,

new insights were established into so far only vaguely formulated scientific problems in order to obtain precise models and equations as well as structure preserving and efficient numerical methods for problems involving interfaces and free boundaries.

The workshop was attended by 47 participants from Europe, Asia and America with an expertise in analysis of PDEs, modeling, numerical analysis and scientific computing. In addition, six researchers participated online. The scientific program consisted of 28 plenary talks. In addition, six young researchers were given the opportunity to present their research in twenty minutes talks on Tuesday and Thursday evening.

The workshop had a focus on free and moving boundary problems, phase field equations and their singular limits, bulk-surface interactions, geometric variational and geometric evolution problems, problems involving bending energies, stochastic PDEs for interfaces and free boundaries and PDEs on surfaces. We will now briefly discuss the relevant contributions.

Free and moving boundary problems: John King discussed new developments for moving boundary problems for singular reaction-diffusion equations with a focus on applications in tissue and tumor growth. Sara Zahedi introduced new divergence preserving cut finite elements which are important for two-phase flow moving boundary problems. Julian Fischer established a weak-strong uniqueness principle for varifold solutions to the Mullins-Sekerka problem. Richard Schubert showed convergence to a planar interface for the Mullins-Sekerka evolution where in particular the fact that one has to work on unbounded domains causes major difficulties. James Sethian presented numerical approaches for highly complex models related to fluid interfaces in industrial painting. Amal Alphonse studied free boundaries in quasi-variational problems arising in thermo-elasticity.

Phase field models and their singular limits: Helmut Abels considered a sharp interface limit of a Navier-Stokes/Allen-Cahn system using both matched asymptotic expansions and the relative entropy method. Maurizio Grasselli showed new results on multi-component phase-field systems and in particular showed strict separation properties. Matthias Röger studied phase separation on varying surfaces and considered the convergence of diffuse interface approximations. Chun Liu used non-equilibrium thermodynamics to study temperature effects for chemical reactions and in particular could derive non-isothermal models for phase transitions in the Cahn-Hilliard context. Changyou Wang used axisymmetric Ginzburg-Landau approximated solutions of the Ericksen-Leslie system to show existence of weak solutions. Dennis Trautwein introduced a new viscoelastic phase field model for tumor growth and showed existence of solutions via a stable finite element approximation. Clemens Ullrich introduced and analysed a phase field model for the evolution of surfactants.

Geometric variational and geometric evolution problems: Lia Bronsard studied non-local isoperimetric problems leading to double bubbles and core-shells with applications to triblock copolymers. Also in the talk of Matteo Novaga, a non-local energy was minimized. However, in his case the non-locality originated from

a charge repulsion. Antonin Chambolle considered discrete to continuous crystalline curvature flows using a fully discrete version of the Luckhaus-Sturzenhecker scheme. Alexandra Pluda studied another geometric evolution problem, namely the network curvature flow. Here, results can help to understand coarsening in poly-crystalline materials. Paola Pozzi studied the anisotropic curvature flow for networks and in particular showed stability results. Björn Stinner showed convergence of finite element schemes with mesh smoothing for geometric evolution problems. Klaus Deckelnick was able to introduce a new tangential motion for fourth order geometric curve evolutions which made it possible to rigorously study the convergence of related finite element discretizations. Alice Marveggio studied the multiphase mean curvature flow and was able to show stability beyond a circular topology change in the planar case.

Bulk-surface interactions: Balázs Kovács studied a bulk-surface model for tumor growth and was able to provide a convergence analysis for a finite element scheme. Patrik Knopf considered two-phase flow with moving contact lines and modeled the bulk-surface interaction with the help of a phase field model with dynamic boundary conditions. Dieter Bothe introduced new sharp interface models for dynamic contact lines which have the potential to deal with the contact line paradox.

Problems involving bending energies: Sören Bartels studied the Babuška paradox related to an instability of certain fourth order problems. He in particular also considered the paradox for nonlinear versions. Maxim Olshanskii studied equilibrium shapes for deformable liquid surfaces taking curvature energies into account. The talk of Tom Ranner dealt with microswimmer locomotion and he was able to model the motion of real swimmers with the help of a Cosserat rod model.

PDEs on surfaces: Axel Voigt and Robert Nürnberg both discussed fluid deformable models involving surface Navier-Stokes equations and bending energies. Tom Sales studied a (tangential) Navier-Stokes/Cahn-Hilliard system on an evolving surface which is an evolving surface analogue of the "Model H" of Hohenberg and Halperin. Achilleas Mavrakis analysed a surface finite element method for surface Stokes equations, and Andrea Poiatti considered several models for phase separation on evolving surfaces.

Stochastic PDEs for interfaces and free boundaries: Günther Grün was able to show finite speed of propagation properties for stochastic thin film equations and Ana Djurdjevac studied multilevel repesentations of isotropic random fields on the sphere.

Workshop: Interfaces, Free Boundaries and Geometric Partial Differential Equations

Table of Contents

Abstracts

Some moving-boundary problems for singular reaction-diffusion equations
John King

The quasilinear reaction-diffusion equation

$$\frac{\partial u}{\partial t} = \frac{\partial}{\partial x}\left(D(u)\frac{\partial u}{\partial x} \right) + f(u)$$

is derived from a simple two-phase model for tissue (or biofilm) growth, where u is the volume fraction of cellular material, so that $0 \leqslant u \leqslant 1$. There is specific interest in allowing D and f to take power-law forms in each of the limits $u \to 0$ and $u \to 1$; the ultimate behaviour can then exhibit a large variety of distinct types of phenomena (involving a number of classes of both linear and superlinear growth rates) and these are classified in terms of the various power-law exponents. A specific focus is on regimes in which moving-boundary problems naturally arise, either at $u = 0$ (usually associated with the case of 'slow' diffusion and leading to a clearly defined tissue boundary) and/or at $u = 1$ (whereby considerations associated with the contact inhibition of cell division necessarily arise through close packing and lead to obstacle-problem-like formulations). The analyses in question involve a combination of formal asymptotic methods alongside a comprehensive characterisation of the possible solutions branches.

Babuška's paradox in linear and nonlinear bending theories
Sören Bartels
(joint work with Andrea Bonito, Peter Hornung, and Philipp Tscherner)

The plate bending or Babuška paradox refers to an instability of certain fourth order problems with respect to the approximation of the underlying domain by polygonally bounded domains. In particular, for the minimization of the bending energy

$$I(\omega, u) = \frac{\sigma}{2} \int_{\omega} |\Delta u|^2 \, \mathrm{d}x + \frac{1-\sigma}{2} \int_{\omega} |D^2 u|^2 \, \mathrm{d}x - \int_{\omega} f u \, \mathrm{d}x$$

subject to simple support boundary conditions

$$u|_{\partial \omega} = 0$$

we have that approximations $u_m \in H^2(\omega_m) \cap H_0^1(\omega_m)$ obtained as minimizers for the funtionals $I(\omega_m, u)$ do not converge to the minimizer $u \in H^2(\omega) \cap H_0^1(\omega)$ if $\partial \omega$ has a curved part and ω_m are polygonal approximations of ω. The failure of convergence can be explained by a curvature contribution in the Euler–Lagrange

equations related to the minimization problem, i.e., the minimizer u for the functional $I(\omega, \cdot)$ solves the equations

$$\Delta^2 u = f \text{ in } \omega, \quad u = 0 \text{ on } \partial\omega, \quad \Delta u + (1 - \sigma)\kappa\partial_n u = 0 \text{ on } \partial\omega,$$

where κ is the curvature of $\partial\omega$. For polygonally bounded domains ω_m, the (distributional) curvature κ_m vanishes away from the corner points while the normal derivative $\partial_n u_m$ vanishes in the corner points if $u_m = 0$ on $\partial\omega_m$. Hence, the minimizers u_m for the functionals $I(\omega_m, \cdot)$ satisfy the equations

$$\Delta^2 u_m = f \text{ in } \omega_m, \quad u_m = 0 \text{ on } \partial\omega_m, \quad \Delta u_m = 0 \text{ on } \partial\omega_m.$$

The disappearance of the material parameter σ indicates that convergence $u_m \to u$ cannot be expected in general. A particular rotationally symmetric example has been specified in [1].

An alternative and more general explanation for the failure of convergence can be obtained by adopting a variational viewpoint. With the help of density results for certain regular functions in the admissible set, one verifies the identity

$$I(\omega, u) = \frac{1}{2}\int_\omega |\Delta u|^2\, \mathrm{d}x + \frac{1 - \sigma}{2}\int_{\partial\omega} \kappa|\partial_n u|^2\, \mathrm{d}s - \int_\omega fu\, \mathrm{d}x,$$

while for polygonally bounded domains ω_m one finds that

$$I(\omega_m, u) = \frac{1}{2}\int_\omega |\Delta u_m|^2\, \mathrm{d}x - \int_{\omega_m} fu_m\, \mathrm{d}x.$$

The representations imply that Γ-convergence $I_m \to I$ cannot apply in general and that a modification of the boundary condition is necessary to guarantee convergence.

Following ideas from [4], an appropriate treatment of the boundary conditions consists in imposing these in the corner points only, i.e., considering the set of admissible functions

$$\mathcal{A}_m = \big\{v \in H^2(\omega_m) : v(c_i) = 0 \text{ for } i = 0, 1, \ldots, m\big\},$$

where $c_i \in \partial\omega$, $i = 0, 1, \ldots, m$, are the corner points of ω_m that are assumed to belong to the boundary of ω. Letting $\widetilde{I}(\omega_m, \cdot)$ denote the application of $I(\omega_m, \cdot)$ to funtions in $\mathcal{A}_m$ one easily establishes the variational convergence of the functionals $\widetilde{I}_m$ to I. The construction of a so-called recovery sequence is simply realized via the restriction of functions $u \in H^2(\omega) \cap H_0^1(\omega)$ to the approximating domains $\omega_m \subset \omega$ which provides approximations $u_m \in \mathcal{A}_m$.

In finite element settings it is crucial that the discrete boundary conditions are satisfied by nodal interpolants in the approximating triangulated domains of functions $u \in H^3(\omega) \cap H_0^1(\omega)$. Then, convergence of discrete minimizers can be established for conforming and nonconforming finite element methods, cf. [3].

The Babuška paradox is difficult to observe in real experiments since the Kirchhoff bending model only applies to small deflections. The paradox may thus be an artifact related to an oversimplistic modelling. That this is not the case can be seen by considering nonlinear bending problems. An interesting case results from the description of thin-sheet folding problems, in which a given crease line

allows for discontinuities in the deformation gradient. The mathematical model obtained in [2] seeks a deformation $y : \omega \to \mathbb{R}^3$ that is continuous in ω and twice weakly differentiable away from the crease line S, i.e., it belongs to the set $H^2(\omega \setminus S; \mathbb{R}^3) \cap W^{1,\infty}(\omega; \mathbb{R}^3)$, and minimizes the functional

$$I_{\mathrm{fold}}(\omega, S, y) = \frac{1}{2} \int_{\omega \setminus S} |D^2 y|^2 \, \mathrm{d}x - \int_\omega f \cdot y \, \mathrm{d}x$$

subject to boundary conditions $L_{\mathrm{bc}}(y) = \ell_{\mathrm{bc}}$ and the isometry condition

$$(\nabla y)^T \nabla y = \mathrm{id}.$$

The latter condition imposes the constraint that no shearing or stretching occurs. Simple experiments show that singularities occur if a smooth crease line S is approximated by piecewise straight crease lines S_m. In fact, it is possible to prove that deformations $y_m \in H^2(\omega \setminus S_m; \mathbb{R}^3) \cap W^{1,\infty}(\omega; \mathbb{R}^3)$ with polygonal arcs S_m always belong to $H^2(\omega; \mathbb{R}^3)$, i.e., they cannot be folded. By following the ideas for the linear Kirchhoff model discussed above, a convergent approximation is obtained by imposing continuity only in the corner points of S_m which corresponds to using slit crease line segments in practice.

References

[1] I. Babuška and J. Pitkäranta, *The plate paradox for hard and soft simple support*, SIAM J. Math. Anal. **21** (1990), 551–576.

[2] S. Bartels, A. Bonito, and P. Hornung, *Modeling and simulation of thin sheet folding*, Interfaces Free Bound. **24** (2022), 459–485.

[3] S. Bartels and P. Tscherner, *Necessary and sufficient conditions for avoiding Babuška's paradox on simplicial meshes*, arXiv eprint 2401.05897 (2024).

[4] R. Rannacher, *Finite element approximation of simply supported plates and the Babuška paradox*, Z. Angew. Math. Mech. **59** (1979), T73–T76.

Sharp Interface Limit of a Navier-Stokes/Allen-Cahn System with Vanishing Mobility

Helmut Abels

(joint work with Mingwen Fei, Julian Fischer, and Maximilian Moser)

We consider the singular limit $\varepsilon \to 0$ of the following system:

$$\text{(1)} \qquad \partial_t \mathbf{v}_\varepsilon + \mathbf{v}_\varepsilon \cdot \nabla \mathbf{v}_\varepsilon - \mathrm{div}(2\nu(c_\varepsilon) D\mathbf{v}_\varepsilon) + \nabla p_\varepsilon = -\varepsilon \, \mathrm{div}(\nabla c_\varepsilon \otimes \nabla c_\varepsilon),$$

$$\text{(2)} \qquad \mathrm{div}\, \mathbf{v}_\varepsilon = 0,$$

$$\text{(3)} \qquad \partial_t c_\varepsilon + \mathbf{v}_\varepsilon \cdot \nabla c_\varepsilon = m_\varepsilon(\Delta c_\varepsilon - \tfrac{1}{\varepsilon^2} f'(c_\varepsilon)),$$

in $\Omega \times (0, T_0)$ together with

$$\text{(4)} \qquad (\mathbf{v}_\varepsilon, c_\varepsilon)|_{\partial \Omega} = (0, -1) \qquad \text{on } \partial \Omega \times (0, T_0),$$

$$\text{(5)} \qquad (\mathbf{v}_\varepsilon, c_\varepsilon)|_{t=0} = (\mathbf{v}_{0,\varepsilon}, c_{0,\varepsilon}) \quad \text{in } \Omega$$

Here $\mathbf{v}_\varepsilon, p_\varepsilon$ are the velocity and the pressure of the fluid mixture, c_ε is the order parameter, which is related to the concentration difference of the fluids, $\nu(c_\varepsilon)$

describes the viscosity in dependence on c_ε, and f is a suitable smooth double well potential, e.g., $f(c) = \frac{1}{8}(c^2 - 1)^2$. Moreover, $D\mathbf{v}_\varepsilon = \frac{1}{2}(\nabla\mathbf{v}_\varepsilon + (\nabla\mathbf{v}_\varepsilon)^T)$, $\Omega \subseteq \mathbb{R}^2$ is a bounded domain with smooth boundary, and $m_\varepsilon > 0$ is mobility coefficient such that $m_\varepsilon \to_{\varepsilon \to 0} 0$ suitably. We prove the convergence of (1)-(3) to the following sharp interface limit system:

$$(6) \quad \partial_t \mathbf{v}_0^\pm + \mathbf{v}_0^\pm \cdot \nabla \mathbf{v}_0^\pm - \nu^\pm \Delta \mathbf{v}_0^\pm + \nabla p_0^\pm = 0 \qquad \text{in } \Omega^\pm(t), t \in (0, T_0),$$

$$(7) \qquad\qquad\qquad\qquad\qquad\qquad \text{div } \mathbf{v}_0^\pm = 0 \qquad \text{in } \Omega^\pm(t), t \in (0, T_0),$$

$$(8) \qquad\qquad\qquad [\![2\nu^\pm D\mathbf{v}_0^\pm - p_0^\pm \mathbf{I}]\!]\mathbf{n}_{\Gamma_t} = -\sigma H_{\Gamma_t}\mathbf{n}_{\Gamma_t} \qquad \text{on } \Gamma_t, t \in (0, T_0),$$

$$(9) \qquad\qquad\qquad\qquad\qquad\qquad\qquad [\![\mathbf{v}_0^\pm]\!] = 0 \qquad \text{on } \Gamma_t, t \in (0, T_0),$$

$$(10) \qquad\qquad\qquad\qquad\qquad\qquad V_{\Gamma_t} = \mathbf{n}_{\Gamma_t} \cdot \mathbf{v}_0^\pm \qquad \text{on } \Gamma_t, t \in (0, T_0),$$

$$(11) \qquad\qquad\qquad\qquad\qquad\qquad\qquad \mathbf{v}_0^- |_{\partial\Omega} = 0 \qquad \text{on } \partial\Omega \times (0, T_0)$$

$$(12) \qquad\qquad\qquad\qquad\qquad (\mathbf{v}_0^\pm, \Gamma_t)|_{t=0} = (\mathbf{v}_{0,0}^\pm, \Gamma_0),$$

where $\nu^\pm = \nu(\pm 1)$, Ω is the disjoint union of $\Omega^+(t), \Omega^-(t)$, and Γ_t for every $t \in [0, T_0]$, $\Omega^\pm(t)$ are smooth domains, $\Gamma_t = \partial\Omega^+(t)$, and $\mathbf{n}_{\Gamma_t}$ is the interior normal of Γ_t with respect to $\Omega^+(t)$. Moreover,

$$[\![u]\!](p, t) = \lim_{h \to 0+} [u(p + \mathbf{n}_{\Gamma_t}(p)h) - u(p - \mathbf{n}_{\Gamma_t}(p)h)]$$

is the jump of a function $u \colon \Omega \times [0, T_0] \to \mathbb{R}^2$ at Γ_t in direction of $\mathbf{n}_{\Gamma_t}$, H_{Γ_t} and V_{Γ_t} are the curvature and the normal velocity of Γ_t, both with respect to $\mathbf{n}_{\Gamma_t}$. Furthermore, $\sigma = \int_{\mathbb{R}} \theta_0'(\rho)^2 \, d\rho$, where θ_0 is the so-called optimal profile that is the unique solution of

$$-\theta_0''(\rho) + f'(\theta_0(\rho)) = 0 \quad \text{for all } \rho \in \mathbb{R}, \qquad \lim_{\rho \to \pm\infty} \theta_0(\rho) = \pm 1, \quad \theta_0(0) = 0.$$

As first convergence result we have shown in [1]:

Theorem 1. *Let $T_0 > 0$, $m_\varepsilon = \sqrt{\varepsilon}$ for all $\varepsilon > 0$, and $(\mathbf{v}_0^\pm, \Gamma)$ be a smooth solution of the two-phase Navier-Stokes system with surface tension (6)-(12) on $[0, T_0]$ and $c_{0,\varepsilon}(x, t) \in [-1, 1]$ for all $(x, t) \in \overline{\Omega} \times [0, T_0]$, $\varepsilon \in (0, 1]$. Let $N \in \mathbb{N}$, $N \geq 3$. Then there exist $c_A = c_A(N, \varepsilon), \mathbf{v}_A = \mathbf{v}_A(N, \varepsilon) \in H^1(0, T_0; L^2(\Omega)) \cap L^2(0, T_0; H^2(\Omega))$ for $\varepsilon \in (0, 1]$, uniformly bounded in these spaces and $\|c_A\|_\infty \leq 1 + c$ with $c > 0$ independent of $\varepsilon \in (0, 1]$, such that the following holds:*

Let $(\mathbf{v}_\varepsilon, c_\varepsilon)$ be strong solutions of (1)-(5) with initial values $\mathbf{v}_{0,\varepsilon}, c_{0,\varepsilon}$ such that

$$\|c_{0,\varepsilon} - c_A|_{t=0}\|_{L^2(\Omega)} + \varepsilon^2 \|\nabla(c_{0,\varepsilon} - c_A|_{t=0})\|_{L^2(\Omega)}$$

$$(13) \qquad\qquad + \|\mathbf{v}_{0,\varepsilon} - \mathbf{v}_A|_{t=0}\|_{L^2(\Omega)} \leq C\varepsilon^{N+\frac{1}{2}}$$

for all $\varepsilon \in (0, 1]$ and some $C > 0$. Then there are some $\varepsilon_0 \in (0, 1]$, $R > 0$ and $T_1 \in (0, T_0]$ small such that for all $\varepsilon \in (0, \varepsilon_0]$ and some $C_R > 0$ it holds for

$\overline{c}_\varepsilon := c_\varepsilon - c_A$ and $\overline{\mathbf{v}}_\varepsilon := \mathbf{v}_\varepsilon - \mathbf{v}_A$

$$(14) \qquad \|\overline{c}_\varepsilon\|_{L^\infty(0,T_1;L^2(\Omega))} + \varepsilon^{\frac{1}{4}}\|\nabla\overline{c}_\varepsilon\|_{L^2((\Omega\times(0,T_1))\setminus\Gamma(\delta))} \le R\varepsilon^{N+\frac{1}{2}},$$

$$(15) \qquad \varepsilon^{\frac{1}{4}}\|\nabla_{\boldsymbol{\tau}_\varepsilon}\overline{c}_\varepsilon\|_{L^2((\Omega\times(0,T_1))\cap\Gamma(2\delta))} + \varepsilon\|\nabla\overline{c}_\varepsilon\|_{L^2((\Omega\times(0,T_1))\cap\Gamma(2\delta))} \le R\varepsilon^{N+\frac{1}{2}},$$

$$(16) \qquad \varepsilon^2\|\nabla\overline{c}_\varepsilon\|_{L^\infty(0,T_1;L^2(\Omega))} + \varepsilon^{2+\frac{1}{4}}\|\nabla^2\overline{c}_\varepsilon\|_{L^2(\Omega\times(0,T_1))} \le R\varepsilon^{N+\frac{1}{2}},$$

$$(17) \qquad \|\overline{\mathbf{v}}_\varepsilon\|_{H^{\frac{1}{2}}(0,T_1;L^2(\Omega))} + \|\overline{\mathbf{v}}_\varepsilon\|_{L^\infty(0,T_1;L^2(\Omega))\cap L^2(0,T_1;H^1(\Omega))} \le C_R\varepsilon^{N+\frac{1}{4}},$$

where $\Gamma(\tilde{\delta})$ are standard tubular neighbourhoods for $\tilde{\delta} \in [0,3\delta]$, $\delta > 0$ small and $\nabla_{\boldsymbol{\tau}_\varepsilon}$ is a suitable (approximate) tangential gradient. Moreover, let d_Γ be the signed distance to Γ. Then

$$(18) \quad c_A = \zeta(d_\Gamma)\theta_0(\rho_\varepsilon) \pm \chi_{\Omega^\pm}(1 - \zeta(d_\Gamma)) + O(\varepsilon^{\frac{3}{2}}) \qquad in \ L^\infty((0,T_0)\times\Omega),$$

$$(19) \quad \mathbf{v}_A = \mathbf{v}_0^+(x,t)\eta(\rho_\varepsilon) + \mathbf{v}_0^-(x,t)(1 - \eta(\rho_\varepsilon)) + O(\sqrt{\varepsilon}) \qquad in \ L^\infty(0,T_0;L^p(\Omega)),$$

where $\varepsilon\rho_\varepsilon = d_\Gamma + O(\sqrt{\varepsilon})$ in $\Gamma(3\delta)$, $p \in [1,\infty)$ is arbitrary, $\zeta\colon\mathbb{R}\to[0,1]$ is smooth such that $\operatorname{supp}\zeta \subseteq [-2\delta,2\delta]$ and $\zeta \equiv 1$ on $[-\delta,\delta]$, and $\eta\colon\mathbb{R}\to[0,1]$ is smooth such that $\eta = 0$ in $(-\infty,-1]$, $\eta = 1$ in $[1,\infty)$, $\eta - \frac{1}{2}$ is odd and $\eta' \ge 0$ in $\mathbb{R}$. In particular,

$$\lim_{\varepsilon\to 0} c_A = \pm 1 \qquad uniformly \ on \ compact \ subsets \ of \quad \Omega^\pm.$$

For the proof an approximate solution $(\mathbf{v}_A, p_A, c_A)$ is constructed using finitely many terms from formally matched asymptotic calculations and a novel ansatz for a critical highest order term. Then the error $c_A - c_\varepsilon$ is estimated with the aid of a refined spectral estimate for the linearized Allen-Cahn operator. We refer to [1] for the details.

With the aid of relative entropy method we have shown in [2]:

Theorem 2. Let $\nu(c_\varepsilon) = \nu$ be independent of c_ε, $m_\varepsilon := m_0\varepsilon^\beta$ for $\varepsilon > 0$, where $m_0 > 0$ and $\beta \in (0,2)$ are fixed, $q = 2$ if $d = 2$, and $q = \frac{4}{3}$ if $d = 3$. Moreover, let $T_0 > 0$ be such that the two-phase Navier-Stokes system with surface tension (6)-(12) has a smooth solution $(\mathbf{v}_0^\pm, p_0^\pm, \Gamma)$ on $[0,T_0]$. Let $(\mathbf{v}_\varepsilon, \varphi_\varepsilon)$ with $\mathbf{v}_\varepsilon \in L^\infty(0,T_0;L^2_\sigma(\Omega))\cap L^2(0,T_0;H^1_0(\Omega)^d)$, $c_\varepsilon \in L^2(0,T_0;H^2(\Omega))\cap W^1_q(0,T_0;L^2(\Omega))$ for $\varepsilon > 0$ be energy-dissipating weak solutions to the Navier-Stokes/Allen-Cahn system (1)-(5) on $[0,T_0]$ for the constant mobility m_ε and for initial data $(\mathbf{v}_{0,\varepsilon}, c_{0,\varepsilon})$ with energy uniformly bounded with respect to ε and satisfying

$$(20) \quad \begin{aligned} \sum_\pm \int_{\Omega_0^\pm} \frac{1}{2}|\mathbf{v}_{0,\varepsilon} - \mathbf{v}_{0,0}^\pm|^2\,dx + \int_\Omega \frac{\varepsilon}{2}|\nabla c_{0,\varepsilon}|^2 + \frac{1}{\varepsilon}W(c_{0,\varepsilon}) - (\xi\cdot\nabla\psi_{0,\varepsilon})\,dx \\ + \int_\Omega |\sigma\chi_{\Omega_0^+} - \psi_{0,\varepsilon}|\min\{d_{\Gamma_0},1\}\,dx \le C\frac{\varepsilon^2}{m_\varepsilon} \end{aligned}$$

for $\varepsilon > 0$ sufficiently small, where $\psi(r) := \int_{-1}^r \sqrt{2W(s)}\,ds$ and $\psi_{0,\varepsilon} := \psi(c_{0,\varepsilon})$. Set $\psi_\varepsilon := \psi(c_\varepsilon)$.

Then for $\varepsilon > 0$ small and a.e. $T \in [0, T_0]$ it holds

(21a) $\|(\mathbf{v}_\varepsilon - \mathbf{v}^0)(., T)\|_{L^2(\Omega)} + \|\sigma \chi_{\Omega_T^+} - \psi_\varepsilon(., T)\|_{L^1(\Omega)} \leq C \left(\dfrac{\varepsilon}{\sqrt{m_\varepsilon}} + m_\varepsilon \right)$

(21b) $\|\nabla \mathbf{v}_\varepsilon - \nabla \mathbf{v}^0\|_{L^2(0, T_0; L^2(\Omega))} \leq C \left(\dfrac{\varepsilon}{\sqrt{m_\varepsilon}} + m_\varepsilon \right)$

for some $C > 0$ independent of $\varepsilon > 0$ and $T \in [0, T_0]$. Finally, there are well-prepared initial data $(\mathbf{v}_{0,\varepsilon}, c_{0,\varepsilon})$ for $\varepsilon > 0$ small in the sense that (20) is satisfied, even with rate ε^2.

References

[1] H. Abels, M. Fei, and M. Moser, *Sharp Interface Limit for a Navier-Stokes/Allen-CahnSystem in the Case of a Vanishing Mobility*, Preprint **arXiv:2304.12096** (2023).
[2] H. Abels, J. Fischer, and M. Moser, *Approximation of Classical Two-Phase Flows of Viscous Incompressible Fluids by a Navier-Stokes/Allen-Cahn System*, Preprint **arXiv:2311.02997** (2023).

Multi-component Cahn-Hilliard and conserved Allen-Cahn equations

MAURIZIO GRASSELLI

(joint work with Ciprian G. Gal, Andrea Poiatti, and Joseph L. Shomberg)

"Not only is phase separation intuitive, but it seems to be everywhere. Droplets of proteins and RNAs are turning up in bacteria, fungi, plants and animals. Phase separation at the wrong place or time could create clogs or aggregate of molecules linked to neurodegenerative diseases, and poorly formed droplets could contribute to cancers and might help explain the ageing process."

[E. Dolgin, What lava lamps and vinaigrette can teach us about cell biology, Nat. 555, 300-302 (2018)]

Phase separation phenomena often involves many interacting species (see, for instance, [7]). Thus, it follows the necessity of introducing and analyzing multi-component versions of the well-known Cahn-Hilliard equation as well as of the conserved Allen-Cahn equation (see [6]). Assume to have $N \geq 2$ components u_i, such that

$$\sum_{i=1}^{N} u_i = 1, \quad 0 \leq u_i \leq 1, \quad \forall i = 1, \dots, N.$$

Each component is defined in a space-time domain $\Omega \times [0, T]$, where $\Omega \subset \mathbb{R}^d$, $d = 2, 3$, is an open bounded domain and $T > 0$ is given. Following [3], we set

$$\boldsymbol{F}(\mathbf{u}) := \sum_{i=1}^{N} \psi(\varphi_i) - \frac{1}{2} \mathbf{u} \cdot \mathbf{A} \mathbf{u}$$

with $\mathbf{A}$ positive definite matrix and

$$\psi(s) := \theta s \ln s, \quad \theta > 0$$

so that

$$\mathcal{E}(\mathbf{u}) := \int_\Omega \boldsymbol{F}(\mathbf{u})dx + \frac{\gamma}{2}\int_\Omega |\nabla\mathbf{u}|^2 dx, \quad \gamma > 0.$$

We also introduce a mobility matrix $\boldsymbol{\alpha} \in \mathbb{R}^{N \times N}$ symmetric and positive semidefinite such that

$$\boldsymbol{\alpha\eta}\cdot\boldsymbol{\eta} \geq C_0|\boldsymbol{\eta}|^2 \quad \forall\boldsymbol{\eta}: \ \sum_{i=1}^N \eta_i = 0,$$

for some $C_0 > 0$, and observe that

$$Ker(\boldsymbol{\alpha}) = span\{[1, 1, \ldots, 1]^T\}.$$

Then we consider the following initial and boundary value problem for the Cahn-Hilliard multi-component equation

$$\begin{cases} \partial_t\mathbf{u} - \operatorname{div}(\boldsymbol{\alpha}(\nabla\boldsymbol{\mu})) = \mathbf{0} & \text{in } \Omega \times (0, T) \\ \boldsymbol{\mu} = -\gamma\Delta\mathbf{u} + \boldsymbol{F}'(\mathbf{u}) & \text{in } \Omega \times (0, T) \\ (\nabla\mathbf{u})\mathbf{n} = \mathbf{0} & \text{on } \partial\Omega \times (0, T) \\ (\boldsymbol{\alpha}\nabla\boldsymbol{\mu})\mathbf{n} = \mathbf{0} & \text{on } \partial\Omega \times (0, T) \end{cases}$$

and a similar problem for the conserved Allen-Cahn multi-component equation

$$\begin{cases} \partial_t\mathbf{u} + \boldsymbol{\alpha}(\boldsymbol{\mu} - \overline{\boldsymbol{\mu}}) = \mathbf{0} & \text{in } \Omega \times (0, T) \\ \boldsymbol{\mu} = -\gamma\Delta\mathbf{u} + \boldsymbol{F}'(\mathbf{u}) & \text{in } \Omega \times (0, T) \\ (\nabla\mathbf{u})\mathbf{n} = \mathbf{0} & \text{on } \partial\Omega \times (0, T). \end{cases}$$

The matrix $\boldsymbol{\alpha}$ is positive semidefinite, so we need to introduce the following projector

$$(\mathbf{P}\boldsymbol{\eta})_i := \eta_i - \frac{1}{N}\sum_{j=1}^N \eta_j$$

and reformulate both problems in terms of

$$\mathbf{w} := \mathbf{P}\boldsymbol{\mu} = \left[\mu_i - \frac{1}{N}\sum_{j=1}^N \mu_j\right]_{i=1,\ldots,N}.$$

This gives, respectively,

$$(1) \quad \begin{cases} \partial_t\mathbf{u} - \operatorname{div}(\boldsymbol{\alpha}\nabla\mathbf{w}) = \mathbf{0} & \text{in } \Omega \times (0, T) \\ \mathbf{w} = -\gamma\Delta\mathbf{u} + \mathbf{P}\boldsymbol{F}'(\mathbf{u}) & \text{in } \Omega \times (0, T) \\ (\nabla\mathbf{u})\mathbf{n} = \mathbf{0} & \text{on } \partial\Omega \times (0, T) \\ (\boldsymbol{\alpha}\nabla\mathbf{w})\mathbf{n} = \mathbf{0} & \text{on } \partial\Omega \times (0, T) \\ \mathbf{u}(0) = \mathbf{u}_0 & \text{in } \Omega \end{cases}$$

and

$$(2) \quad \begin{cases} \partial_t \mathbf{u} + \boldsymbol{\alpha}(\mathbf{w} - \overline{\mathbf{w}}) = \mathbf{0} & \text{in } \Omega \times (0, T) \\ \mathbf{w} = -\gamma \Delta \mathbf{u} + \mathbf{P}\boldsymbol{F}'(\mathbf{u}) & \text{in } \Omega \times (0, T) \\ (\nabla \mathbf{u})\mathbf{n} = \mathbf{0} & \text{on } \partial\Omega \times (0, T) \\ \mathbf{u}(0) = \mathbf{u}_0 & \text{in } \Omega. \end{cases}$$

We call *finite energy solution* to problem (1), a solution which satisfies the identity

$$\frac{d}{dt}\mathcal{E}(\mathbf{u}) + \int_\Omega \boldsymbol{\alpha}\nabla\mathbf{w} : \nabla\mathbf{w}\,dx = 0,$$

while a energy solution to the problem (2) satisfies the identity

$$\frac{d}{dt}\mathcal{E}(\mathbf{u}) + \int_\Omega \boldsymbol{\alpha}(\mathbf{w} - \overline{\mathbf{w}}) \cdot (\mathbf{w} - \overline{\mathbf{w}})\,dx = 0.$$

Both the identities are essential to establish the existence of (finite energy) solutions and to analyze their longtime behavior.

Regarding problem (1), the following results are proven in [4] (see also [1] for a model which accounts for hydrodynamics)

- well-posedness for finite energy solutions (refinement of [3])
- instantaneous regularization of finite energy solutions
- instantaneous uniform strict separation property if $d = 2$
- existence of global and, if $d = 2$, exponential attractors for the corresponding dissipative dynamical system
- convergence of any energy solution to a single stationary state (extension of [2] to the multi-component case)
- validity of the strict separation property for large times if $d = 3$.

By *strict separation property* we mean the existence of a $\delta \in (0, 1)$ such that $\delta \leq u_i \leq 1 - \delta$ for all $i \in \{1, \ldots, N\}$. This δ might be uniform with respect to the initial datum. Such a property is crucial to investigate several further properties of a solution (e.g., additional regularity, existence of an exponential attractor). Moreover, it rigorously justifies the use of smooth approximations of mixing entropy density.

The following results are valid for problem (2) (see [5])

- existence of finite energy solutions
- continuous dependence on the initial datum if $\boldsymbol{\alpha}$ has, for instance, the following structure

$$\boldsymbol{\alpha} = \xi \begin{bmatrix} N-1 & -1 & \ldots & -1 \\ -1 & N-1 & \ldots & -1 \\ \vdots & \vdots & \vdots & \vdots \\ -1 & \ldots & \ldots & N-1 \end{bmatrix} \quad \text{with } \xi > 0.$$

Assuming the well-posedness hypotheses, further properties are shown, namely,

- instantaneous regularization of finite energy solutions
- instantaneous uniform strict separation property

- existence of global and exponential attractors for the corresponding dissipative dynamical system
- convergence of any energy solution to a single equilibrium.

References

[1] H. Abels, H. Garcke, A. Poiatti, *Mathematical analysis of a diffuse interface model for multi-phase flows of incompressible viscous fluids with different densities*, J. Math. Fluid Mech., to appear.

[2] H. Abels, M. Wilke, *Convergence to equilibrium for the Cahn–Hilliard equation with a logarithmic free energy*, Nonlinear Anal. **67** (2007) 3176–3193.

[3] C.M. Elliott, S. Luckhaus, *A generalized diffusion equation for phase separation of a multi component mixture with interfacial free energy*, IMA Preprint Series # **887**, 1991.

[4] C.G. Gal, M. Grasselli, A. Poiatti, J.L. Shomberg, *Multi-component Cahn-Hilliard systems with singular potentials: theoretical results*, Appl. Math. Optim. **88**, Paper No. 73, 46 pp., 2023.

[5] M. Grasselli, A. Poiatti, *Multi-component Allen-Cahn equations*, Interfaces Free Bound., in press.

[6] J. Rubinstein, P. Sternberg, *Nonlocal reaction-diffusion equations and nucleation*, IMA J. Appl. Math. **48** (1992), 249–264.

[7] D. Zwicker, L. Laan, *Evolved interactions stabilize many coexisting phases in multicomponent liquids*, Proc. Natl. Acad. Sci. USA **119** (2022), (28) e2201250119.

Nonlocal isoperimetric problems: double-bubbles and core-shells, and a new partitioning problem

LIA BRONSARD

(joint work with Stan Alama, XinYang Lu, Chong Wang, Silas Vriend, and Mike Novack)

We first present a nonlocal isoperimetric problem for three interacting phase domains, related to the Nakazawa-Ohta ternary inhibitory system which describes domain morphologies in a triblock copolymer. We consider global minimizers on the two-dimensional torus, in a limit in which two of the species have vanishingly small mass but the interaction strength is correspondingly large. In this limit there is splitting of the masses, and each vanishing component rescales to a minimizer of an isoperimetric problem for clusters in $2D$. Depending on the relative strengths of the coefficients of the interaction terms we may see different structures for the global minimizers, ranging from a lattice of isolated simple droplets of each minority species to double-bubbles or core-shells. These results have led to a new type of partitioning problem that I will also describe. These represent work with S. Alama, X. Lu, C. Wang for the triblock copolymer problems, and with S. Alama and S. Vriend, and separately with M. Novack on the new partitioning problems.

The partitioning problem for (N, M) clusters introduced in [2] comes from the study of triblock copolymer models in the 2D torus by Alama-Bronsard-Lu-Wang in [3]. In [1], these authors study a partitioning problem in the torus with three phases, one of which occupies nearly all of the total area with the other two accounting for only a tiny fraction. In that case, the global minimizers form

weighted double-bubble or core-shell patterns depending on the parameters. In [3], they consider this partitioning problem but with two of the phases occupying nearly all of the total area and the third accounting for only a tiny fraction. In that case, we expect minimizers of the nonlocal triblock copolymer energy to form a lamellar pattern with the two majority phases, with tiny droplets of the third phase aligned on each lamellar stripe. By blowing up the droplets in the limit of vanishing area of the third phase we expect to recover the lens shape in the plane, and the characterization of the *vesica piscis* as the unique minimizer (up to symmetries) of this problem is critical to the analysis of the small-area limit of the triblock problem.

The classical double bubble theorem characterizes the minimizing partitions of $\mathbb{R}^n$ into three chambers, two of which have prescribed finite volume. In the article with M. Novack, [4] we prove a variant of the double bubble theorem in which two of the chambers have infinite volume. Such a configuration is an example of a *(1,2)-cluster*, or a partition of $\mathbb{R}^n$ into three chambers, two of which have infinite volume and only one of which has finite volume [2]. A $(1, 2)$-cluster is locally minimizing with respect to a family of weights $\{c_{jk}\}$ if for any $B_r(0)$, it minimizes the interfacial energy $\sum_{j<k} c_{jk} H^n(\partial \mathcal{X}(j) \cap \partial \mathcal{X}(k) \cap B_r(0))$ among all variations with compact support in $B_r(0)$ which preserve the volume of $\mathcal{X}(1)$. For $(1, 2)$ clusters, the analogue of the weighted double bubble is the *weighted lens cluster*, and we show that it is locally minimizing. Furthermore, under a symmetry assumption on $\{c_{jk}\}$ that includes the case of equal weights, the weighted lens cluster is the unique local minimizer in $\mathbb{R}^n$ for $n \leq 7$, with the same uniqueness holding in $\mathbb{R}^n$ for $n \geq 8$ under a natural growth assumption. We also obtain a closure theorem for locally minimizing $(N, 2)$-clusters.

In the article with Michael Novack [4], we study $(1, 2)$-clusters $\{\mathcal{X}(j)\}_{j=1}^3$, where $|\mathcal{X}(1)| < \infty$, and the weighted energy $\sum_{j<k} c_{jk} H^n(\partial^* \mathcal{X}(j) \cap \partial^* \mathcal{X}(k))$, where the family of weights satisfies standard positivity and triangularity conditions, and first show that the standard weighted lens cluster is locally minimizing. Our main result can be summarized as follows:

Theorem. *If $c_{12} = c_{13}$, then, up to rigid motions of $\mathbb{R}^n$, the standard weighed lens cluster is the unique locally minimizing $(1, 2)$-cluster in $\mathbb{R}^n$ for $n \leq 7$. The same uniqueness holds in $\mathbb{R}^n$ for $n \geq 8$ among locally minimizing $(1, 2)$-clusters with planar growth at infinity.*

We also include a proof of the equivalence between the above notion of local minimality and another natural one and use it to strengthen the closure theorem from [5] when there are two chambers with infinite volume, and also provide a characterization of the asymptotic behavior of the local minimizers of the $(N, 2)$ partitioning problem.

References

[1] S. Alama, L. Bronsard, X. Lu, and C. Wang. *Core shells and double bubbles in a weighted nonlocal isoperimetric problem*, accepted in SIAM Math Anal, 2023.

[2] S. Alama, L. Bronsard, and S. Vriend. *The standard lens cluster in R2 uniquely minimizes relative perimeter*, accepted in Trans AMS, 2023.

[3] S. Alama, L. Bronsard, X. Lu, and C. Wang. *Decorated phases in a model of tri-block co-polymers*, in preparation.

[4] L. Bronsard and M. Novack, *An Infinite Double Bubble Theorem*, preprint, arXiv:2401.08063

[5] M. Novaga, E. Paolini, and V. M. Tortorelli. *Locally isoperimetric partitions*, preprint 2023.

Temperature effects for chemical reaction dynamics

Chun Liu

(joint work with Jan-Eric Sulzbach)

Most existing research in fluid dynamics revolves around a fixed temperature setting, but it is becoming increasingly more in demand to incorporate non-isothermal conditions in practical applications. With advances in industries and technologies, it is crucial to provide a theoretical foundation for these complex systems. The key challenge is to find a way to unite the concepts from non-equilibrium thermodynamics with ideas from fluid mechanics. With this research we try to breach the gap between these two theories, by presenting a novel approach to model non-isothermal fluid systems.

For non-isothermal fluids, the temperature changes with the flow in both space and time. When a fluid is subjected to a change in temperature, its material properties, such as density, viscosity and pressure, change accordingly. In addition, for large enough deviations from a constant temperature there is a substantial influence on the flow field. Since the fluid can transport heat, the temperature field is, in turn, affected by changes in the flow field. This two-way coupling between fluid flow and heat transfer is a phenomenon that is common in heat engines, chemical reactions and atmospheric flows.

The theory of non-equilibrium thermodynamics derived from irreversible processes has been developed almost 100 years ago. It started from the 1930s seminal work by Onsager ([10], [11]) where he formulated the principles of irreversible thermodynamics with some underlying assumptions. The idea is to extend the concept of state from continuum thermostatics to a local description of material a point in the continuum, i.e., every material point that constructs the continuum is assumed to be close to a local thermodynamic equilibrium state at any given instant. Therefore, we can define the state variables and state functions such as temperature and entropy past their definition in equilibrium thermostatics. This theory is known as Classical Irreversible Thermodynamics (CIT) (cf. [7]). Besides the classical set of state variables, thermodynamic fluxes are introduced to describe irreversible processes. In particular, the rate of change of entropy within a region is contributed by an entropy flux through the boundary of that region and entropy production inside the region. In CIT the entropy flux only depends on the heat flux. The non-negativity of the entropy production rate grants the irreversibility of the dissipative process and states the second law of thermodynamics. Extensions of this theory beyond this local equilibrium hypothesis and incorporating a variational structure leads to the works by [5, 6, 1, 3].

The new approach developed in [8, 9, 2, 12] combines the ideas from non-equilibrium thermodynamics with the energetic variational approach (EnVarA) [4]. A key advantage is that we can provide a practical user's manual that can be employed in a wide variety of physical models:

- We will adopt a starting point as the free energy $\Psi(f,\theta)$ of the system, which includes both mechanical (resolved) and temperature/heat (under-resolved) contributions. From this free energy one can derive the thermo-dynamic state functions entropy $s(f,\theta) = -\partial_\theta \Psi(f,\theta)$ and internal energy $e(f,\theta) = \Psi(f,\theta) + \theta s(f,\theta)$.
- In the next step we will need to specify the kinematics of the mechanical state variables f. For instance when f corresponds to a density or concentration, the kinematics would be conservation of mass.
- Next we also need to specify the kinematics of the temperature. Here, the question is whether the temperature moves with the particle or if it stays on a fixed or moving background.
- In the next step, we derive the conservative and dissipative forces by using the Energetic Variational Approach (with prescribed mechanical dissipation) and combine them with Newton's force balance.
- In order to obtain the equations for the thermal quantities we apply the laws of thermodynamics.
- In the last step we connect the different thermal quantities by making use of constitutive relations such as the Duhem relation and Fourier's law.

One example of this framework can be found in [8], where the ideal gas equation is studied. Starting with a free energy of the form $\Psi(\rho,\theta) = k_2\theta\rho\log\rho - k_1\rho\theta\log\theta$ we obtain the non-isothermal Brinkman fluid with ideal gas equilibrium

$$\partial_t\rho + \nabla\cdot(\rho u) = 0, \quad \nabla p = \mu\Delta u - \nu\rho u,$$

$$\partial_t s + \nabla\cdot(su) = \nabla\cdot\left(\frac{\kappa\nabla\theta}{\theta}\right) + \tilde{\Delta},$$

where the entropy production is given by

$$\tilde{\Delta} = \frac{1}{\theta}\left(\mu|\nabla u|^2 + \nu|u|^2 + \frac{\kappa|\nabla\theta|^2}{\theta}\right)$$

and the entropy and pressure are

$$-s(\rho,\theta) = k\rho\left(\log\rho - \frac{3}{2}(\log\theta + 1)\right), \quad p(\rho,\theta) = k\rho\theta.$$

Besides the derivation of the model the paper focuses on establishing the existence of local-in-time weak solutions for the above system. Key steps in the proof are to obtain the existence of solutions for a regularized system, where an artificial viscosity term is used to regularize the continuity equation and the entropy equation is replaced by a regularized balance of internal energy equation. The next steps are to pass to the limit in each of the regularization parameters. Besides standard methods we apply the Div-Curl Lemma and weak compactness results in L^1, where passing to the limit in the entropy equation is the key challenge.

A second example of the general framework can be found in [9]. In this work we derive a model for the non-isothermal reaction-diffusion equation with law of mass action kinetics. This work extends the isothermal system derived in [13]. Here, we consider a chemical reaction of the form $\alpha A + \beta B \rightleftharpoons \gamma C$ with free energy

$$\psi(c, \theta) = \sum_{i=1}^{3} c_i \big(k_i^c \theta \ln c_i - k_i^\theta \theta \ln \theta \big),$$

where we assume that each species c_i has the free energy of an ideal gas, which is the case for ideal mixing. The general non-isothermal system now has the form

$$\partial_t c_i + \nabla \cdot (c_i u_i) = -\sigma R_t, \quad \eta_i(c_i, \theta) u_i = -k^c \nabla c_i \theta$$

$$\partial_t s + \nabla \cdot \left(\sum_{i=1}^{3} s_i u_i \right) = \nabla \cdot \left(\frac{\kappa \nabla \theta}{\theta} \right) + \frac{1}{\theta} \sum_i \big(\eta_i(c_i, \theta) |u_i|^2 \big)$$

$$+ \frac{1}{\theta} \left(\left(\sum_i \sigma_i \mu_i \right)^2 + \frac{\kappa |\nabla \theta|^2}{\theta} \right)$$

where the reaction rate R_t, chemical potential μ_i and entropy s are given by

$$R_t = k^c \ln \left(\frac{c_A c_B}{c_C} \right) + k^\theta \ln \theta - k^c$$

$$\mu_i = k^c \theta (\ln c_i + 1) - k^\theta \theta \ln \theta$$

$$s = \sum_i s_i = -\sum_i c_i \big(k^c \ln c_i - k^\theta (\ln \theta + 1) \big)$$

From this system we recover a linearized model close to the equilibrium state and analyze the global-in-time well-posedness of the system for small initial data in a critical Besov space.

Further applications and extensions can be found in [2] for phase transitions in the Cahn-Hilliard system and ongoing projects.

REFERENCES

[1] A.N. Beris and B.J. Edwards, Thermodynamics of flowing systems: with internal microstructure, Oxford University Press, USA, 1994

[2] F. De Anna, C. Liu, A. Schlömerkemper and J.E. Sulzbach, *Temperature dependent extensions of the Cahn–Hilliard equation*, Nonlinear Analysis: Real World Applications, **77** (2024), 104056

[3] M. Frémond, Non-Smooth Thermomechanics, Springer, Berlin, 2002

[4] M.-H. Giga, A. Kirshtein and C. Liu, *Variational modeling and complex fluids*, In: Handbook of mathematical analysis in mechanics of viscous fluids (2017), pp. 1–41

[5] M. Grmela and H. Öttinger, *Dynamics and thermodynamics of complex fluids. i. development of a general formalism*, Phys. Rev. E, **56** (6) (1997), p. 6620

[6] M. Grmela and H. Öttinger, *Dynamics and thermodynamics of complex fluids. ii. illustrations of a general formalism*, Phys. Rev. E, **56** (6) (1997), p. 6633

[7] S.R. De Groot and P. Mazur, Non-equilibrium thermodynamics, North-Holland Publ. Co., Amsterdam, 1962

[8] C. Liu and J.-E. Sulzbach, *The Brinkman-Fourier System with Ideal Gas Equilibrium*, Discrete & Continuous Dynamical Systems **42** (1) (2022), pp. 425–462

[9] C. Liu and J.-E. Sulzbach, *Well-Posedness for the Reaction-Diffusion Equation with Temperature in a critical Besov Space*, Journal of Differential Equations **325** (2022), pp. 119–149

[10] L. Onsager,*Reciprocal Relations in Irreversible Processes. I*, Phys. Rev. **37** (4) (1931), pp. 405–426

[11] L. Onsager,*Reciprocal Relations in Irreversible Processes. II*, Phys. Rev. **38** (12) (1931), pp. 2265–2279

[12] J.E. Sulzbach *Thermal Effects in Fluid Dynamics*, Ph.D. Thesis, Illinois Institute of Technology, Chicago, 2021

[13] Y. Wang, C. Liu, P. Liu and B. Eisenberg, *Field theory of reaction-diffusion: Mass action with an energetic variational approach*, Phys. Rev. E **102** (2020)

Discrete to continuous crystalline curvature flows

ANTONIN CHAMBOLLE

(joint work with Daniele DeGennaro and Massimiliano Morini)

This talk is an evolution and improvement from a previous talk in a MFO workshop (#2357), two months before. In a work soon online, we investigated a fully discrete version of the Almgren-Taylor-Wang / Luckhaus-Sturzenhecker scheme [1, 9] for building mean curvature flows. This scheme, after some rewriting, can be described as follows: given a set E^0, and d_{E^0} the *signed distance function* to its boundary, we solve in $\mathbb{R}^d$, for $h > 0$ small and each $n \geq 1$:

$$(1) \qquad \begin{cases} -h \operatorname{div} z^n + u^n = d_{E^{n-1}}\,, \\ |z^n| \leq 1, \quad z^n \cdot Du^n = |Du^n| \end{cases}$$

which is formally the Euler-Lagrange equation of

$$\min_u \int |Du| + \frac{1}{2h} \int (u - d_{E^{n-1}})^2 dx$$

(yet this energy is infinite in the whole space). We let then $E^n = \{x : u^n(x) \leq 0\}$. Equation (1) means that the level set 0 of u^n is at a distance from the boundary of E^{n-1} which is equal to h times its mean curvature: this corresponds to an implicit time-discretization of the mean curvature flow. By translational invariance and comparison, u^n is trivially 1-Lipschitz (since $d_{E^{n-1}}$ is), in particular the second condition in (1) reads $z \in \partial |\cdot|(\nabla d)$ a.e. in $\mathbb{R}^d$ (the subgradient of the Euclidean norm). One also deduces that $d_{E^n} \geq u^n$ in $\{u^n > 0\}$, and $d_{E^n} \leq u^n$ in $\{u^n < 0\}$. Hence,

$$\frac{d^n - d^{n-1}}{h} \geq \operatorname{div} z^n$$

out of E^n. Getting some control on d^n in time and $\operatorname{div} z^n$ in space allows then to pass to the limit and deduce the existence of $E \subset \mathbb{R}^d \times [0, \infty)$ (the Hausdorff limit of $\bigcup_{n \geq 0} E^n \times \{nh\}$) a closed set such that

$$(2) \qquad \partial_t d \geq \operatorname{div} z \quad \text{in} \quad \mathcal{D}'((\mathbb{R}^d \times (0, \infty)) \setminus E), \qquad z \in \partial |\cdot|(\nabla_x d) \text{ a.e.}$$

with $d(x, t) = \operatorname{dist}(x, E(t))$ for all x, t. Reasoning with the complement, one finds a similar equation for $A \subset E$, the complement of the Hausdorff limit of $\bigcup_{n \geq 0} (\mathbb{R}^d \setminus E^n) \times \{nh\}$.

This equation, which holds in the distributional or measure sense, is seen to hold also in the viscosity sense [6, 5] and hence characterizes the mean curvature flow (with a possible, but exceptional, fattening of the set $E \setminus A$), as shown in [10]. An important step in proving the convergence is an estimate of the solution of (1) with the right-hand side replaced with $|x|$, first computed in [3], this is crucial to estimate the variation of d^n in time as well as div z^n from above where $d^n > 0$.

Now, in [6, 4], it is also shown that the same scheme (and the same proof) can be applied to build and characterize anisotropic, or crystalline flows. Sticking to the simpler case of [6], and given φ a convex norm (with possibly polyhedral level sets) we replace Du above with $\varphi(Du)$, the distance with the φ° distance ($\varphi^\circ(x) = \sup\{x \cdot \nu : \varphi(\nu) \leq 1\}$), the condition on z^n in (1) with $z^n \in \partial\varphi(\nabla u^n)$ and end up with a distributional definition of a well posed *crystalline* mean curvature flow (see [6] for a comparison result which guarantees the uniqueness, in general, of the limit—when A is the interior of E). In this case, the motion is still described by (2) yet the second condition is $z \in \partial\varphi(\nabla_x d)$ and d is the φ°-distance to E. We observe that an alternative definition of the crystalline flow (which in general coincides) is based on the notion of viscosity solutions and was proposed by Giga and Giga [7] in 2D and Giga and Požár [8] in arbitrary dimension.

In the work presented at the workshop, together with M. Morini (Parma) and our student D. DeGennaro (Ceremade), we propose to solve a fully discrete equation, which reads (for $h, \varepsilon > 0$, small time and space steps)

$$\begin{cases} h(D_\varepsilon^* z^n)_i + u_i^n = d_i^{n-1} & \text{for } i \in \varepsilon\mathbb{Z}^d \\ |z_{i,j}^n| \leq \beta_{\frac{j-i}{\varepsilon}}, \quad z_{i,j}^n(u_j - u_i) = \beta_{\frac{j-i}{\varepsilon}}|u_j - u_i| \end{cases}$$

where $D_\varepsilon : \mathbb{R}^{\varepsilon\mathbb{Z}^d} \to \mathbb{R}^{\varepsilon\mathbb{Z}^d \times \varepsilon\mathbb{Z}^d}$ is defined by $(D_\varepsilon u)_{i,j} = (u_j - u_i)/\varepsilon$, D^* is its adjoint (for the standard scalar product), and β_k, $k \in \mathbb{Z}^d$, is a finitely supported family of positive weights (positive at least on a basis of $\mathbb{Z}^d$). One then sends $h, \varepsilon \to 0$. We show that we can adapt the techniques above to show again the convergence to (2), for the crystalline anisotropy $\varphi(p) = \sum_{k \in \mathbb{Z}^d} \beta_k |k \cdot p|$. Surprisingly, this happens for $\varepsilon \ll h$ (as expected), but also in case $\varepsilon = h$, and also, in case the weights $\beta_\bullet$ are *rational*, regardless of the ratio ε/h as both go to zero. To ensure this property, we have to define d^n from u^n with a sort of interpolation scheme (defined by suitable inf/sup convolutions with the distance φ°), so that the limiting evolution is precisely given by (2) without any drift, contrarily to the dicrete scheme introduced previously in [2], which was the starting point for our study, and where a rounding occurs at each step which accumulates in the limit.

References

[1] F. Almgren, J. E. Taylor, and L.-H. Wang. Curvature-driven flows: a variational approach. *SIAM J. Control Optim.*, 31(2):387–438, 1993.

[2] Andrea Braides, Maria Stella Gelli, and Matteo Novaga. Motion and pinning of discrete interfaces. *Arch. Ration. Mech. Anal.*, 195(2):469–498, 2010.

[3] Vicent Caselles and Antonin Chambolle. Anisotropic curvature-driven flow of convex sets. *Nonlinear Anal.*, 65(8):1547–1577, 2006.

[4] Antonin Chambolle, Massimiliano Morini, Matteo Novaga, and Marcello Ponsiglione. Existence and uniqueness for anisotropic and crystalline mean curvature flows. *J. Amer. Math. Soc.*, 32(3):779–824, 2019.

[5] Antonin Chambolle, Massimiliano Morini, Matteo Novaga, and Marcello Ponsiglione. Generalized crystalline evolutions as limits of flows with smooth anisotropies. *Anal. PDE*, 12(3):789–813, 2019.

[6] Antonin Chambolle, Massimiliano Morini, and Marcello Ponsiglione. Existence and uniqueness for a crystalline mean curvature flow. *Comm. Pure Appl. Math.*, 70(6):1084–1114, 2017.

[7] Mi-Ho Giga and Yoshikazu Giga. Generalized motion by nonlocal curvature in the plane. *Arch. Ration. Mech. Anal.*, 159(4):295–333, 2001.

[8] Yoshikazu Giga and Norbert Požár. A level set crystalline mean curvature flow of surfaces. *Adv. Differential Equations*, 21(7-8):631–698, 2016.

[9] Stephan Luckhaus and Thomas Sturzenhecker. Implicit time discretization for the mean curvature flow equation. *Calc. Var. Partial Differential Equations*, 3(2):253–271, 1995.

[10] Halil Mete Soner. Motion of a set by the curvature of its boundary. *J. Differential Equations*, 101(2):313–372, 1993.

Divergence Preserving Cut Finite Element Methods

SARA ZAHEDI

(joint work with Thomas Frachon, Peter Hansbo, and Erik Nilsson)

I introduce Cut Finite Element Methods (CutFEM) for interface problems and discuss our recent developments in achieving pointwise divergence-free velocity approximations in the case of incompressible flows.

The cut finite element method belongs to the class of unfitted finite element methods, providing an alternative to standard finite element methods when a fitted mesh is complicated and/or expensive to generate. The basic ideas of CutFEM were first introduced in [1] for an elliptic partial differential equation. In Cut-FEM, we begin with a regular mesh covering the computational domain, which is not required to conform to external and/or internal boundaries (interfaces). We then define active unfitted meshes, on which appropriate finite element spaces are defined, and a weak formulation where interface and boundary conditions are imposed weakly. A common approach to ensure accurate and robust discretization, regardless of the interface position relative to the computational mesh, is to add stabilization terms in the weak form. Ghost penalty stabilization [2] has been demonstrated to work well with low as well as high order elements using both continuous and discontinuous elements.

We present a cut finite element discretization of the Stokes interface problem using Taylor-Hood elements and standard ghost penalty stabilization. While this method accurately approximates discontinuities across interfaces on unfitted meshes [3, 4], the incompressibility condition does not hold pointwise.

To address this issue, we explore the Darcy interface problem to elucidate how to enforce the incompressibility condition discretely. Our proposed discretization is based on the mixed finite element pairs $\mathbf{RT}_k \times Q_k$ [5], where Q_k is the space

of discontinuous polynomial functions of degree $k \geq 0$ and $\mathbf{RT}_k$ is the Raviart-Thomas space. We demonstrate that the divergence-free property of the Raviart-Thomas element is compromised when the standard ghost penalty stabilization for the pressure is added in the weak form. We propose a modification of the pressure stabilization term, allowing for optimal divergence approximation in the unfitted setting.

Utilizing $\mathbf{H}^{\mathrm{div}}$-conforming finite elements and the new stabilization terms, we introduce cut finite element methods for the Stokes equations [6]. These methods demonstrate optimal convergence rates for velocity, pointwise divergence-free velocity fields, and well-posed linear systems, irrespective of the position of the boundary/interface relative to the computational mesh.

Finally, we discuss how to achieve pressure-robustness on unfitted meshes [6]. We demonstrate that pressure-robustness relies on accurate enforcement of boundary conditions and may not hold when boundary conditions are imposed weakly, even when the incompressibility condition is met pointwise. Two approaches for weakly imposing the normal component of the velocity at the boundary are examined: Nitsche's method (or a penalty method) and a Lagrange multiplier method. While pressure-robustness can be maintained with both approaches by minimizing errors at the boundary, the resulting linear systems' condition number are higher when the boundary conditions are weakly imposed, regardless of whether the mesh is fitted or unfitted to the boundary.

References

[1] A. Hansbo and P. Hansbo, *An unfitted finite element method, based on Nitsche's method, for elliptic interface problems*, Comput. Methods Appl. Mech. Engrg., **191** (2002), 5537–5552.

[2] Burman, E.: *Ghost penalty*, C. R. Acad. Sci. Paris, Ser. I **348**(21-22) (2010), 1217 – 1220.

[3] P. Hansbo, M. G. Larson, S. Zahedi, *A cut finite element method for a Stokes interface problem*, Appl. Numer. Math., **85** (2014), 90–114.

[4] T. Frachon, S. Zahedi, *A cut finite element method for two-phase flows with insoluble surfactants*, J. Comput. Phys., **473** (2023), 111734.

[5] T. Frachon, P. Hansbo, E. Nilsson, S. Zahedi, *A divergence preserving cut finite element method for Darcy flow*, accepted for publication in SISC, arXiv:2205.12023, (2023).

[6] T. Frachon, E. Nilsson, S. Zahedi, *Divergence-free cut finite element methods for Stokes flow*, arXiv:2304.14230, (2023).

Fluid deformable surfaces

Axel Voigt

(joint work with Veit Krause, Ingo Nitschke, Michael Nestler, and Maik Porrmann)

We consider surface finite elements and a semi-implicit time stepping scheme to simulate fluid deformable surfaces. Fluid deformable surfaces are thin fluidic sheets of soft materials exhibiting a solid–fluid duality. While they store elastic energy when stretched or bent, as solid shells, under in-plane shear, they flow as viscous two-dimensional fluids. This duality has several consequences: it establishes a

tight interplay between tangential flow and surface deformation. In the presence of curvature, any shape change is accompanied by tangential flow and, vice versa, the surface deforms due to tangential flow. Such surfaces are modeled by incompressible surface Navier-Stokes equations with bending forces. We consider closed surfaces and enforce conservation of the enclosed volume. The numerical approach builds on higher order surface parameterizations, a Taylor-Hood element for the surface Navier-Stokes part, appropriate approximations of the geometric quantities of the surface, mesh redistribution and a Lagrange multiplier for the constraint. The considered computational examples highlight the solid-fluid duality of fluid deformable surfaces and demonstrate convergence properties that are known to be optimal for different sub-problems, see, e.g., [1, 2]. The numerical approach and its validation is described in detail in [3]. With the aim to model the underlying mechanics of epithelial tissue in morphogenetic evolution we add an active driving forces which solely depends on curvature. Such geometric odd elastic forces, which act in response to mean curvature gradients and are directed perpendicularly to this gradient have been introduced in [4].

The overall model reads

$$\partial_t \boldsymbol{u} + \nabla_{\boldsymbol{v}} \boldsymbol{u} = -\nabla_{\mathcal{S}} p - p\mathcal{H}\boldsymbol{\nu} + \frac{2}{\mathrm{Re}} \operatorname{div}_{\boldsymbol{P}} \boldsymbol{\sigma} - \lambda\boldsymbol{\nu} + \mathbf{b} + \frac{\mathrm{Ac}}{2}\boldsymbol{\nu} \times \nabla_{\mathcal{S}}\mathcal{H}$$

(1)
$$\operatorname{div}_{\boldsymbol{P}} \boldsymbol{u} = 0$$

$$\int_{\mathcal{S}} \boldsymbol{u} \cdot \boldsymbol{\nu} \, \mathrm{d}\mathcal{S} = 0$$

which is defined on a surface $\mathcal{S} = \mathcal{S}(t)$, which is given by a parametrization $\boldsymbol{X}$. Related to $\mathcal{S}$ we denote the surface normal $\boldsymbol{\nu}$, the shape operator $\boldsymbol{B}$ with $B_{ij} = -\nabla_{\mathcal{S}}^i \nu_j$, the mean curvature $\mathcal{H} = \operatorname{tr} \boldsymbol{B}$ and the surface projection $\boldsymbol{P} = \mathbf{I} - \boldsymbol{\nu} \otimes \boldsymbol{\nu}$. Let $\nabla_{\mathcal{S}}$ and $\operatorname{div}_{\mathcal{S}}$ be the surface differential operators with respect to the covariant derivative. Those operators are well defined for vector fields in the tangent bundle of $\mathcal{S}$. For a non-tangential vector field $\boldsymbol{u} \colon \mathcal{S} \to \mathbb{R}^3$ we use the tangential derivative $\nabla_{\boldsymbol{P}} \boldsymbol{u} = \boldsymbol{P}\nabla \boldsymbol{u}^e \boldsymbol{P}$ and the tangential divergence $\operatorname{div}_{\boldsymbol{P}} \boldsymbol{u} = \operatorname{tr}[\boldsymbol{P}\nabla \boldsymbol{u}^e]$ where $\boldsymbol{u}^e$ is an extension of $\boldsymbol{u}$ constant in normal direction and ∇ the gradient of the embedding space $\mathbb{R}^3$. $\nabla_{\boldsymbol{P}} \boldsymbol{u}$ is a pure tangential tensor field and relates to the covariant operator by $\nabla_{\boldsymbol{P}} \boldsymbol{u} = \nabla_{\mathcal{S}}(\boldsymbol{P}\boldsymbol{u}) - (\boldsymbol{u} \cdot \boldsymbol{\nu})\boldsymbol{B}$. Similarly, it holds that $\operatorname{div}_{\boldsymbol{P}} \boldsymbol{u} = \operatorname{div}_{\mathcal{S}}(\boldsymbol{P}\boldsymbol{u}) - (\boldsymbol{u} \cdot \boldsymbol{\nu})\mathcal{H}$, see [2]. In the above equation $\boldsymbol{u}$ is the surface fluid velocity, p the surface pressure, $\boldsymbol{\sigma} = \frac{1}{2}(\nabla_{\boldsymbol{P}} \boldsymbol{u} + \nabla_{\boldsymbol{P}} \boldsymbol{u}^T)$ the rate of deformation tensor, Re the Reynolds number and $\mathbf{b}$ an acting force. The convection term is defined by $[\nabla_{\boldsymbol{v}} \boldsymbol{u}]_i = \nabla_{\mathcal{S}} u_i \cdot \boldsymbol{v}$, $i = 1, 2, 3$ where $\boldsymbol{v}$ is the relative material velocity of the surface. The surface fluid velocity is related to the parametrization by $(\boldsymbol{u} \cdot \boldsymbol{\nu})\boldsymbol{\nu} = \partial_t \boldsymbol{X}$. This formulation thus provides an Eulerian approach in tangential direction but a Lagrangian approach in normal direction. While conservation of the surface area $|\mathcal{S}|$ is enforced as a consequence of the local inextensibility constraint. To enforce conservation of the enclosed volume, e.g. $\int_{\mathcal{S}} \boldsymbol{u} \cdot \boldsymbol{\nu} = 0$, we consider the scalar Lagrange multiplier λ. Elastic properties of the surface $\mathcal{S}$ if deformed in normal direction are considered by $\mathbf{b}$, which result from the Helfrich energy and

read

$$(2) \qquad \mathbf{b} = \frac{1}{\mathrm{Be}}(-\Delta_{\mathcal{S}}\mathcal{H} - \mathcal{H}(\|\boldsymbol{B}\|^2 - \frac{1}{2}\operatorname{tr}(\boldsymbol{B})^2)\boldsymbol{\nu},$$

with the bending capillary number Be. The remaining term models the active forcing with Ac an activity parameter.

Figure 1 shows snapshots of the evolution. The initial condition is a local minimum of the Helfrich energy. The active forcing induces a chiral flow, which induces a shape instability. The instability leads to a global shape change terminating in shape which has a lower Helfrich energy and continuously circulating flows in opposite direction on both sides.
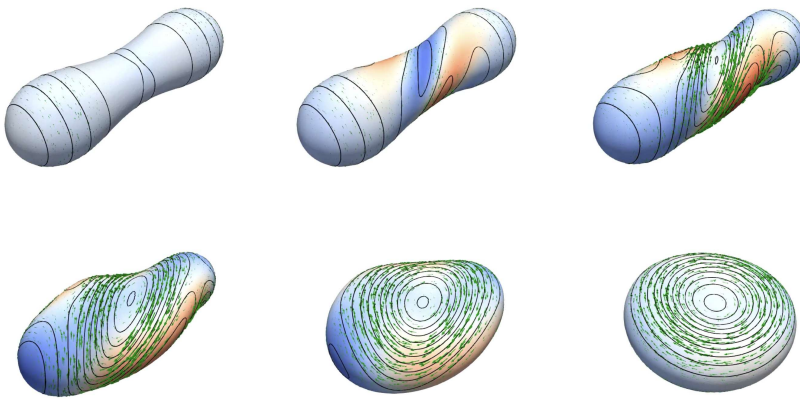
FIGURE 1. Snapshots of evolution: Isolines correspond to mean curvature, the color to the shape evolution in normal direction (blue - inwards, red - outwards) and the arrows to the tangential flow.

The full parameter space, varying the reduced volume, the bending capillary number and the stregth of activity is currently explored.

References

[1] G. Dziuk, *Computational parametric Willmore flow*, Num. Math. **111** (2008) 55–80.

[2] P. Brandner, T. Jankuhn, S. Praetorius, A. Reusken, A. Voigt, *Finite element discretization methods for velocity-pressure and stream function formulations of surface Stokes equations*, SIAM J. Sci. Comput. **44** (2022), A1807-A1832.

[3] V. Krause, A. Voigt, *Anumerical approach for fluid deformable surfaces with conserved enclosed volume*, J. Comput. Phys. **486** (2023), 112097.

[4] S.C. Al-Izzi, G. Alexander, *Chiral active membranes: Odd mechanics, spontaneous flows, and shape instabilities*, Phys. Rev. Research **5** (2023) 043227

An isoperimetric problem with capacitary repulsion

Matteo Novaga

(joint work with Michael Goldman and Berardo Ruffini)

We will consider a variational problem motivated by models for charged liquid drops recently studied in a series of papers [7, 8, 9, 10, 11, 2]. One of the main features of this problem is the competition between surface tension and charge repulsion; in particular, as opposed to the Gamow liquid drop model (see for instance [1] and references therein), the non-local effects often dominate the cohesive forces leading to singular behaviors.

Let us introduce the model: Given $\alpha \in (0, N)$ and a measurable set $E \subset \mathbb{R}^N$, we define the Riesz energy

$$(1) \qquad \mathcal{I}_\alpha(E) = \inf_{\mu(E)=1} \int_{\mathbb{R}^N \times \mathbb{R}^N} \frac{d\mu(x)\, d\mu(y)}{|x-y|^{N-\alpha}}.$$

Letting $P(E)$ denote the perimeter of E, we consider the functional

$$\mathcal{F}_{\alpha,Q}(E) = P(E) + Q^2 \mathcal{I}_\alpha(E),$$

for a charge $Q > 0$.

We are interested in studying the minimum problem

$$(2) \qquad \min_{|E|=m} \mathcal{F}_{\alpha,Q}(E),$$

for a fixed volume $m > 0$.

This question is motivated by the model for an electrically charged liquid drop in absence of gravity, introduced by Lord Rayleigh [12] in the physically relevant case $N = 3$ and $\alpha = 2$, and later investigated by many authors (see for instance [13, 14, 3, 7, 10, 11]).

In [7] it has been proved that, quite surprisingly, for any $\alpha \in (1, N)$ (in particular for the Coulombic case $\alpha = 2$) the problem is ill-posed. Indeed one can show that

$$\inf_{|E|=m} \mathcal{F}_{\alpha,Q}(E) = P(B_r),$$

where r is such that $|B_r| = m$. To restore well-posedness of the problem one needs to impose some extra regularity conditions such as bounds on the curvature [7], entropic terms [10] or the convexity of competitors [8].

It was shown in [11] that, for $N = 2$ and $\alpha = 1$, the ball is the unique minimizer of the problem, as long as Q is below an explicit threshold, and that nonexistence occurs otherwise.

This result was later extended in [9] to the general case $N \geq 2$ and $\alpha \in (1, N)$. More precisely, the following result holds:

Theorem. *Let $N \geq 2$. For $\alpha \in (1, N)$ and $Q > 0$, there are no minimizers of problem* (2).

Conversely, for $\alpha \in (0, 1]$ there exists $Q_0 = Q_0(N, \alpha) > 0$ such that for every $Q \leq Q_0$, balls are the only minimizers of (2).

References

[1] CHOKSI, R., MURATOV, C. B., AND TOPALOGLU, I. An old problem resurfaces nonlocally: Gamow's liquid drops inspire today's research and applications. *Notices Amer. Math. Soc.* 64, 11 (2017), 1275–1283.

[2] DE PHILIPPIS, G., HIRSCH, J., AND VESCOVO, G. Regularity of minimizers for a model of charged droplets. *ArXiv e-prints 1901.02546, to appear on Comm. Math. Phys.*

[3] FONTELOS, M. A., AND FRIEDMAN, A. Symmetry-breaking bifurcations of charged drops. *Arch. Ration. Mech. Anal. 172*, 2 (2004), 267–294.

[4] FRANK, R. L., AND LIEB, E. H. A compactness lemma and its application to the existence of minimizers for the liquid drop model. *SIAM J. Math. Anal. 47*, 6 (2015), 4436–4450.

[5] GOLDMAN, M., AND NOVAGA, M. Volume-constrained minimizers for the prescribed curvature problem in periodic media. *Calc. Var. Partial Differential Equations 44*, 3-4 (2012), 297–318.

[6] GOLDMAN, M., NOVAGA, M., AND RUFFINI, B. Reifenberg flatness for almost minimizers of the perimeter under minimal assumptions. *Proc. Amer. Math. Soc.*.

[7] GOLDMAN, M., NOVAGA, M., AND RUFFINI, B. Existence and stability for a non-local isoperimetric model of charged liquid drops. *Arch. Ration. Mech. Anal. 217*, 1 (2015), 1–36.

[8] GOLDMAN, M., NOVAGA, M., AND RUFFINI, B. On minimizers of an isoperimetric problem with long-range interactions under a convexity constraint. *Anal. PDE 11*, 5 (2018), 1113–1142.

[9] GOLDMAN, M., NOVAGA, M., AND RUFFINI, B. Rigidity of the ball for an isoperimetric problem with strong capacitary repulsion. *to appear on J. Eur. Math. Soc.*

[10] MURATOV, C. B., AND NOVAGA, M. On well-posedness of variational models of charged drops. *Proc. R. Soc. Lond. Ser. A 472*, 2187 (2016).

[11] MURATOV, C. B., NOVAGA, M., AND RUFFINI, B. On equilibrium shape of charged flat drops. *Comm. Pure Appl. Math. 71*, 6 (2018), 1049–1073.

[12] RAYLEIGH, L. On the equilibrium of liquid conducting masses charged with electricity. *Phil. Mag. 14* (1882), 184–186.

[13] TAYLOR, G. Disintegration of water drops in an electric field. *Proc. Roy. Soc. Lond. A 280* (1964), 383–397.

[14] ZELENY, J. Instability of elecrtrified liquid surfaces. *Phys. Rev. 10* (1917), 1–6.

A diffuse-interface model for two-phase flows with moving contact lines, variable contact angles and bulk-surface interaction

PATRIK KNOPF

(joint work with Andrea Giorgini)

The description of two-phase flows is an important but very challenging topic of modern continuum fluid dynamics with various applications in biology, chemistry and engineering. To represent the interface separating the different components, two fundamental approaches have been developed, namely *sharp-interface methods* and *diffuse-interface methods* (see, e.g., [1] and the references therein).

In sharp-interface models, the interface is represented as an evolving hypersurface contained in the surrounding domain. The time evolution of the interface is the described by a free boundary problem.

In diffuse-interface models (also referred to as phase-field models), the interface is approximated by a thin layer whose thickness is proportional to a small parameter $\varepsilon > 0$. The concentrations (or volume fractions) are represented by

an order parameter, the so-called phase-field, which attains the values -1 and 1, respectively, in the regions where the single fluids are present. This phase-field is expected to exhibit a continuous transition between -1 and 1 at the diffuse-interface separating the fluids. The main advantage of this approach is that the time evolution of the phase-field can be described via an Eulerian formulation as a PDE on the whole domain. This avoids an explicit description of the interface as in free boundary problems. If a proper scaling with respect to the interface parameter ε is used, the corresponding sharp-interface model can be recovered (in most cases at least formally) as the *sharp-interface limit* (see, e.g., [1]).

The "Abels–Garcke–Grün model". A very popular thermodynamically consistent diffuse-interface model for viscous incompressible two-phase flows with possibly *unmatched* densities is the *Abels–Garcke–Grün model* (or *AGG model*), which was derived in [2]. The system of equations reads as follows:

$$(1a) \qquad \partial_t\big(\rho(\phi)\boldsymbol{v}\big) + \operatorname{div}\big(\boldsymbol{v}\otimes(\rho(\phi)\boldsymbol{v}+\mathbf{J})\big) - \operatorname{div}\big(2\nu(\phi)\,\mathbf{D}\boldsymbol{v}\big) + \nabla p$$
$$= -\varepsilon\operatorname{div}\big(\nabla\phi\otimes\nabla\phi\big) \qquad\qquad \text{in } Q,$$

$$(1b) \qquad \operatorname{div}\boldsymbol{v} = 0 \qquad\qquad\qquad\qquad\qquad\qquad\qquad\qquad \text{in } Q,$$

$$(1c) \qquad \rho(\phi) = \tilde{\rho}_1\frac{1+\phi}{2} + \tilde{\rho}_2\frac{1-\phi}{2}, \quad \mathbf{J} = -\tfrac{1}{2}(\tilde{\rho}_2-\tilde{\rho}_1)m_\Omega(\phi)\nabla\mu \quad \text{in } Q,$$

$$(1d) \qquad \partial_t\phi + \operatorname{div}(\phi\boldsymbol{v}) = \operatorname{div}\big(m_\Omega(\phi)\nabla\mu\big) \qquad\qquad\qquad \text{in } Q,$$

$$(1e) \qquad \mu = -\varepsilon\Delta\phi + \varepsilon^{-1}F'(\phi) \qquad\qquad\qquad\qquad\qquad \text{in } Q.$$

Here, $\Omega\subset\mathbb{R}^d$ with $d=2,3$ is a bounded Lipschitz domain with boundary Γ, $T>0$ is a given final time, and $Q := \Omega\times(0,T)$. Moreover, $\boldsymbol{v}$ is the velocity field associated with the mixture, p denotes the pressure, ϕ is the phase-field (representing the difference of the fluid concentrations), and μ represents the chemical potential. Moreover, ν is the concentration depending viscosity, $\mathbf{D}$ is the symmetric gradient operator, ε is a positive parameter related to the thickness of the diffuse interface, m_Ω is the (bulk) mobility function and F is a double-well potential. The concentration depending density $\rho(\phi)$, where $\tilde{\rho}_1$ and $\tilde{\rho}_2$ are the constant individual densities of the two fluids, requires the inclusion of an additional mass flux term $\mathbf{J}$ in the Navier–Stokes equation to make the model thermodynamically consistent. The AGG model is usually supplemented with the classical boundary conditions

$$(2) \qquad\qquad\qquad \boldsymbol{v} = \mathbf{0}, \quad \partial_\mathbf{n}\phi = 0, \quad \partial_\mathbf{n}\mu = 0 \quad \text{on } \Sigma.$$

Here, $\Sigma := \Gamma\times(0,T)$ and $\mathbf{n}$ denotes the outward unit normal vector field on the boundary Γ.

Limitations of the AGG model with classical boundary conditions. Even though the AGG model ((1),(2)) is already very sophisticated and capable of describing the challenging case where the two fluids have unmatched specific densities, the classical boundary conditions (2) still entail some important limitations.

- (L1) The boundary condition $(2)_2$ enforces the diffuse interface separating the two fluids to always intersect the boundary Γ at a perfect right angle. Certainly, this will not always be satisfied in concrete applications, where the

contact angle of the interface might not only deviate from ninety degrees but even change dynamically over the course of time.

(L2) As shown, for instance, in [5], the boundary condition $(2)_1$ is not very suitable for the description of moving contact line phenomena since the motion of the fluid at the boundary is totally neglected.

(L3) The conditions $(2)_1$ and $(2)_3$ ensure mass conservation in the bulk, meaning that $\int_\Omega \phi(t)\,\mathrm{d}x$ is constant in time. Therefore, no transfer of material between bulk and surface (e.g., absorption processes) can be described.

A variant of the AGG model with dynamic boundary conditions. In order to overcome the aforementioned limitations (L1)–(L3), we derived and investigated a new class of thermodynamically consistent Navier–Stokes–Cahn–Hilliard systems with dynamic boundary conditions in the recent paper [3]. Similar to [2], our model derivation is based on local mass balance laws, both in the bulk and on the surface, with a priori unknown mass fluxes. We also consider local energy dissipation laws involving additional energy flux terms. Eventually, we employ the Lagrange multiplier approach (where the chemical potentials μ and θ act as the Lagrange multipliers) to complete our model derivation by identifying the mass and energy fluxes. The resulting system of equations reads as:

$$
\text{(3a)} \quad \partial_t\big(\rho(\phi)\boldsymbol{v}\big) + \mathrm{div}\big(\boldsymbol{v}\otimes(\rho(\phi)\boldsymbol{v}+\mathbf{J})\big) - \mathrm{div}\big(2\nu(\phi)\,\mathbf{D}\boldsymbol{v}\big) + \nabla p
$$
$$
= -\varepsilon\,\mathrm{div}\big(\nabla\phi\otimes\nabla\phi\big) \qquad\qquad \text{in } Q,
$$

$$
\text{(3b)} \quad \mathrm{div}\,\boldsymbol{v} = 0, \qquad\qquad\qquad \text{in } Q,
$$

$$
\text{(3c)} \quad \rho(\phi) = \tilde{\rho}_1\frac{1+\phi}{2} + \tilde{\rho}_2\frac{1-\phi}{2}, \quad \mathbf{J} = -\tfrac{1}{2}(\tilde{\rho}_2-\tilde{\rho}_1)m_\Omega(\phi)\nabla\mu \qquad \text{in } Q,
$$

$$
\text{(3d)} \quad \partial_t\phi + \mathrm{div}(\phi\boldsymbol{v}) = \mathrm{div}\big(m_\Omega(\phi)\nabla\mu\big) \qquad\qquad \text{in } Q,
$$

$$
\text{(3e)} \quad \mu = -\varepsilon\Delta\phi + \varepsilon^{-1}F'(\phi) \qquad\qquad\qquad \text{in } Q,
$$

$$
\text{(3f)} \quad \partial_t\psi + \mathrm{div}_\Gamma(\psi\boldsymbol{v}_\tau) = \mathrm{div}_\Gamma\big(m_\Gamma(\psi)\nabla_\Gamma\theta\big) - \beta m_\Omega(\psi)\,\partial_\mathbf{n}\mu \qquad \text{on } \Sigma,
$$

$$
\text{(3g)} \quad \theta = -\delta\kappa\Delta_\Gamma\psi + \delta^{-1}G'(\psi) + \varepsilon\partial_\mathbf{n}\phi \qquad\qquad \text{on } \Sigma,
$$

$$
\text{(3h)} \quad \phi|_\Gamma = \psi, \quad
\begin{cases}
Lm_\Omega(\psi)\,\partial_\mathbf{n}\mu = \beta\theta - \mu & \text{if } L\in[0,\infty), \\
m_\Omega(\psi)\,\partial_\mathbf{n}\mu = 0 & \text{if } L = \infty
\end{cases} \qquad \text{on } \Sigma,
$$

$$
\text{(3i)} \quad \boldsymbol{v}\cdot\mathbf{n} = 0, \quad \big[2\nu(\psi)(\mathbf{D}\boldsymbol{v}\cdot\mathbf{n}) + \gamma(\psi)\boldsymbol{v}\big]_\tau = \big[-\psi\nabla_\Gamma\theta + \tfrac{1}{2}\,(\mathbf{J}\cdot\mathbf{n})\,\boldsymbol{v}\big]_\tau \quad \text{on } \Sigma,
$$

$$
\text{(3j)} \quad \boldsymbol{v}|_{t=0} = \boldsymbol{v}_0, \quad \phi|_{t=0} = \phi_0 \qquad\qquad\qquad \text{in } \Omega,
$$

$$
\text{(3k)} \quad \psi|_{t=0} = \psi_0 \qquad\qquad\qquad\qquad \text{on } \Gamma.
$$

In addition to the quantities introduced in (1), ψ is a surface phase-field, θ is a surface chemical potential, and G is a double-well potential. The nonnegative function m_Γ represents the mobility on the boundary. The parameter $\delta > 0$ is related to the thickness of the diffuse interface on the boundary, and the constant $\kappa \geq 0$ acts as a weight for smoothing effects on the surface. We further prescribe the constants $\beta \in \mathbb{R}$ and $L \in [0,\infty]$. Moreover, the subscript τ indicates the tangential component of a vector field on Γ.

As it was shown in [4], the underlying Cahn–Hilliard subsystem with dynamic boundary conditions (3d)–(3h) is capable of overcoming the limitations (L1) and (L3). Moreover, as discussed in [5], the Navier-slip boundary condition $(3i)_2$ provides a better description of the convection-induced motion of the contact line. Therefore, it helps to overcome limitation (L2).

First analytic results in the case of matched densities. In [3], we also presented some first analytical results. There, we restricted ourselves to consider the case of matched densities (i.e., $\rho(\phi) \equiv \tilde\rho_1 = \tilde\rho_2$) as well as regular potentials F and G. Concerning the coupling condition for the chemical potentials, we investigated the case $L = 0$ with $\beta > 0$. In this setting, we proved the existence of global weak solutions in two and three dimensions as well as the uniqueness of the weak solution in two dimensions.

REFERENCES

[1] H. Abels and H. Garcke, *Weak solutions and diffuse interface models for incompressible two-phase flows*, Handbook of mathematical analysis in mechanics of viscous fluids, Springer, Cham (2018), 1267–1327.

[2] H. Abels, H. Garcke and G. Grün, *Thermodynamically consistent, frame indifferent diffuse interface models for incompressible two-phase flows with different densities*, Math. Models Methods Appl. Sci. **22** (2012), no.3, 1150013, 40 pp.

[3] A. Giorgini and P. Knopf, *Two-phase flows with bulk-surface interaction: thermodynamically consistent Navier-Stokes-Cahn-Hilliard models with dynamic boundary conditions*, J. Math. Fluid Mech. **25** (2023), no.3, Paper No. 65, 44 pp.

[4] P. Knopf, K. F. Lam, C. Liu and S. Metzger, *Phase-field dynamics with transfer of materials: the Cahn-Hilliard equation with reaction rate dependent dynamic boundary conditions*, ESAIM Math. Model. Numer. Anal. **55** (2021), no.1, 229–282.

[5] T. Qian, X.-P. Wang, and P. Sheng, *A variational approach to moving contact line hydrodynamics*, J. Fluid Mech. **564** (2006), 333–360.

Multilevel Representations of Isotropic Gaussian Random Fields on the Sphere

ANA DJURDJEVAC

(joint work with Markus Bachmayr)

Representation of random fields on hypersurfaces is important in many applications such as (cell) biology, climatology and astrophysics. Furthermore, if we are considering a partial differential equation with random coefficient on a hypersurface, one of the main questions is how to represent those random fields. For example, let Γ be a hypersurface and $(\Omega, \mathcal{F}, \mathbb{P})$ a probability space and we are considering the diffusion problem

$$(1) \qquad\qquad -\nabla_\Gamma \cdot (a(\omega)\nabla_\Gamma q) = f$$

where a is a random field. Two standard choices for the field a are: uniformly bounded or log-normal random field. In this report we are interested in the case when $a = \exp(u)$, where u is an isotropic Gaussian random field on a sphere $\Gamma = \mathbb{S}^2$.

One of the main questions is how to approximate the solution mapping. For that purpose, we are interested in the representations of the Gaussian random field u of the form

$$(2) \qquad u(\omega, s) = \sum_{i=1}^{\infty} z_i(\omega) \varphi_i(s), \quad s \in \mathbb{S}^2.$$

The standard representation of that form is the so-called Karhunen-Loève (KL) expansion, where in this case $(z_i)_{i \in \mathbb{N}}$ is a sequence of independent scalar Gaussian random variables and functions $\varphi_i \in L_2(\mathbb{S}^2)$ are determined as eigenfunctions of the covariance operator of u. Since we are considering the random field on a sphere, the expansion is in terms of spherical harmonics $Y_{\ell m}$, $\ell \geq 0$, $m = -\ell, \ldots, \ell$, which are eigenfunctions of the Laplace-Beltrami operator on $\mathbb{S}^2$ and $z_{\ell m} \sim \mathcal{N}(0, A_\ell)$, where the positive real sequence $\mathsf{A} = (A_\ell)_{\ell \in \mathbb{N}_0}$ is called the *power spectrum* of u. Hence the expansion has the form

$$(3) \qquad u = \sum_{\ell=0}^{\infty} \sum_{m=-\infty}^{\infty} z_{\ell m} Y_{\ell m}.$$

For more details, see for example [6].

While this expansion yields the most rapid convergence in L_2-norm, the functions φ_i typically exhibit global oscillations. This has the direct consequence of the error of the best n-term Hermite approximation of the solution q of (1). The reason is that the error directly depends on the summability properties of coefficients φ_i from the expansion of the coefficient (2), see for example [2]. Hence, motivated by the work in [2], our main goal (presented in [4]) is to construct a series expansions of isotropic Gaussian random fields on $\mathbb{S}^2$ with independent Gaussian coefficients and localised basis functions. Such representations with multilevel localized structure provide an alternative to the standard Karhunen-Loève expansion.

We are exploring an alternative expansion that is based on spherical needlets [8]. These are functions ψ_{jk} with a scale parameter $j \in \mathbb{N}_0$ and an angular index $k \in \{1, \ldots, n_j\}$, which have localisation properties of the following type: for each ψ_{jk} there exists a point $\xi_{jk} \in \mathbb{S}^2$ such that

$$(4) \qquad |\psi_{jk}(s)| \leq \frac{C 2^j}{1 + \left(2^j d(s, \xi_{jk})\right)^r}, \quad s \in \mathbb{S}^2,$$

for some $r \in \mathbb{N}$ with $C = C(r) > 0$ and with the geodesic distance

$$(5) \qquad d(s, s') = \arccos(s \cdot s')$$

on $\mathbb{S}^2$. Hence, ψ_{jk} is concentrated near ξ_{jk} and decays rapidly with increasing angular distance to this point. One can show (see [8]) that the points ξ_{jk} can be chosen in a such a way that the family $\{\psi_{jk} \colon j \in \mathbb{N}_0, k = 1, \ldots, n_j\}$ is a *Parseval frame* of $L_2(\mathbb{S}^2)$, meaning that

$$\|f\|_{L_2(\mathbb{S}^2)}^2 = \sum_{j,k} |\langle f, \psi_{jk} \rangle|^2 \quad \text{and} \quad f = \sum_{j,k} \langle f, \psi_{jk} \rangle_{L_2(\mathbb{S}^2)} \psi_{jk},$$

for any $f \in L_2(\mathbb{S}^2)$. If we were to directly use spherical harmonics in the expansion of the isotropic Gaussian field u, the problem would be that even though we have the localized spatial functions, we lose the independence of the coefficients. Namely, in [1], it was shown that the needlet coefficients $\langle u, \psi_{jk} \rangle_{L_2(\mathbb{S}^2)}$ of a weakly isotropic Gaussian random field u on $\mathbb{S}^2$, are just *asymptotically uncorrelated*. We show that there exist modified needlets ψ_{jk}^{A} such that one has the expansion

$$
(6) \qquad\qquad u = \sum_{j=0}^{\infty} \sum_{k=1}^{n_j} y_{jk} \psi_{jk}^{\mathsf{A}}
$$

in terms of independent scalar Gaussian random variables $y_{jk} \sim \mathcal{N}(0,1)$ and the modified needlets ψ_{jk}^{A} still have the same localisation property (4) as the standard needlets ψ_{jk}, but with r limited by certain features of the power spectrum of u.

In order to construct such modified needlets, we apply the result from [7] that states that one obtains such an expansion exactly when the family $\{\psi_{jk}^{\mathsf{A}}\}$ is a Parseval frame of the reproducing kernel Hilbert space $\mathcal{H}$. For that purpose, we consider the factorization of the covariance operator $T\colon C(\mathbb{S}^2)' \to C(\mathbb{S}^2)$, because if one has the factorization of the form $T = SS'$ and if $\{\varphi_i\}_{i \in \mathbb{N}}$ is a Parseval frame of the domain of S, then $\{S\varphi_i\}_{i \in \mathbb{N}}$ is a Parseval frame of the reproducing kernel Hilbert space of u, for more details see [7, Prop. 1]. Hence, we choose

$$
(7) \qquad\qquad Sf := \sum_{\ell=0}^{\infty} \sqrt{A_\ell} \sum_{m=-\ell}^{\ell} \left(\int_{\mathbb{S}^2} Y_{\ell m} f \, \mathrm{d}\sigma \right) Y_{\ell m} \,.
$$

For a given power spectrum A, we now define modified needlets by

$$
(8) \quad \psi_{jk}^{\mathsf{A}}(s) := \sqrt{\lambda_{jk}} K_j^{\mathsf{A}}(s \cdot \xi_{jk}), \quad K_j^{\mathsf{A}}(s \cdot \xi_{jk}) := \sum_{\ell=0}^{\infty} b_j(\ell) \sqrt{A_\ell} \frac{2\ell+1}{4\pi} P_\ell(s \cdot \xi_{jk}).
$$

It is now straightforward to verify that (6) holds for these functions.

Furthermore, we show that under appropriate conditions on forward differences of $\sqrt{A_\ell}$ the localisation properties of the form (4) of the standard needlets ψ_{jk} are preserved in the modified needlets ψ_{jk}^{A}.

Next we revisit the equation (1), and now for the expansion of the log-normal coefficient $a = \exp(u)$ we use the modified needlet expansion of the form (6). As already mentioned at the beginning, integrability and approximation of the random solution q depends on the summability properties of ψ_{jk}^{A}. We show that the best n-term product Hermite polynomial approximations q_n converge in L_2 as $\mathcal{O}(n^{-s})$ for any s up to $\beta/2$, where under certain assumptions, β is precisely the limiting order of Hölder regularity of the random field u (and hence of a). Note that here we rely crucially on the localisation of the random field expansion, and no such convergence result is available for KL expansions in spherical harmonics.

<div align="center">REFERENCES</div>

[1] P. Baldi, G. Kerkyacharian, D. Marinucci, and D. Picard, *Asymptotics for spherical needlets*, The Annals of Statistics **37** (2009), no. 3, 1150–1171.

[2] M. Bachmayr, A. Cohen, and G. Migliorati, *Representations of Gaussian random fields and approximation of elliptic PDEs with lognormal coefficients*, J. Fourier Anal. Appl. **24** (2018), no. 3, 621–649.

[3] M. Bachmayr, A. Cohen, R. DeVore, and G. Migliorati, *Sparse polynomial approximation of parametric elliptic PDEs. Part II: lognormal coefficients*, ESAIM: Mathematical Modelling and Numerical Analysis **51** (2017), no. 1, 341–363.

[4] M. Bachmayr, A. Djurdjevac, *Multilevel representations of isotropic Gaussian random fields on the sphere*, IMA Journal of Numerical Analysis, **43** (2023), no. 4, 1970–2000.

[5] L. Herrmann, A. Lang, and C. Schwab, *Numerical analysis of lognormal diffusions on the sphere*, Stoch. Partial Differ. Equ., Anal. Comput. **6** (2018), no. 1, 1–44 (English).

[6] A. Lang and C. Schwab, *Isotropic Gaussian random fields on the sphere: regularity, fast simulation and stochastic partial differential equations*, Ann. Appl. Probab. **25** (2015), no. 6, 3047–3094.

[7] H. Luschgy and G. Pagès, *Expansions for Gaussian processes and Parseval frames*, Electronic Journal of Probability **14** (2009), 1198–1221.

[8] F. J. Narcowich, P. Petrushev, and J. D. Ward, *Localized tight frames on spheres*, SIAM J. Math. Anal. **38** (2006), no. 2, 574–594.

Coarsening in the network flow

Alessandra Pluda

Solids have a crystalline structure, and a piece of metal is actually (much) more complicated than a unique crystal. Most of the technological materials are poly-crystalline: they are composed of several pieces (grains) in which the crystal lattice is rotated in different ways, delimited by grain boundaries. Grain boundaries have a profound impact on materials properties (for instance electrical and thermal conductivity) and therefore their performance. The challenge in polycrystals is then the development of process technology, in other words the way we make materials, that will allow us to arrange grains in a way that gives us the property we desire, these properties can be said strength, toughness, electrical resistivity.

One way that the grain structure is tailored or engineered is through grain growth. To model grain growth is an old problem and it attracted the attention of applied scientists and then mathematicians. Already in 1956, Mullins considered the 2-dimensional version in thin films and observed that the grain boundaries of a recrystallized metal, when annealed, move with a velocity proportional to the curvature [10]. Thus, in a first approximation, the grain boundary and the grain growth can be described as a finite union of curves that meet at junctions (a network) that moves by curvature (the normal velocity of each curvature at each point and time is its curvature). The system evolves so as to reduce the energy, hence we consider the L^2-gradient flow of the length functional and we expect to see networks with only triple junctions at almost all times. The equilibrium state should actually be a single crystal and one of the defining features of evolution is that the network undergoes changes in topology.

It is fair to say that in the last years there have been progresses concerning both in situ–experiments, simulations and mathematical models [1, 4, 5, 7]. Unfortunately at the moment experiments cannot give us precise information about the

dynamics of the motion of grain boundaries, thus we still have to relies on good models and simulations.

The first attempt to study the network flow from a mathematical point of view has been by Brakke [2], who developed a geometric-measure-theoretic method to define the evolution. While his definition is very powerful and useful in its own way (it provides global existence), it does not give a very detailed picture of the evolution itself, hence the need of a definition based on classical PDE solutions. My final goal is the study of evolution by curvature of cluster of surfaces as a simplified model of grain growth. Concerning the 2-dimensional version, I aim to a complete analysis of the network flow in a PDE framework, from well–posedness, to the study of long–time behaviour and asymptotic analysis as time goes to infinity [9, 12].

A precise analysis of singularities in some special cases can be used as a benchmark on the reliability of simulations. On the other hand, simulations can be an inspiration for the theoretical study of the flow.

In numerical simulations we see that the networks completely rearrange itself any time we have a topological discontinuity and larger grains "eat" smaller ones. The most prominent features that eyes pick up is the increasing average size of (surviving) grains [3, 6].

Between the period of critical events we know exactly how the area of a grain grows with time: the grains follow the so-called Von Neumann rule. Consider indeed a grain bounded by a loop ℓ composed of m curves. By Gauss–Bonnet we have

$$\partial_t A = \int_\ell k \, \mathrm{d}s = \left(\frac{m}{3} - 2\right)\pi \,,$$

hence the area of grains bounded by more than six curves grows linearly, by less than six curves decreases linearly and the area of hexagonal cells remains constant. Moreover, by Hölder inequality

$$\left|2 - \frac{m}{3}\right|\pi \le \int_\ell |k| \le \left(\int_\ell \kappa^2\right)^{\frac{1}{2}} \sqrt{\mathrm{L}(\ell)} \,,$$

that is

$$\int_\ell \kappa^2 \, \mathrm{d}s \ge \frac{C}{\mathrm{L}(\ell)} \,,$$

with C that is different from zero for non–hexagonal cells. If we suppose that all grains are very similar to each other and the percentage of non–hexagonal grains is sufficiently high during evolution, we can actually formally prove that the average area of the (surviving) grains grows linearly. Consider an initial network composed of N^2 grains in the flat torus and let it evolve by the network flow. We pass from the above estimate on a single grain to the estimate on the entire network simply by multiplying by the number of grains and keeping in mind that the average length of a single loop is of order $1/N$:

$$\int_{\mathcal{N}} k^2 \, \mathrm{d}s \gtrsim N\sharp\,(\text{non–hexagonal grains}) = N^3 \,.$$

The evolution law of the the total length of the network reads

$$\frac{d}{dt}L(\mathcal{N}) = -\int_{\mathcal{N}} k^2 \, \mathrm{d}s \,.$$

Now we use the fact that the length of the network is of order N and we put together the last two formula, getting the differential inequality:

$$\frac{d}{dt}N(t) \lesssim -N^3(t) \,,$$

Thus the average area (that is of order $1/N^2$) grows at least linearly in time

$$\frac{1}{N(t)^2} \geq 2Ct \,.$$
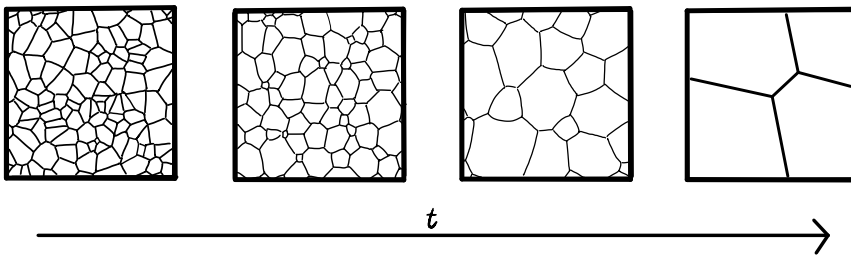
FIGURE 1. Expected evolution of a complicated network

It is not difficult to show another property of the flow that indicates that the structure/topology of the networks should be simplified during the evolution. When the flow develops a multiple junction where at most five curves, then the multiple junction will be split in triple junctions and locally all the flowouts will be without loops. Hence, by an easy computation involving the Euler characteristic, one shows that the total number of curves decreases at least by three and the total number of triple junctions decreases at least by two.

To conclude, in my talk I also showed a quantitative estimate of the size of the basin of local minimality of regular networks with straight segments. The estimate, obtained by local calibrations [11], indicates that the volume of the basin of attraction of all the many critical points of the length functional is expected to be small in the space of networks hence it is unlikely that the flow gets stuck in a configuration composed of lots of hexagonal grains.

REFERENCES

[1] P. Bardsley, K. Barmak, E. Eggeling, Y. Epshteyn, D. Kinderlehrer, and S. Ta'asan, *Towards a gradient flow for microstructure*, Atti Accad. Naz. Lincei Rend. Lincei Mat. Appl., 28 no.4 (2017) 777–805.

[2] K. A. Brakke, *"The Motion of a Surface by its Mean Curvature"*, Princeton University Press, Princeton, NJ , 1978.

[3] K. A. Brakke, `https://facstaff.susqu.edu/brakke/`, personal web page.

[4] Y. Epshteyn, C. Liu, M. Mizuno, *Motion of grain boundaries with dynamic lattice misorientations and with triple junctions drag*, SIAM J. Math. Anal. 53 no.3 (2021) 3072–3097.

[5] Y. Epshteyn, C. Liu, M. Mizuno, *Large time asymptotic behavior of grain boundaries motion with dynamic lattice misorientations and with triple junctions drag*, Commun. Math. Sci. 19 no.5 (2021) 1403–1428.

[6] S. Esedoglu, `http://www.math.lsa.umich.edu/~esedoglu/research.html`, personal web page.

[7] T. Kagaya, M. Mizuno, and K. Takasao, *Long time behavior for a curvature flow of networks related to grain bundary motion with the effect of lattice misoriantations*, 2021, arXiv:2112.11069.

[8] C. Mantegazza, M. Novaga, and A. Pluda, *Type–0 singularities in the network flow – Evolution of trees*, J. Reine Angew. Math., 2022, no.792 (2022), 189-221

[9] C. Mantegazza, M. Novaga, A. Pluda, and F. Schulze, *Evolution of network with multiple junctions*, to appear Astérisque, preprint ArXiv:1611.08254.

[10] W. M. Mullins, *Two–dimensional motion of idealized grain boundaries*, J. Appl. Phys., 27 (1956) 900–904.

[11] A. Pluda and M. Pozzetta, *Minimizing properties of networks via global and local calibrations*, Bull. Lond. Math. Soc., 55 no. 6 (2023) 3029–3052.

[12] A. Pluda, Y. Tonegawa, *Coarsening phenomena in the network flow*, arXiv preprint 2024.

A (tangential) Navier–Stokes–Cahn–Hilliard system on an evolving surface

Thomas Sales

(joint work with Charles M. Elliott)

This talk was concerned with a system of partial differential equations on an evolving surface which can be understood as an evolving surface analogue of the "Model H" of Hohenberg and Halperin [4]. Two derivations were outlined. The first of these was by using rational mechanics/thermodynamics arguments (in the style of [3]) for which one obtains the system

$$(1) \qquad \rho \partial^{\bullet} \mathbf{u} = -\nabla_\Gamma p + pH\boldsymbol{\nu} + \nabla_\Gamma \cdot (2\eta(\varphi)\mathbb{E}(\mathbf{u})) - \varepsilon \nabla_\Gamma \cdot (\nabla_\Gamma \varphi \otimes \nabla_\Gamma \varphi),$$

$$(2) \qquad \nabla_\Gamma \cdot \mathbf{u} = 0,$$

$$(3) \qquad \partial^{\bullet} \varphi = \nabla_\Gamma \cdot (M(\varphi)\nabla_\Gamma \mu),$$

$$(4) \qquad \mu = -\varepsilon \Delta_\Gamma \varphi + \frac{1}{\varepsilon} F'(\varphi),$$

posed on $\Gamma(t)$.

Here the motion of $\Gamma(t)$ is determined by the velocity $\mathbf{u}$ which is split into a tangential and normal component, the latter of which induces the geometric evolution of $\Gamma(t)$. The notation above can be split into various categories as follows.

(1) Fluidic quantities: ρ is the constant density of the fluid. $\mathbf{u}$ is the fluid velocity. p is the pressure induced by the fluid. $\eta(\cdot)$ is the viscosity, which varies with the phase field variables.

(2) Geometric quantities: H is the mean curvature of $\Gamma(t)$ and $\boldsymbol{\nu}$ is the outer unit normal to $\Gamma(t)$.

(3) Phase field quantities: φ is the difference of the concentrations of the two fluidic components. μ is the chemical potential. $M(\cdot)$ is the mobility function. ε is the interface width associated with the diffuse interface approximation.

(4) Differential operators: $\partial^\bullet$ is the material derivative following the flow $\mathbf{u}$. ∇_Γ is the surface gradient/covariant derivative. $\mathbb{E}(\cdot) = \frac{1}{2}\left(\nabla_\Gamma(\cdot) + \nabla_\Gamma(\cdot)^T\right)$ is the rate of strain operator.

The second derivation is via a thin film limit (in the style of [5]) where one prescribes the normal evolution of $\Gamma(t)$. The resulting equations are the same as (1)-(4) up to a term in the normal direction. This discrepancy can be seen as a Lagrange multiplier enforcing the prescribed normal evolution of $\Gamma(t)$.

When one considers the full problem (1)-(4) one has to solve the equations on a domain which is also to be found. Our simplifying assumption, as in [6], is to consider the normal evolution as being prescribed so that one obtains a purely tangential system of equations

$$
(5) \qquad \rho\left(\mathbb{P}\partial^\circ\mathbf{u}_T + (\nabla_\Gamma\mathbf{u}_T)\mathbf{u}_T + V_N\mathbb{H}\mathbf{u}_T - \frac{1}{2}\nabla_\Gamma V_N^2\right),
$$
$$
= -\nabla_\Gamma\tilde{p} + \mathbb{P}\nabla_\Gamma\cdot(2\eta(\varphi)\mathbb{E}(\mathbf{u}_T)) + \mu\nabla_\Gamma\varphi
$$

$$
(6) \qquad \nabla_\Gamma\cdot\mathbf{u}_T = -HV_N,
$$

$$
(7) \qquad \partial^\circ\varphi + \nabla_\Gamma\varphi\cdot\mathbf{u}_T = \nabla_\Gamma\cdot(M(\varphi)\nabla_\Gamma\mu),
$$

$$
(8) \qquad \mu = -\varepsilon\Delta_\Gamma\varphi + \frac{1}{\varepsilon}F'(\varphi).
$$

Where here ∂° is the normal time derivative (i.e. following the flow of only the normal component of the velocity), $\mathbb{P}$ is the projection onto the tangent space of $\Gamma(t)$, V_N is the prescribed normal velocity, and $\mathbb{H}$ is the Weingarten map. We similarly have a new pressure, $\tilde{p}$, which functionally plays the same role p above. Moreover, the prescribed evolution is assumed to be such that

$$
|\Gamma(t)| = |\Gamma(0)|.
$$

The main results of the associated preprint [2] are on the well-posedness of the system (5)-(8) for a constant mobility $M(\cdot) \equiv 1$. In particular we establish the existence and uniqueness for suitable weak solutions (using the framework of [1]) for regular potentials, for example the quartic double well potential

$$
F(r) = \frac{(1-r^2)^2}{4},
$$

and the singular logarithmic potential

$$
F(r) = \frac{\theta}{2}\left((1+r)\log(1+r) - (1-r)\log(1-r)\right) + \frac{1-r^2}{2},
$$

for some constant $\theta \in (0,1)$. The latter case naturally has some constraints on the choice of initial data for φ.

REFERENCES

[1] A. Alphonse, C. M. Elliott, and B. Stinner, *An abstract framework for parabolic PDEs on evolving spaces.* Portugaliae Mathematica **72**(1) (2015), 1–46.
[2] C. M. Elliott, and T. Sales, *Navier-Stokes-Cahn-Hilliard equations on evolving surfaces.* arXiv preprint arXiv:2401.12044 (2024).
[3] M. E. Gurtin, D. Polignone, and J. Viñals, *Two-phase binary fluids and immiscible fluids described by an order parameter.* Mathematical Models and Methods in Applied Sciences **6**(6) (1996), 815–831.
[4] P. C. Hohenberg, and B. I. Halperin, *Theory of dynamic critical phenomena*, Reviews of Modern Physics **49**(3) (1977), 435–479.
[5] T. H. Miura, *On singular limit equations for incompressible fluids in moving thin domains.* Quarterly of Applied Mathematics **76**(2) (2018), 215–251.
[6] M. A. Olshanskii, A. Reusken, and A. Zhiliakov, *Tangential Navier–Stokes equations on evolving surfaces: Analysis and simulations.* Mathematical Models and Methods in Applied Sciences **32**(14) (2022), 2817–2852.

Stability of multiphase mean curvature flow beyond a circular topology change

ALICE MARVEGGIO

(joint work with Julian Fischer, Sebastian Hensel, and Maximilian Moser)

The evolution of a network of interfaces by mean curvature flow features the occurrence of topology changes and geometric singularities. Therefore, existence and uniqueness results for classical strong solutions are in general limited to a finite time horizon. On the other side, the evolution beyond topology changes can be described only in the framework of weak solution concepts, whose uniqueness may fail (e.g., Brakke solutions).

In a recent work [1], Fischer, Hensel, Laux and Simon have established a weak-strong uniqueness principle for weak BV solutions to planar multiphase mean curvature flow: *As long as a unique strong solution exists, any energy dissipating weak BV solution with the same initial data must coincide with it.* In particular, their result follows from a stability estimate, which is formulated in terms of an error functional (measuring the error between a strong and a weak solution) and holds *prior to the first topology change* of the strong solution. Our aim is to extend the stability result of [1] *beyond* the formation of *a circular topology change*.

The stability result in [1] holds for weak BV solution concepts, more precisely for BV solutions in the sense of Laux and Otto [5] and for the varifold-BV solution concept recently introduced by Stuvard and Tonegawa [7]. Denoting the strong solution by the partition $\Omega^s = (\Omega_1^s, ..., \Omega_P^s)$ of $\mathbb{R}^2$ on the time interval $[0, T_{ext})$ and the weak BV solution by the partition $\Omega^w = (\Omega_1^w, ..., \Omega_P^w)$ of $\mathbb{R}^2$ on $[0, \infty)$, the study of the time evolution of a suitable error functional $E[\Omega^w | \Omega^s]$ yields (by means of a Gronwall type argument) a weak-strong stability estimate holding prior to the first topology change of the strong solution. The estimate does not guarantee stability past topology changes as the time-dependent constant $C(t)$ in
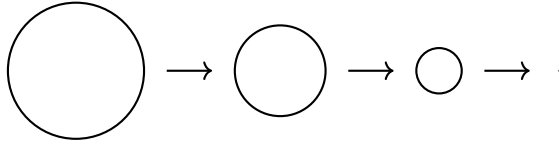
FIGURE 1. Evolution of a circle by mean curvature flow, i.e., $r'(t) = -\frac{1}{r(t)}$ for any $t \in (0, T_{ext})$, $r(0) = r_0$ and $T_{ext} = \frac{1}{2}r_0^2$.

the Gronwall inequality of [1]

$$\frac{\mathrm{d}}{\mathrm{d}t} E[\Omega^w | \Omega^s](t) \leq C(t) E[\Omega^w | \Omega^s](t) \quad \text{for any } t \in [0, T_{ext}) \tag{1}$$

is given by $C(t) \sim (T_{ext} - t)^{-1}$. Since $C(t)$ is borderline non-integrable, this requires the study of the stability of the leading-order contributions in (1) at the singularity $t = T_{ext}$.

We aim to extend the weak-strong stability estimate following from (1) beyond the formation of the simplest topology change [6], i.e., a circular one of length scale $r(t)$. More precisely, in our statement, a two-phase strong solution is given by some smooth, bounded, open and simply connected initial set $\Omega_1^s(0) \subset \mathbb{R}^2$ with boundary $\partial\Omega_1^s(0)$ evolving in time into $\partial\Omega_1^s(t)$ by mean curvature flow. Hence, by the works of Gage and Hamilton [3] and of Grayson [4], $\partial\Omega_1^s(t)$ becomes circular in the process, in the sense that $\partial\Omega_1^s(t)$ gets asymptotically close to a circle of radius $r(t) := \sqrt{2(T_{ext} - t)}$, and it shrinks to a point at the extinction time $T_{ext} = \frac{\text{vol}(\Omega_1^s(0))}{\pi}$ (cf. Figure (1) for the evolution of an exact circle). On the other side, our result applies to *multiphase* weak BV solutions, which may additionally feature other types of topology changes and singularities.

Our result on the stability for weak BV solutions to planar multiphase mean curvature flow beyond a circular topology change reads as follows.

Theorem. *Let $P \geq 2$. Consider a weak BV solution $\Omega^w = (\Omega_1^w, ..., \Omega_P^w)$ on $[0, \infty)$ and a two-phase strong solution $\Omega^s = (\Omega_1^s, \mathbb{R}^2 \setminus \Omega_1^s, \emptyset, ..., \emptyset)$ on $[0, \infty)$ asymptotically close to a circle of length scale $r(t) := \sqrt{2(T_{ext} - t)}$ and evolving approximately self-similarly. Then, there exists $\delta_0 \in (0, 1)$ such that for $\delta \in (0, \delta_0)$*

$$E[\Omega^w | \Omega^s](0) \leq \delta r_0$$

implies quantitative weak-strong stability up to space-time shift: $\exists (z, T) : [0, \infty) \to \mathbb{R}^2 \times [0, \infty)$ Lipschitz such that T is increasing, $(z(0), T(0)) = (0, 0)$, $\|z\|_{L_t^\infty} \lesssim \delta^{1/2} r_0$, $\|T - \text{Id}\|_{L_t^\infty} \lesssim \delta^{1/2} r_0^2$, and

$$E[\Omega^w | \Omega_{z,T}^s](t) \leq E[\Omega^w | \Omega_{z,T}^s](0) \left(\frac{r(T(t))}{r_0}\right)^\alpha \quad \text{for } \alpha \in (1, 5) \tag{2}$$

for all $0 \leq t < t_\chi := \sup\{t : T(t) < \frac{1}{2}r_0^2\}$, where $\Omega_{z,T}^s(t) = z(t) + \Omega^s(T(t))$.

We overcome the issue of the blowing-up constant $C(t) \sim (T_{ext} - t)^{-1}$ in (1) at the singular time T_{ext} by developing a weak-strong stability theory for circular
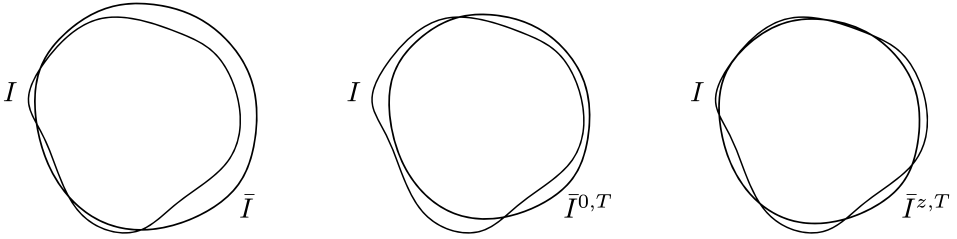
FIGURE 2. The interface $\bar{I} = \partial\Omega_1^s$ is dynamically adapted to $I = \partial^*\Omega_1^w$ by means of the space-time shift (z, T).

topology change up to dynamic space-time shift $(z(t), T(t)) \in \mathbb{R}^2 \times \mathbb{R}$. The role of the space-time shift is that of dynamically adapting the strong solution to the weak BV solution so that the leading-order non-integrable contributions in the inequality (1) are compensated - see Figure 2. As a result, we obtain an inequality of the form

$$\frac{\mathrm{d}}{\mathrm{d}t} E[\Omega^w | \Omega_{z,T}^s](t) \leq -\frac{\alpha}{r^2(T(t))} E[\Omega^w | \Omega_{z,T}^s](t) \quad \text{for } \alpha \in (1,5),$$

whence we infer the weak-strong stability estimate (2). Note that the exponent $\alpha < 5$ in (2) is optimal in the sense that is consistent with the result obtained by Gage and Hamilton in [3].

In order to prove weak-strong stability for a circular topology change up to dynamic space-time shift, we work in two different regimes for the weak BV solution. The non-perturbative regime correspond to the times $t \in (0, t_\chi)$ at which the energy dissipation term satisfies

$$\frac{1}{2} \sum_{\substack{i,j=1 \\ i \neq j}}^{P} \int_{I_{i,j}(t)} |H_{i,j}(t)|^2 \, \mathrm{d}\mathcal{H}^1 \geq \frac{\Lambda}{r(T(t))},$$

where $I_{i,j} = \partial^*\Omega_i^w \cap \partial^*\Omega_j^w$, $H_{i,j}$ is the mean curvature of $I_{i,j}$, and the constant $\Lambda > 0$ is chosen such that the dissipation dominates all the contributions from the time evolution of the error functional. In particular, one obtains the desired stability estimate by a trivial argument. On the other side, the perturbative regime corresponds to the times at which the energy dissipation term is strictly bounded by $\frac{\Lambda}{r(T(t))}$. Indeed, together with the smallness of the error one can show that the weak solution reduces to a graph over the strong solution with small Lipschitz norm. This structure can then be exploited to compensate the leading-order contributions by means of an explicit computation and choosing the space-time shift correctly.

At last, we note that we expect that our method may provide the starting point to study other types of dynamically stable shrinkers [6], as well as to prove quantitative convergence of the phase-field (Allen-Cahn) approximation for planar mean curvature flow [2] beyond the associated singularities.

REFERENCES

[1] J. Fischer, S. Hensel, T. Laux, and T. Simon, *The local structure of the energy landscape in multiphase mean curvature flow: Weak-strong uniqueness and stability of evolutions*, to appear in J. Eur. Math. Soc. (2024).

[2] J. Fischer, T. Laux, and T. Simon, *Convergence rates of the Allen-Cahn equation to mean curvature flow: A short proof based on relative entropies*, SIAM J. Math. Anal. **52(6)** (2020), 6222–6233.

[3] M. Gage and R. Hamilton, *The heat equation shrinking convex plane curves*, J. Diff. Geom **23** (1986), 69–95.

[4] M. A. Grayson. *The heat equation shrinks embedded plane curves to round points*, J. Diff. Geom. **25(2)** (1987), 285–314.

[5] T. Laux and F. Otto, *Convergence of the thresholding scheme for multi-phase mean curvature flow*, Calc. Var. Partial Differential Equations **55(5)** (2016), 129.

[6] C. Mantegazza, M. Novaga, A. Pluda, and F. Schulze, *Evolution of networks with multiple junctions*, to appear in Astérisque (2024).

[7] S. Stuvard and Y. Tonegawa. *On the existence of canonical multi-phase Brakke flows*, Advances in Calculus of Variations **17(1)** (2024), 33–78.

Viscoelastic two-phase models for tumour growth

Dennis Trautwein

(joint work with Harald Garcke and Balázs Kovács)

We introduce the topic of two-phase models with viscoelasticity, focusing on the challenges in modelling, analysis and numerical approximations. The primary aspect is their application to tumour growth [2, 4], but these models also find relevance in the context of two-phase flows and fluid–structure interaction [6].

Two-phase models generally describe the evolution and interaction of two unmixed materials separated by an interface, which can be either *diffuse*, with a smooth transition between phases, or *sharp*, resulting in a free boundary problem. The diffuse interface models are described using Cahn–Hilliard type systems for an order parameter, while sharp interface models depend on geometric quantities like the mean curvature of the evolving interface. The interface model is coupled to a Navier–Stokes equation or Stokes equation for an internal velocity, incorporating an elastic stress tensor described by an Oldroyd-B type model for the left Cauchy–Green tensor. We discuss various biological, chemical and mechanical factors contributing to unstable tumour growth and their inclusion in the mathematical models [2, 3, 4, 5].

The integration of different subsystems in the mathematical models poses significant challenges, necessitating a simultaneous treatment of these difficulties. Understanding the physical properties of the subsystems is crucial. Based on [1, 2, 4], we discuss the most important properties and demonstrate how they can be used for constructing suitable numerical approximations using the finite element method and for existence analysis. Finally, we will present the applicability of these numerical schemes from [2, 4] with accompanying results.

REFERENCES

[1] J. W. Barrett, S. Boyaval, *Existence and approximation of a (regularized) Oldroyd-B model*, Math. Models Methods Appl. Sci. **21** (2011), 1783–1837.
[2] H. Garcke, B. Kovács, D. Trautwein, *Viscoelastic Cahn–Hilliard models for tumour growth*, Math. Models Methods Appl. Sci. **32** (2022), 2673–2758.
[3] H. Garcke, K. F. Lam, E. Sitka, V. Styles, *A Cahn–Hilliard–Darcy model for tumour growth with chemotaxis and active transport*, Math. Models Methods Appl. Sci. **26** (2016), 1095–1148.
[4] H. Garcke, D. Trautwein, *Approximation and existence of a viscoelastic phase-field model for tumour growth in two and three dimensions*, Discrete Contin. Dyn. Syst. Ser. S **17** (2024), 221–284.
[5] M. Ebenbeck, H. Garcke, R. Nürnberg, *Cahn–Hilliard–Brinkman systems for tumour growth*, Discrete Contin. Dyn. Syst. Ser. S **14** (2021), 3989–4033.
[6] D. Mokbel, H. Abels, S. Aland, *A phase-field model for fluid–structure interaction*, J. Comput. Phys. **372** (2018), 823–840.

On finite speed of propagation for a class of stochastic thin-film equations

GÜNTHER GRÜN

(joint work with Lorenz Klein)

In 2005, Davidovitch, Moro, and Stone [3] introduced the stochastic thin-film equation

$$du_t + (u^3 u_{xxx})_x dt = (u^{3/2} dW_t)_x$$

as a model to capture effects of thermal noise in surface-tension driven thin-film flow[1]. Based on numerical experiments, they conjectured that noise enhances droplet spreading, affecting corresponding rates, too.

In recent years, first existence and nonnegativity results for stochastic thin-film equations were established in various parameter regimes (see [1, 2, 5, 6, 13, 8, 14, 15]. It turned out that in the case of surface-tension driven evolution (see above), the Stratonovich interpretation of noise provides an additional regularizing term which seems to be essential for basic existence results (cf. [6] and subsequent work). In this contribution, we assume the noise to be colored in space and white in time and to be explicitly given by a Q-Wiener process $W_t(x) := \sum_{k \in \mathbb{Z}} \mu_k \beta_k(t) g_k(x)$ where

- the g_k, $k \in \mathbb{Z}$, are the standard sine, cosine eigenfunctions of the Laplacian under periodic boundary conditions,
- the β_k, $k \in \mathbb{Z}$, are independent standard Brownian motions on an appropriate filtered probability space $(\Omega, \mathcal{F}, (\mathcal{F}_t)_{t \geq 0}, \mathbb{P})$,
- Q is a Hilbert-Schmidt operator on $L^2(\mathcal{O})$ such that $Q g_k = \mu_k^2 g_k$ for all $k \in \mathbb{Z}$,
- $\sum_{k \in \mathbb{Z}} \mu_k^2 k^4 < \infty$.

---

[1]For a derivation of stochastic thin-film equations for dewetting scenarios, see [12].

If we choose Q to be an integral operator with a nonnegative, compactly supported, symmetric kernel, and if the index k indicates the frequency of the eigenfunction g_k, then the nonnegative numbers μ_k, $k \in \mathbb{Z}$, satisfy $\mu_k = \mu_{-k}$ for all $k \in \mathbb{N}$, and the stochastic thin-film equation reads in the Stratonovich formulation simply as

$$(1) \qquad du_t + (u^n u_{xxx})_x dt - (C_{Strat} + S)(u^{n-2} u_x)_x dt = (u^{n/2} dW_t)_x$$

for mobility exponents $n > 0$, a positive parameter $C_{Strat} = C_{Strat}((\mu)_{k \in \mathbb{N}_0}, n)$ and the parameter S – at this stage – chosen to be zero. Taking the specific form of the porous-media-type Stratonovich correction term into account, it becomes evident that results on finite speed of propagation cannot be expected for $n < 2$. From the deterministic setting, we expect weighted versions of the energy estimate

$$(2) \qquad \tfrac{1}{2} \int_{\mathcal{O}} v_x^2(t) dx + \int_0^t \int_{\mathcal{O}} v^n v_{xxx}^2 dx ds \leq \tfrac{1}{2} \int_{\mathcal{O}} v_{0x}^2 dx$$

to be a crucial ingredient for results on finite speed of propagation in the parameter regime $n \in (2, 3)$. Therefore, we look for martingale solutions with compactly supported initial data which dissipate energy, i.e. which satisfy a stochastic analogue of (2). More precisely, the starting point for our analysis on finite speed of propagation are localized versions of the integral estimate

$$(3) \qquad \begin{aligned} \mathbb{E}\left[\sup_{t \in [0,T]} \tfrac{1}{2} \int_{\mathcal{O}} |u_x(\cdot, t)|^2 + \sup_{t \in [0,T]} \tfrac{1}{\eta+1} \int_{\mathcal{O}} u(\cdot, t)^{\eta+1} + c \int_{\mathcal{O}_T} \left(u^{\frac{n+2}{6}} \right)_x^6 \right] \\ \leq \tfrac{1}{2} \int_{\mathcal{O}} |(u_0)_x|^2 + \tfrac{1}{\eta+1} \int_{\mathcal{O}} u_0^{\eta+1} \end{aligned}$$

with $\eta \in (0, 1/2)$ and c an appropriate positive constant. Surprisingly, it turns out that so far[2] the existence of such energy dissipating solutions can only be proven if the parameter S in (1) is chosen positive and sufficiently large – for instance $S > \frac{3(n-2)^2}{4(3-n)} C_{Strat}$ (see [10] for an existence result).

We employ the following notion of finite speed of propagation.

Definition. *Let u be an energy-dissipating martingale solution to equation (1) related to a stochastic basis $(\Omega, \mathcal{F}, (\mathcal{F}_t)_{t \geq 0}, \mathbb{P})$. Let us assume initial data to be compactly supported on $\mathcal{O}$ and deterministic. We say the process u to exhibit finite speed of propagation if, for any point $x_0 \in \mathcal{O}$ and any $R > 0$ such that $B_R(x_0) \subset \mathcal{O}$ and $\operatorname{supp} u_0 \cap B_R(x_0) = \emptyset$, there is for any $r \in (0, R)$ an almost surely positive stopping time T_{r,R,x_0} such that*

$$(4) \qquad \int_0^{T_{r,R,x_0}} \int_{B_r(x_0)} |u(\cdot, \cdot, \omega)| dx dt = 0$$

holds for all $\omega \in \Omega$.

In this sense, we prove finite speed of propagation (cf. [9, 10, 11]) in the parameter regime $n \in (2, 3)$ with the parameter S satisfying the assumption above.

---

[2]The solutions constructed in [2, 15] use another solution concept and are not "energy dissipating".

Our result is based on two main ingredients. First, we establish existence of energy dissipating solutions to equation (1) with compactly supported initial data. For this, we generalize ideas of [5, 8] to the case of nonlinear conservative noise with $n \in (2,3)$. A crucial technical detail is a discrete, nonsmooth version of the identity

$$\int_{\mathcal{O}} u^{n-2} u_x u_{xxx} = -\int_{\mathcal{O}} u^{n-2} u_{xx}^2 + \frac{(n-2)(n-3)}{3} \int_{\mathcal{O}} u^{n-4} u_x^4.$$

Weighted versions of (3) are the starting point for the proof of finite speed of propagation. The scaling transition in the deterministic part of the equation (thin-film operator versus porous-media operator) gives rise to a sum of power-type nonlinearities on the right-hand side of these integral estimates. Combining the ansatz of [7] to rearrange different power-type nonlinearities with the ideas of [4] to transfer deterministic methods to the stochastic setting – in [4] applied to stochastic porous-media equations with source-term noise, – we succeed to set up a new iteration technique tailored for the stochastic thin-film equation and to prove finite speed of propagation in the sense of the definition above (see [11]).

To the best of our knowledge, this is the first result on finite speed of propagation for a stochastic version of a degenerate parabolic equation with conservative (instead of source-term) noise – and at the same time for a degenerate parabolic equation of higher order.

References

[1] K. Dareiotis, B. Gess, M.V. Gnann, G. Grün, *Nonnegative Martingale Solutions to the Stochastic Thin-Film Equation with Nonlinear Gradient Noise*, Arch. Rational Mech. Anal., **242** (2021), 179–234.

[2] K. Dareiotis, B. Gess, M.V. Gnann, M. Sauerbrey, *Solutions to the stochastic thin-film equation for initial values with non-full support*, arXiv:2305.06017, 2023.

[3] B. Davidovitch, E. Moro, H.A. Stone, *Spreading of Viscous Fluid Drops on a Solid Substrate Assisted by Thermal Fluctuations*, Phys. Rev. Lett., **95** (2005), 244505.

[4] J. Fischer, G. Grün, *Finite speed of propagation and waiting times for the stochastic porous medium equation – a unifying approach*, SIAM J. Math. Anal., **47** (2015), 825–854.

[5] J. Fischer, G. Grün, *Existence of positive solutions to stochastic thin-film equations*, SIAM J. Math. Anal., **50** (2018), 411–455.

[6] B. Gess, M.V. Gnann, *The stochastic thin-film equation: existence of nonnegative martingale solutions*, Stoch. Process. Appl., **130** (2020), 7260–7302.

[7] L. Giacomelli, A. Shishkov, *Propagation of support in one-dimensional convected thin-film flow*, Indiana Univ. Math. J., **54** (2005), 1181–1215.

[8] G. Grün, L. Klein, *Zero-contact angle solutions to stochastic thin-film equations*, J. Evol. Eq., **22** (2022), 1–37.

[9] G. Grün, L. Klein, *Existence of positive solutions to stochastic thin-film equations – the case of weak slippage*, in preparation.

[10] G. Grün, L. Klein, *Existence of energy-dissipating solutions to stochastic thin-film equations with compactly supported initial data – the case of weak slippage*, in preparation.

[11] G. Grün, L. Klein, *Finite speed of propagation for a class of stochastic thin-film equations*, in preparation.

[12] G. Grün, K. Mecke, M. Rauscher, *Thin-film flow influenced by thermal noise*, J. Stat. Phys., **122** (2006), 1261–1291.

[13] S. Metzger, G. Grün, *Existence of nonnegative solutions to stochastic thin-film equations in two space dimensions*, Interfaces Free Bound., **24** (2022), 307–387.

[14] M. Sauerbrey, *Martingale solutions to the stochastic thin-film equation in two dimensions*, arXiv:2108.05754, 2021.

[15] M. Sauerbrey, *Solutions to the stochastic thin-film equation for the range of mobility exponents* $n \in (2, 3)$, arXiv:22310.02765, 2023.

Existence and compactness of global weak solutions of three dimensional axisymmetric Ericksen-Leslie system

Changyou Wang

(joint work with Joshua Kortum)

In this talk, I will describe a recent joint work with Joshua Kortum (University of Würzburg, Germany) in which we establish, in dimension three, the existence of global weak solutions to the axisymmetric simplified Ericksen-Leslie system without swirl. This is achieved by analyzing weak convergence of solutions of the axisymmetric Ginzburg-Landau approximated solutions as ε tends to zero. The proof relies on the one hand on the use of a blow-up argument to rule out energy concentration off the z-axis, which exploits the topological restrictions of the axisymmetry. On the other hand, possible limiting energy concentrations on the z-axis can be dealt with by a cancellation argument at the origin. Once more, the axisymmetry plays a substantial role. We will also show that the space of axisymmetric solutions without swirl (u, d) to the simplified Ericksen-Leslie system is compact under weak convergence in $L_t^2 L_x^2 \times L_t^2 H_x^1$.

More precisely, we study the following simplified version of the celebrated Ericksen-Leslie system that models the hydrodynamics of nematic liquid crystals. For an axisymmetric domain $\Omega \subset \mathbb{R}^3$, let $(u, d, P) : \Omega \times [0, \infty) \to \mathbb{R}^3 \times \mathbb{S}^2 \times \mathbb{R}$ be a triple of axisymmetric functions without swirl, namely,

$$(u, d, P) = (u^r(r, z, t)\mathbf{e}_r + u^z(r, z, t)\mathbf{e}_z, \sin \phi(r, z, t)\mathbf{e}_r + \cos \phi(r, z, t)\mathbf{e}_z, P(r, z, t)),$$

which solves

$$\left(\partial_t + b \cdot \nabla - L + \frac{1}{r^2}\right) u^r + P_r = -\left(L\varphi - \frac{\sin 2\varphi}{2r^2}\right) \varphi_r, \tag{1}$$

$$(\partial_t + b \cdot \nabla - L) u^z + P_z = -\left(L\varphi - \frac{\sin 2\varphi}{2r^2}\right) \varphi_z, \tag{2}$$

$$\frac{1}{r}(ru^r)_r + (u^z)_z = 0, \tag{3}$$

$$(\partial_t + b \cdot \nabla - L) \varphi = -\frac{\sin 2\varphi}{2r^2}, \tag{4}$$

where

$$\mathbf{e}_r = (\cos \theta, \sin \theta, 0), \ \ \mathbf{e}_z = (0, 0, 1),$$
$$b = u^r \mathbf{e}_r + u^z \mathbf{e}_z,$$
$$L := \partial_r^2 + \frac{1}{r}\partial_r + \partial_z^2.$$

Our main theorem states as follows.

Theorem. *Suppose $u_0 \in L^2_{div}(\Omega)$ and $d_0 \in H^1(\Omega, \mathbb{S}^2)$ are axisymmetric without swirl. Then there exists a global weak solution $(u, d, P) : \Omega \times [0, \infty) \to \mathbb{R}^3 \times \mathbb{S}^2 \times \mathbb{R}$ to (1)–(4) that is axisymmetric without swirl, subject to the initial and boundary condition $(u, d) = (u_0, d_0)$ on $\Omega \times \{0\} \cup \partial\Omega \times (0, \infty)$.*

REFERENCES

[1] Joshua Kortum, Changyou Wang *Existence and compactness of global weak solutions of three dimensional axisymmetric Ericksen-Leslie system.* Preprint (2024).
[2] Fanghua Lin, Changyou Wang, *Global existence of weak solutions of the nematic liquid crystal flow in dimension three.* Comm. Pure Appl. Math. **69** (2016), 1532–1571.

On anisotropic curve shortening flow for planar networks

PAOLA POZZI

(joint work with Michael Gößwein, Heiko Kröner, and Matteo Novaga)

Recent results for anisotropic curve shortening flow of networks are presented. For simplicity of exposition we consider a simple network Γ composed of three curves, joined through one triple junction and with three fixed endpoints which coincide with given distinct points $P^i \in \mathbb{R}^2$, $i = 1, 2, 3$ in the plane. The curves are parametrized by some regular immersed maps $u^i : [0, 1] \to \mathbb{R}^1$, $u^i = u^i(x)$ such that $u^i(1) = P^i$, $i = 1, 2, 3$ and $u^1(0) = u^2(0) = u^3(0)$. The anisotropic length of Γ is given by

$$E(\Gamma) := \sum_{i=1}^{3} \int_0^1 \varphi^\circ(\nu^i)|u_x^i|dx,$$

where $\nu^i = (\tau^i)^\perp$ is the Euclidean unit normal, $\tau^i = \frac{u_x^i}{|u_x^i|}$ the Euclidean unit tangent, and $\varphi^\circ : \mathbb{R}^2 \to [0, \infty)$ a smooth elliptic anisotropy map. We study an L^2-gradient flow for the above functional, i.e. we let each curve of the triod evolve according to the geometric motion

$$(u_t^i \cdot \nu^i)\nu^i = \varphi^\circ(\nu^i)\kappa_\varphi^i \nu^i \qquad \text{on } (0, T) \times (0, 1), \qquad i = 1, 2, 3,$$

where κ_φ^i denotes the anisotropic curvature given by $\kappa_\varphi^i = D^2\varphi^\circ(\nu^i)\tau^i \cdot \tau^i \kappa$ with κ the Euclidean curvature. The topology of the triod is maintained during evolution and natural boundary conditions are imposed.

After giving a definition of geometric solutions and admissible initial networks, we prove short-time existence of the flow in suitable Hölder spaces and show that, if the maximal time of existence of the evolution is finite, then either one of the lengths of the curves goes to zero or the L^2-norm of the (anisotropic) curvature blows up (see [2] for details). Unlike the case of evolution of a single closed immersed curve where the maximum principle can be applied (see [1]), in the network setting, due to the triple junction and the interaction between the curves, we have to rely on delicate integral estimates. The latter depend on the anisotropy,

making a possible extension of the ideas presented in [1] problematic. Hence it remains an open question if and how we can use the anisotropic curve shortening flow of networks with smooth elliptic energies to approximate anisotropic motion for general (in particular crystalline) anisotropies.

Next we show that the functional E fulfills a Łojasiewicz-Simon gradient inequality and employ this result, together with a suitable graph representation of the solution, to derive a stability statement for the flow. Precisely, we show that, for any initial configuration which is $C^{2+\alpha}$-close to a (local) energy minimizer, the flow exists globally and converges to a possibly different energy minimum. In the specific and elementary setting we have chosen (a simple triod), and exploiting the assumptions on φ°, it is possible to derive convergence to the unique minimum for E (if the latter is non-degenerate, i.e. its triple junction is a distinct point from P^i, $i = 1, 2, 3$). The stability results are discussed in [3].

All results presented are generalizations to the anisotropic setting of the corresponding statements in the isotropic setting: see [2] and [3] for appropriate references.

References

[1] G. Mercier, M. Novaga, P. Pozzi *Anisotropic curvature flow of immersed curves*, Comm. Anal. Geom. **27** (2019), no. 4, 937–964.

[2] H. Kröner, M. Novaga, P. Pozzi *Anisotropic curvature flow of immersed networks*, Milan J. Math. **89** (2021), 147–186.

[3] M. Gößwein, M. Novaga, P. Pozzi *Stability analysis for the anisotropic curve shortening flow of planar networks.*, Preprint (2023), https://arxiv.org/abs/2310.05596.

Modeling of Paint Atomization in Rotary Bell Spray Painting

James A. Sethian

(joint work with Robert I. Saye)

In manufacturing settings, paints are frequently applied by an electrostatic rotary bell atomizer: paint flows to a cup rotating at 10,000-70,000 rpm and is driven by centrifugal forces to form thin sheets and tendrils at the cup edge, where it then atomizes into droplets.

Rotary Bell: Schematic of paint flow and air currents

The goal of computational modeling of this process is to both understand the dynamics, and to optimize flow characteristics. This includes

- Optimizing the atomization process for higher paint flow rates, trying to obtain more uniform and consistent atomization.
- Studying the atomization process as a function of paint fluid properties (such as density, viscosity, and surface tension) and physical properties, such as fluid delivery rates, bell rotation speeds and shaping air currents.
- Analyzing film dynamics, particularly in the immediate atomization at the cup edge, including the dynamics of filament formation and droplet size, distribution and trajectories.

However, the fluid mechanics of this problem make it particularly challenging:

- Bell speeds range from 30,000 to 70,000 rpm, creating enormous centrifugal forces.
- The paint quickly transitions from thin sheets to filaments to tiny droplets.
- Fluid interfaces undergo rapid changes in geometry as they contort and tear apart.
- Paints are non-Newtonian and require careful calculation of associated shear forces.

From a computational point of view, these challenges impose several requirements. First, we need appropriate equations of motion in a moving, rotating coordinate system referencing curved surfaces. Second, hybrid interface solvers which couple interface jump conditions with highly contorted interfaces are required. Third, highly accurate fluid solvers are needed to deal with complex geometry and rapidly varying dynamics in time and space such as fast moving shaping air currents. Fourth, adaptive mesh refinement is needed, because of the vast scales between the smallest droplets and the extent of the computational domain. And fifth, the sheer scales of the time step and space discretization require use of advanced high performance computing capabilities, replete with attention to massively parallel processing on multi-core architectures.

In an earlier (2019) Oberwolfach meeting, we described our plan to build a numerical methodology that can accurately compute the underlying dynamics. Here, we report on that work, giving a brief idea of the algorithms and summarizing the numerical results. Here, we describe discussion and results which appeared in [5].

Our methodology combines (1) level set methods to track the paint/air fluid interface, in a way that is able to deal with significant distortions, tearing, breakup and merger [1, 2, 4, 6]; (2) implicit mesh discontinuous Galerkin methods for high order accurate computation of the underlying flow and interface dynamics, employing on-the-fly body-fitted DG meshes in order to impose complex interface jump conditions [3]; (3) an adaptive mesh refinement scheme to resolve fluid droplets, in which subdivision criteria are based on width/thickness of paint film, as well as curvature; and (4) advanced efficient parallel implementation on high performance multi-core architectures.

Level Set Methods: We use level set methods to track the paint/air fluid interfaces. These methods rely on an implicit embedding of the interface as the zero level set of a higher-dimensional function, whose evolution satisfies an initial value

partial differential equation containing a transport velocity term which captures the underlying physics.

**DG methods:** The fluid equations are solved as follows:

- The equations of two-phase non-Newtonian incompressible fluid flow are solved using a discontinuous Galerkin (DG) approach.
- A level set function is used in a finite difference setting on a background mesh to implicitly determine where the interface is located.
- On the fly, the method constructs a body-fitted DG mesh (just for that time step) so that jump conditions are accurately resolved.

For details, see [3].

Adaptivity: Because the thin films break into tiny bubbles, we need to build a version of adaptive mesh refinement that dynamically refines the background level set (and hence DG mesh) to accurately track small particles. Our approach is as follows:

We subdivide the DG cells that contain the paint/air interface into smaller subcells:

- Subdivision criteria based on width/thickness of paint film, as well as curvature.
- Cells subdivide and coarsen appropriately in response to subdivision criteria.
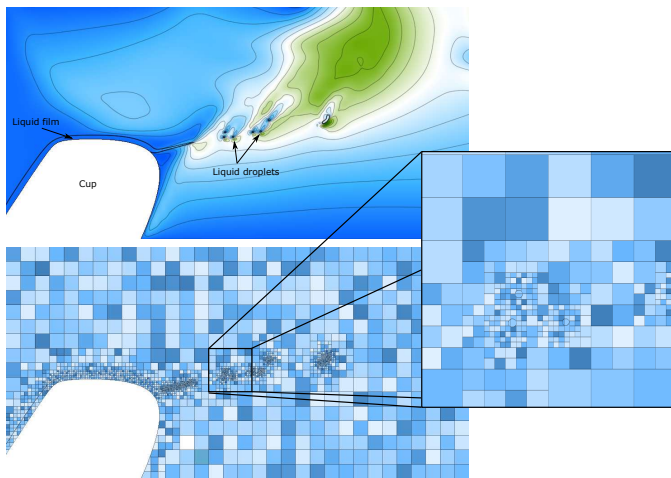
High Performance Computing: All the codes/algorithms have been converted to massively parallel implementations. The time step, spatial resolution, and physics make it impossible to model the entire bell atomization process. On the biggest, fastest, parallel supercomputer (ORNL, NERSC, etc) on millions of cores, we can only model a small angular wedge of the cup. Nonetheless, quantitative results can be obtained.

$t = 472.5\,\mu\text{s}$ $t = 535.0\,\mu\text{s}$ $t = 597.5\,\mu\text{s}$

FIGURE 1. **Time- and spatially-varying inflow film thickness, high mesh resolution, and shaping air currents simulating nozzle inlets.** Three-dimensional model results using a high-resolution computational mesh together with accurate smooth cup geometry. Two viewpoints at the same time frame are given: a top-down perspective and a side-on view to show the vertical drifting of the shedding droplets, being pushed upwards by the shaping air currents. The liquid surface is colored copper, with the bell cup situated beneath.

Results:

See Figure 1.

REFERENCES

[1] Sethian, J.A., *Level Set Methods and Fast Marching Methods: Evolving Interfaces in Geometry, Fluid Mechanics, Computer Vision, and Materials Sciences*, Cambridge University Press, 1999.
[2] Osher, S. and Sethian, J.A., *Fronts Propagating with Curvature–Dependent Speed: Algorithms Based on Hamilton–Jacobi Formulations*, Journal Computational Physics, 1988.
[3] Saye, R.I., *Implicit Mesh discontinuous Galerkin methods and interfacial gauge methods for high-order accurate interface dynamics, with applications to surface tension dynamics, rigid body fluid-structure interaction, and free surface flow, Parts I and II*, Journal Computational Physics, 2017.
[4] Saye, R.I., Sethian, J.A., *Analysis and applications of the Voronoi Implicit Interface Method*, Journal of Computational Physics, 231, 18, July 2012.
[5] Saye, R.I., Sethian, J.A., Petrouskie, B., and Rock, R., *Insights from high-fidelity modeling of industrial rotary bell atomization*, Proceedings of the National Academy of Sciences, 120, Jan, 2023.
[6] Yu, J.D., Sakai, S., and Sethian, J.A., *Two-phase viscoelastic jetting*, Journal of Computational Physics, 220, 2, Jan. 2007.

Finding equilibrium states of fluid membranes
Maxim Olshanskii

We consider an inextensible Boussinesq–Scriven viscous membrane represented by a time-dependent surface $\Gamma(t)$ with a density distribution $\rho(x,t)$. The governing equations for the motion of the membrane are based on conservation of mass and linear momentum for an arbitrary material area $\gamma(t) \subset \Gamma(t)$ (see, e.g., [1]). The system of equations reads: Find a velocity field $\mathbf{u}$ of the density flow on $\Gamma(t)$ together with a surface pressure p and the surface normal velocity V_Γ satisfying

(1)
$$\begin{cases} \rho\dot{\mathbf{u}} = -\nabla_\Gamma p + 2\mu\operatorname{div}_\Gamma(\mathbf{D}_\Gamma(\mathbf{u})) + \mathbf{b} + p\kappa\mathbf{n}, \\ \operatorname{div}_\Gamma \mathbf{u} = 0, \\ \quad\dot{\rho} = 0, \\ \quad V_\Gamma = \mathbf{u}\cdot\mathbf{n} \end{cases} \qquad \text{on } \Gamma(t).$$

Here, κ is the double mean curvature, p is the surface pressure, μ is the viscosity, $\mathbf{D}_\Gamma(\mathbf{u}) = \frac{1}{2}(\nabla_\Gamma\mathbf{u} + \nabla_\Gamma\mathbf{u}^T)$ is the surface rate-of-strain tensor, $\dot{\rho}$, $\dot{\mathbf{u}}$ are material derivatives of ρ and $\mathbf{u}$, and $\mathbf{b}$ represents area forces, which include elastic and external forces. For definitions of the surface tangential operators we refer to [1].

We assume that $\rho = \text{const.}$ at $t = 0$, and then $\dot{\rho} = 0$ implies $\rho = \text{const.}$ for $t > 0$. The area forces $\mathbf{b}$ consist of the external force given by a constant pressure difference across the membrane and elastic forces generated by the bending and stretching of the membrane,

$$\mathbf{b} = p^{\text{ext}}\mathbf{n} + \mathbf{b}^{\text{elst}}.$$

For the elasticity, we consider the Helfrich model with the Willmore energy functional and zero spontaneous curvature:

$$H = \frac{c_\kappa}{2}\int_\Gamma \kappa^2\,\mathrm{d}s,$$

where $c_\kappa > 0$ has the meaning of bending rigidity. Applying the principle of virtual work and computing the shape derivative of H one finds that the release of the bending energy produces a force in the normal direction to the surface:

(2)
$$\mathbf{b}^{\text{elst}} = c_\kappa(\Delta_\Gamma\kappa + \frac{1}{2}\kappa^3 - 2K\kappa)\mathbf{n}.$$

We were interested in the equilibrium state solutions to the governing equations (1)–(2). The following three conditions of the equilibrium were found: The surface is time-independent in the sense of a shape:

(3)
$$\mathbf{u}\cdot\mathbf{n} = 0.$$

Then, either $\mathbf{u} = 0$, which reduces the problem to the classical one of finding a minimal Willmore surface, or the steady surface of interest should support a nontrivial Killing vector field, i.e. tangential $\mathbf{u} \neq 0$ such that

(4)
$$\mathbf{D}_\Gamma(\mathbf{u}) = 0.$$

According to the third equilibrium condition, the in-surface pressure in an equilibrium state splits into a constant term and a term representing the kinetic energy density:

$$(5) \qquad p - \frac{\rho}{2}|\mathbf{u}|^2 = p_0 \qquad \text{with some} \quad p_0 := const.$$

The shape equation for the surface at equilibrium is found by using (3)–(5) and the particular elasticity model. For the Helfrich model, it reads: Find a smooth connected closed and compact surface Γ of a prescribed area such that its curvatures satisfy

$$(6) \qquad -\rho\mathbf{u}^T\mathbf{H}\mathbf{u} - \frac{\rho}{2}\kappa|\mathbf{u}|^2 = p_0\kappa + c_\kappa(\Delta_\Gamma\kappa + \frac{1}{2}\kappa^3 - 2K\kappa) + p^{\text{ext}} \qquad \text{on } \Gamma.$$
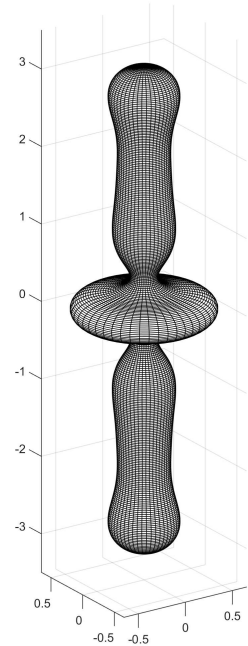
We discussed (see also [2]) that it is plausible to assume that only surfaces of revolution support non-zero Killing fields among closed compact smooth surfaces isometrically embedded in $\mathbb{R}^3$. This motivated us to restrict further considerations to such surfaces. Let Oz be the axis of symmetry for Γ. Then $\mathbf{u}$ satisfying (3)–(4) is a field of rigid rotations given by $\mathbf{u}(\mathbf{x}) = w\,\mathbf{e}_z \times \mathbf{x}, \quad \mathbf{x} \in \Gamma$, with the angular velocity $w\,\mathbf{e}_z$. It can be shown that $\mathbf{u}^T\mathbf{H}\mathbf{u} = \kappa_2|\mathbf{u}|^2$, where κ_2 is the second principal curvature. For an axisymmetric surface the term on the left-hand side of the shape equation takes the form $-\rho\left(\kappa_2 + \frac{\kappa}{2}\right)(w\,r)^2$. Thus, we were interested in the following problem: *Find an axisymmetric Γ, p_0, and p^{ext} such that (6) holds with given ρ, κ, $|w|$, $A = \text{area}(\Gamma)$ and $V = \text{vol}(\Gamma)$.*

We next consider an arc-length parametrization $s : [0, L] \to (r(s), \psi(s))$ of the profile curve, where ψ the tilt angle, so that Γ is generated by rotating the curve around the z-axis in $\mathbb{R}^3$. Writing geometric quantities in terms of r and ψ the problem of finding a stationary shape can be reformulated follows: Given an angular velocity $w \geq 0$, surface area $A > 0$ and volume $V > 0$ (satisfying the isoperimetric inequality $V \leq 1/(6\pi^2)A^{\frac{3}{2}}$), find $L \in \mathbb{R}_+$, $\psi(s), r(s) : [0, L] \to \mathbb{R}$, $p_0, p^{\text{ext}} \in \mathbb{R}$ satisfying the following system of ODEs, integral and boundary conditions:

$$-\rho w^2 r\left(\tfrac{1}{2}r\psi_s + \tfrac{3}{2}\sin\psi\right) = p_0\kappa + c_\kappa\left(r^{-1}(r\kappa_s)_s + \tfrac{1}{2}\kappa^3 - 2K\kappa\right) + p^{\text{ext}},$$

$$\text{with } \kappa = \left(\psi_s + \frac{\sin\psi}{r}\right), \; K = \frac{\psi_s\sin\psi}{r},$$

$$r_s = \cos\psi,$$

$$2\pi \int_0^L r\, ds = A, \quad \pi \int_0^L r^2 \sin\psi \, ds = V$$
$$r(0) = 0, \quad r(L) = 0, \quad \psi(0) = 0, \quad \psi(L) = \pi.$$

We derived a simple and effective second order numerical method to solve this system.

Letting $A = 4\pi^2$ and applying the numerical method we find branches of solutions to (6) parameterized solutions by their reduced volume $\widehat{V} := 3\mathrm{vol}(\Gamma)/(4\pi)$, $\widehat{V}(\Gamma) \in (0,1]$, where $\widehat{V} = 1$ corresponds to the unit sphere, a trivial solution of (6) for $w = 0$ and p_0, p^{ext} satisfying $2p_0 + p^{\mathrm{ext}} = 0$. Several branches of shapes, which are new compared to the classical Willmore shapes, were found and reported in [2]. One of such shapes (with $\widehat{V} = 0.39$, $w = 4$) from the first branch of oblique shapes, in the terminology of [2], is illustrated in the figure above.

References

[1] T. Jankuhn, M. Olshanskii, and A. Reusken, *Incompressible fluid problems on embedded surfaces: Modeling and variational formulations,* Interfaces and Free Boundaries **20** (2018), 353–377.

[2] M. Olshanskii, *On equilibrium states of fluid membranes*, Physics of Fluids **35** (2023), 062111.

Parametric finite element methods for Navier–Stokes equations on evolving surfaces

Robert Nürnberg

(joint work with Harald Garcke)

In this talk we introduce a numerical method for the approximation of a surface Navier–Stokes equation on an evolving surface, where the evolution of the surface is coupled to the flow of the fluid on it. In particular, for an evolving closed oriented hypersurface Γ in $\mathbb{R}^d$, $d = 2$ or 3, we consider the incompressible surface Navier–Stokes equations

$$(1) \qquad \rho\, \partial_t^\bullet \vec{u} - \nabla_s \cdot \underline{\sigma} = \vec{g} + \alpha\, f_\Gamma\, \vec{\nu}, \qquad \nabla_s \cdot \vec{u} = 0, \qquad \mathcal{V} = \vec{u} \cdot \vec{\nu},$$

where $\vec{u}$ denotes the velocity of the fluid on the surface. In addition, $\partial_t^\bullet$ denotes the material time derivative on Γ, $\nabla_s\cdot$ is the surface divergence, $\underline{\sigma}$ is the surface stress tensor, $\vec{\nu}$ is a unit normal on Γ, $\mathcal{V}$ is the normal velocity of the evolving surface Γ, $\vec{g}$ is some external forcing and ρ is the constant density. For the forcing f_Γ we have some intrinsic properties of the surface in mind, and $\alpha \in \mathbb{R}_{\geq 0}$ is a related coefficient. The second condition in (1) models the incompressibility of the surface's material, meaning in particular that the total surface area is conserved. The third equation in (1) means that the surface evolves according to the normal component of the velocity $\vec{u}$. The surface stress tensor is given by

$$\underline{\sigma} = 2\,\mu\, \underline{D}_s(\vec{u}) - p\,\underline{\mathcal{P}},$$

where $\mu \in \mathbb{R}_{\geq 0}$ is the interfacial shear viscosity and p denotes the surface pressure, which acts as a Lagrange multiplier for the incompressibility condition in (1). Here $\underline{\mathcal{P}} = \underline{\mathbf{I}} - \vec{\nu} \otimes \vec{\nu}$ is the projection onto the tangent space of Γ, and $\underline{D}_s(\vec{u}) = \frac{1}{2} \underline{\mathcal{P}} \left(\nabla_s \vec{u} + (\nabla_s \vec{u})^T \right) \underline{\mathcal{P}}$ is the surface rate-of-deformation tensor, where $\nabla_s = \underline{\mathcal{P}} \nabla = (\partial_{s_1}, \ldots, \partial_{s_d})$ denotes the surface gradient and $\nabla_s \vec{u} = \left(\partial_{s_j} u_i \right)_{i,j=1}^d$.

For example, the forcing f_Γ in (1) can be derived from a simple bending energy, e.g.

$$(2) \qquad E(\Gamma) = \tfrac{1}{2} \int_\Gamma \varkappa^2 \, \mathrm{d}\mathcal{H}^{d-1} \,,$$

the well-known Willmore energy. By $\varkappa$ we denote the mean curvature (the sum of the principal curvatures) of Γ and $\mathrm{d}\mathcal{H}^{d-1}$ indicates integration with respect to the $(d-1)$-dimensional surface measure. The forces from the bending energy act in a direction normal to the surface and f is given as minus the first variation of $E(\Gamma)$, i.e.

$$(3) \qquad f_\Gamma = -\Delta_s \varkappa - \varkappa |\nabla_s \vec{\nu}|^2 + \tfrac{1}{2} \varkappa^3 \,,$$

where Δ_s is the surface Laplacian and $\nabla_s \vec{\nu}$ is the Weingarten map.

More generally, if $f_\Gamma = 1$ then α can play the role of a Lagrange multiplier for the side constraint $\int_\Gamma \mathcal{V} \, \mathrm{d}\mathcal{H}^{d-1} = \int_\Gamma \vec{u} \cdot \vec{\nu} \, \mathrm{d}\mathcal{H}^{d-1} = 0$, which would enforce the conservation of the volume enclosed by Γ. We also observe that replacing (2) with the total surface area $\int_\Gamma 1 \, \mathrm{d}\mathcal{H}^{d-1}$ would result in the variation $f_\Gamma = \varkappa$. However, using that forcing in (1) would have no effect on the flow, due to the surface's incompressibility. In particular, the solution to (1) would be independent of the value of α.

The surface Navier–Stokes equations (1), as well as the stationary case, where $\vec{u} \cdot \vec{\nu} = 0$, have recently seen a lot of interest in the literature. We refer to [4, 6] and the references therein. Solutions to (1), (3) are often called fluidic surfaces and play a role as a simplified model for biological membranes, see e.g. [5]. In fact, the system can formally be derived as a limit of the coupled bulk Navier–Stokes/surface Navier–Stokes/Willmore energy model for fluidic biomembranes considered in [1, 2], when the bulk densities and bulk viscosities go to zero.

Solutions of (1), (3) satisfy the energy estimate

$$(4) \qquad \tfrac{1}{2} \frac{\mathrm{d}}{\mathrm{d}t} \left(\rho \langle \vec{u}, \vec{u} \rangle_{\Gamma(t)} + \alpha \langle \vec{\varkappa}, \vec{\varkappa} \rangle_{\Gamma(t)} \right) + 2\mu \langle \underline{D}_s(\vec{u}), \underline{D}_s(\vec{u}) \rangle_{\Gamma(t)} = \langle \vec{g}, \vec{u} \rangle_{\Gamma(t)} \,.$$

The aim of this talk is to introduce a parametric finite element approximation for (1), (3) that mimics (4) on the discrete level. Based on the authors' previous work with John W. Barrett in [2], we first consider a semidiscrete method based on polyhedral approximations $\Gamma^h(t)$ of the evolving surface Γ, together with surface P2P1 Taylor–Hood elements for the approximations $(\vec{U}^h, P^h)$ of velocity and pressure, and P1 approximations of curvature and bending forces. For the discrete stability proof, similarly to the techniques used in [2], it is crucial to identify the (full) discrete velocity $\vec{\mathcal{V}}^h$ of $\Gamma^h(t)$ with $\vec{\pi}_1^h \vec{U}^h$, the piecewise linear interpolant of $\vec{U}^h$. Unfortunately, this indirect reduction in the degrees of freedom of $\vec{U}^h$, and which

| | P1 | P2 | |
1/h	$\|\Gamma^h(T) - \Gamma(T)\|_{L^\infty}$	$\|\Gamma^h(T) - \Gamma(T)\|_{L^\infty}$	EOC
32	3.7052e-02	7.3893e-02	—
64	8.8822e-01	9.3797e-03	2.98
128	1.0081e-00	1.1815e-03	2.99
256	1.0140e-00	1.4784e-04	3.00
512	1.0083e-00	1.8481e-05	3.00

TABLE 1. Errors for the convergence test for $\Gamma(t) = (1+t)\,\mathbb{S}^1$ for P1 and P2 discrete surfaces.

terms they influence, leads to locking phenomena for some numerical experiments for the corresponding fully discrete scheme.

That is why in the second part of the talk we consider piecewise quadratic approximations $\Gamma^h(t)$ of Γ instead, together with the associated isoparametric finite element spaces $S_2^h(\Gamma^h)$ and $S_1^h(\Gamma^h)$ of order P2 and P1. Using isoparametric P2P1 Taylor–Hood elements for $(\vec{U}^h, P^h)$ then means that the proof of the discrete analogue of the stability bound (4) naturally follows the proof in the continuous setting. In particular, the (full) discrete velocity $\vec{\mathcal{V}}^h$ of $\Gamma^h(t)$ now satisfies $\vec{\mathcal{V}}^h = \vec{U}^h \in S_2^h(\Gamma^h)$. In addition, it can be shown that the surface area of the evolving discrete surfaces $\Gamma^m(t)$ is preserved, in line with the corresponding conservation property on the continuous level.

The differences between the P1 and P2 surface approximations in practice can be visualized with the following convergence experiment. To this end, we observe that the family of spheres $\Gamma(t) = r(t)\,\mathbb{S}^{d-1}$, with outer unit normal $\vec{\nu} = \frac{\vec{\mathrm{id}}}{|\vec{\mathrm{id}}|}$, together with $\vec{u}(\cdot, t) = r'(t)\,\vec{\nu}$ and $p(t) = \rho\,\frac{r''(t)\,r(t)}{d-1} + 2\,\mu\,\frac{r'(t)}{r(t)} - \alpha\,\frac{f_\Gamma(t)\,r(t)}{d-1}$ is a solution to (1) with the second equation replaced by $\nabla_s \cdot \vec{u} = (d-1)\,\frac{r'(t)}{r(t)}$. For example, for (2) it holds that

$$(5) \qquad f_\Gamma(t) = \frac{(d-1)^2}{r^3(t)} - \frac{1}{2}\left(\frac{d-1}{r(t)}\right)^3 = \begin{cases} \frac{1}{2\,r^3(t)} & d = 2\,, \\ 0 & d = 3\,. \end{cases}$$

We use this solution to perform a convergence test for both schemes, for the function $r(t) = 1+t$ on the time interval $[0, T]$ with $T = 1$, and for the parameters $d = 2$, $\rho = \mu = \alpha = 1$. See Table 1 for the observed errors. We see that for the P1 case the errors are not converging, while for the P2 surfaces we see a convergence rate of order $\mathcal{O}(h^3)$. The reason for the nonconvergent P1 approximations is locking, as seen in the example in Figure 1.

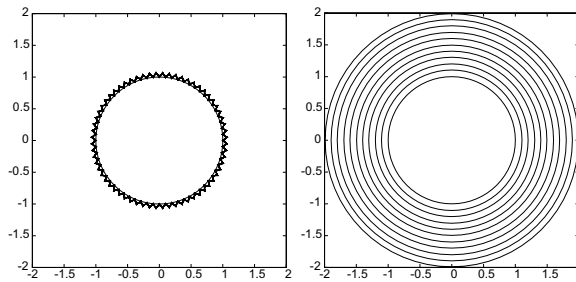The research presented in this talk is work in progress, see [3].

FIGURE 1. Plots of the discrete surface at times $t = 0, 0.1, \ldots, 1$ for the convergence test for $\Gamma(t) = (1 + t)\,\mathbb{S}^1$ for P1 (left) and P2 (right) discrete surfaces.

REFERENCES

[1] M. Arroyo and A. DeSimone, *Relaxation dynamics of fluid membranes*, *Phys. Rev. E* **79** (2009) 031915.

[2] J. W. Barrett, H. Garcke and R. Nürnberg, *A stable numerical method for the dynamics of fluidic membranes*, *Numer. Math.* **134** (2016) 783–822.

[3] H. Garcke and R. Nürnberg, *Parametric finite element methods for Navier–Stokes equations on evolving surfaces*, 2024, (in preparation).

[4] T. Jankuhn, M. A. Olshanskii and A. Reusken, *Incompressible fluid problems on embedded surfaces: modeling and variational formulations*, *Interfaces Free Bound.* **20** (2018) 353–377.

[5] V. Krause and A. Voigt, *A numerical approach for fluid deformable surfaces with conserved enclosed volume*, *J. Comput. Phys.* **486** (2023) 112097.

[6] S. Reuther, I. Nitschke and A. Voigt, *A numerical approach for fluid deformable surfaces*, *J. Fluid Mech.* **900** (2020) R8, 12.

Numerical analysis of an evolving bulk–surface model of tumour growth

BALÁZS KOVÁCS

(joint work with Dominik Edelmann and Christian Lubich)

We have presented some recent results on the numerical analysis of an evolving bulk-surface finite element method for a model of tissue growth (see [2]), which is a modification of the model of Eyles, King and Styles (2019) [1]. The model couples a Poisson equation on the domain with a forced mean curvature flow of the free boundary, with nontrivial bulk–surface coupling in both the velocity law of the evolving surface and the boundary condition of the Poisson equation. The numerical method discretises evolution equations for the mean curvature and the outer normal and it uses a harmonic extension of the surface velocity into the bulk; the strong formulation consists of four coupled groups of equations:
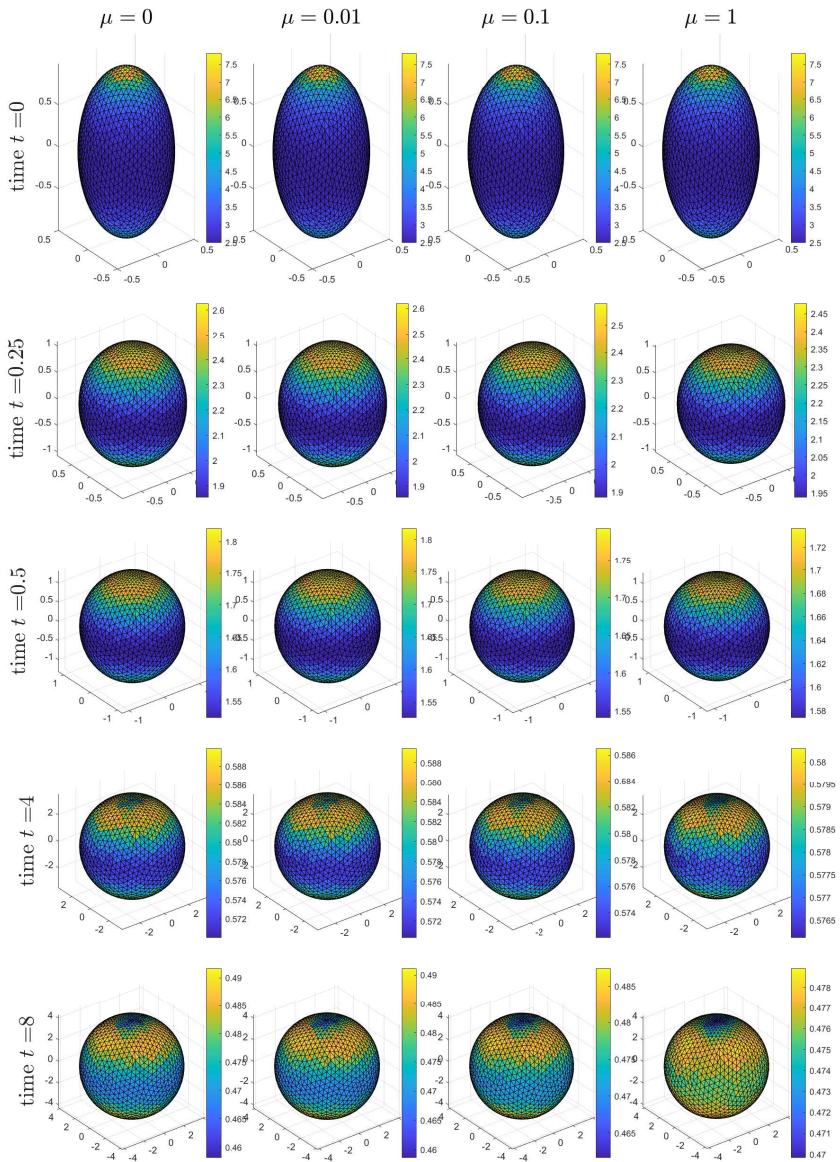
FIGURE 1. Numerical solutions with varying regularisation parameter $\mu = 0$, 0.01, 0.1, 1 (column-wise from left to right).

$$(1) \quad \begin{cases} \quad -\Delta u = -1 & \text{in } \Omega(t), \\ \quad \partial_\nu u - \mu \Delta_\Gamma u + \alpha u = \beta H + Q & \text{on } \Gamma(t); \end{cases}$$

$$(2) \quad \begin{cases} \quad \partial^\bullet \nu = \beta \Delta_\Gamma \nu + \beta |A|^2 \nu - \alpha \nabla_\Gamma u & \text{on } \Gamma(t), \\ \quad \partial^\bullet H = \beta \Delta_\Gamma H + \beta |A|^2 H - \alpha \Delta_\Gamma u - \alpha |A|^2 u & \text{on } \Gamma(t), \\ \quad v_\Gamma = V \nu \quad \text{with } V = -\beta H + \alpha u & \text{on } \Gamma(t); \end{cases}$$

$$(3) \quad \begin{cases} \quad -\Delta v = 0 & \text{in } \Omega(t), \\ \quad v = v_\Gamma & \text{on } \Gamma(t); \end{cases}$$

$$(4) \quad \begin{cases} \quad \partial_t X = v \circ X & \text{on } \Omega^0 \cup \Gamma^0. \end{cases}$$

The term $\mu \Delta_\Gamma u$ in the first equation is a regularisation term, which does not appear in [1], but is required by the presented analysis.

The spatial semi-discretisation using evolving bulk–surface finite elements admits a convergence analysis in the case of continuous finite elements of polynomial degree at least two. The error analysis combines stability estimates and consistency estimates to yield optimal-order H^1-norm error bounds for the computed tissue pressure u and for the surface position X, velocities v_Γ and v, normal vector ν and mean curvature H. We have presented some numerical experiments illustrating and complementing our theoretical results.

A numerical experiment. Figure 1 briefly reports on the minimal effects of the regularisation $\mu = 0$, 0.01, 0.1, 1 (column-wise left to right) with a fixed source $Q = 1.5$, and fixed model parameters $\alpha = 1$ and $\beta = 1$.

REFERENCES

[1] J. Eyles, J. King, and V. Styles, *A tractable mathematical model for tissue growth*, Interfaces Free Bound., **21**(4) (2019), 463–493.
[2] D. Edelmann, B. Kovács, and Ch. Lubich, *Numerical analysis of an evolving bulk–surface model of tumour growth*, (2024), arXiv:2401.09372.

A weak-strong uniqueness principle for De Giorgi type solutions to the Mullins-Sekerka equation

JULIAN FISCHER

(joint work with Sebastian Hensel, Tim Laux, and Theresa Simon)

The Mullins-Sekerka equation describes volume-preserving phase separation and coarsening processes; it arises in particular as the sharp-interface limit of the Cahn-Hilliard equation with double-well potential. In the Mullins-Sekerka equation, the motion of an interface $I(t)$ between two phases $\Omega^+(t) = \{x : \chi(x,t) = 1\}$ and

$\Omega^-(t) = \{x : \chi(x,t) = 0\}$ is determined by the chemical potential $u = u(x,t)$; more precisely, the interface moves with normal velocity V_n given by

$$V_n = n \cdot [[\nabla u]] \qquad \text{on } I(t),$$

where n denotes the surface normal of $I(t)$ and $[[\cdot]]$ denotes the jump across the interface. The system is closed by the piecewise harmonicity of the chemical potential

$$\Delta u = 0 \qquad \text{in } \Omega \setminus I(t)$$

and the Gibbs-Thomson law prescribing the chemical potential u to be equal to the mean curvature H of the phase interface

$$u(x,t) = H(x,t) \qquad \text{on } I(t).$$

Classical solutions to the Mullins-Sekerka equation have been constructed by Chen, Hong, and Yi [2] and by Escher and Simonett [3]. A conditional proof of existence of weak solutions has been given by Luckhaus and Sturzenhecker [10], while Röger [12] provided the first unconditional proof of existence. Recently, Hensel and Stinson developed a notion of weak solutions based on De Giorgi's approach to solutions for gradient flows [9]. Note that the aforementioned weak notions of solutions are formulated in terms of the phase indicator function χ; the harmonicity of the chemical potential and the evolution of the interface are merged into a single equation $\partial_t \chi = \Delta u$ that must be satisfied in the sense of distributions, and the Gibbs-Thomson law is imposed via a weak formulation in terms of the phase indicator function χ.

As our main result, in [5] *we establish a weak-strong uniqueness principle for the two-phase Mullins-Sekerka equation in the planar case*: As long as a classical solution to the evolution problem exists, any weak solution in the sense of Hensel-Stinson [9] must coincide with it. In particular, in the absence of geometric singularities their notion of weak solutions does not introduce a mechanism for (unphysical) nonuniqueness. We also derive a stability estimate with respect to changes in the data. We emphasize that our result in [5] also applies to solutions in the sense of Luckhaus-Sturzenhecker [10], assuming that they satisfy a sharp energy dissipation estimate.

Our method is based on the notion of relative entropies for interface evolution problems: We consider the relative energy given as

$$(1) \qquad E[\chi|\xi] := \int_\Omega 1 - \xi \cdot \frac{\nabla \chi}{|\nabla \chi|} \, d|\nabla \chi|$$

where ξ denotes a suitable extension of the unit normal vector field of the strong solution subject to the length constraint $|\xi| \le 1$. Observe that the relative energy (1) controls quantities like

$$\int_\Omega \left| \frac{\nabla \chi}{|\nabla \chi|} - \xi \right|^2 d|\nabla \chi|,$$

thereby measuring the "difference" between the two interfaces in a tilt-excess-like sense. The general notion of relative entropies goes back to Dafermos and Di Perna;

for geometric quantities, a notion of relative energy for curves was developed by Jerrard and Smets [11] and the above stated analogous notion for interfaces by the second and the first author [6]. A notion of relative energy for partitions based on the concept of calibrations was developed by the four authors [4]. In recent years the relative entropy method has also proven highly useful for the justification of sharp-interface limits [1, 8, 7].

Besides the notion of relative energy (1), two further key ingredients for our weak-strong uniqueness result are

- An estimate showing that whenever the interface in the weak solution is not a graph over the interface of the strong solution, the energy dissipation term from the weak solution dominates all other terms in the evolution of the relative energy and leads to an estimate of the form

$$\frac{d}{dt}E[\chi|\xi] \leq -\frac{1}{2}\int_\Omega |\nabla u|^2 \, dx.$$

- The construction of an auxiliary chemical potential $\tilde{u}$, which is harmonic in each of the phases of the weak solution, but takes the curvature of the strong solution as a boundary condition on the phase interface of the weak solution.

Combining these ingredients with stability properties of the Dirichlet-to-Neumann operator with respect to perturbations of the domain, they allow us to establish a stability estimate for the relative energy of the form

$$\frac{d}{dt}E[\chi|\xi] \leq -\frac{1}{2}\int_\Omega |\nabla u - \nabla \tilde{u}|^2 \, dx + CE[\chi|\xi]$$

and conclude with a Gronwall estimate.

References

[1] H. Abels, J. Fischer, M. Moser, *Approximation of classical two-phase flows of viscous incompressible fluids by a Navier-Stokes/Allen-Cahn system*, Preprint (2023), arXiv:2311.02997.

[2] X. Chen, J. Hong, F. Yi, *Existence, uniqueness, and regularity of classical solutions of the Mullins-Sekerka problem*, Comm. Partial Differential Equations **21** (1996), 1705–1727.

[3] J. Escher, G. Simonett, *Classical solutions for Hele-Shaw models with surface tension*, Adv. Differential Equations **2** (1997), 619–642.

[4] J. Fischer, S. Hensel, T. Laux, T. Simon, *The local structure of the energy landscape in multiphase mean curvature flow: Weak-strong uniqueness and stability of evolutions*, accepted for publication at J. Eur. Math. Soc. (JEMS) (2024), arXiv:2003.05478v2.

[5] J. Fischer, S. Hensel, T. Laux, T. Simon, *A weak-strong uniqueness principle for the Mullins–Sekerka equation*, in preparation (2024).

[6] J. Fischer and S. Hensel, *Weak-strong uniqueness for the Navier-Stokes equation for two fluids with surface tension*, Arch. Ration. Mech. Anal. **236** (2020), 967–1087.

[7] J. Fischer, T. Laux, T. Simon, *Convergence rates of the Allen-Cahn equation to mean curvature flow: a short proof based on relative entropies*, SIAM J. Math. Anal. **52** (2020), 6222–6233.

[8] J. Fischer, A. Marveggio, *Quantitative convergence of the vectorial Allen-Cahn equation towards multiphase mean curvature flow*, accepted for publication in Annales Henri Poincaré C (2024), arXiv:2203.17143.

[9] S. Hensel, K. Stinson, *Weak solutions of Mullins–Sekerka flow as a Hilbert space gradient flow*, Arch. Ration. Mech. Anal. **248** (2024), 8.

[10] S. Luckhaus, T. Sturzenhecker, *Implicit time discretization for the mean curvature flow equation*, Calc. Var. Partial Differential Equations **3** (1995), 253–271.

[11] R. Jerrard and D. Smets, *On the motion of a curve by its binormal curvature*, J. Eur. Math. Soc. (JEMS) **17** (2015), 1487–1515.

[12] M. Röger, *Existence of weak solutions for the Mullins–Sekerka flow*, SIAM J. Math. Anal. **37** (2005), 291–301.

Convergent finite element schemes and mesh smoothing for geometric evolution problems

BJÖRN STINNER

(joint work with Paola Pozzi)

Mesh-based computational methods for geometric evolution problems require adaptation and smoothing to enable long-term simulations. We consider finite element schemes based on classical approaches for geometric evolution equations but augmented with the gradient of the Dirichlet energy, or a variant of it, which is known to produce a tangential mesh movement beneficial for the mesh quality. However, this contribution ideally is accounted for in a way such that the impact on the physics of the evolution is minimal.

We focus on the one-dimensional case, i.e., the geometric evolution of curves. Our general aim is to derive semi-discrete finite element schemes for which convergence can be proved and quantified. Two cases are discussed.

Case 1: Triod evolution by curvature flow. We consider three curves moving by curvature connected at a triple junction at which angles of 120° are prescribed. In [3] an approach for single, closed curves is analysed, which approximates the movement in normal direction. However, some tangential movement is required to ensure that the triple junction can move, too. The approach in [1] provides such an addition. However, with that approach the angle condition at the triple junction is not straightforward to realise.

Our idea has been to use the first approach for the geometric evolution in normal direction and to ensure that the angle condition is met, and then to augment the scheme with the second approach for some tangential movement, scaled with a small parameter $\varepsilon > 0$ that enables to control the impact on the geometric (normal) evolution. The weak formulation of the problem essentially reads:

$$\sum_{i=1}^{3} \left(\int_0^1 (u_t^{(i)} \cdot \nu^{(i)})(\varphi^{(i)} \cdot \nu^{(i)})|u_x^{(i)}| + \varepsilon(u_t^{(i)} \cdot \tau^{(i)})(\varphi^{(i)} \cdot \tau^{(i)})|u_x^{(i)}|^2 dx \right)$$

$$= -\sum_{i=1}^{3} \left(\int_0^1 \tau^{(i)} \cdot \varphi_x^{(i)} + \varepsilon u_x^{(i)} \cdot \varphi_x^{(i)} dx \right).$$

where the functions $u^{(i)} : (0,1) \times (0,T) \to \mathbb{R}^2$, $i = 1, 2, 3$, are parametrisations of the three curves and $\tau^{(i)}$ and $\nu^{(i)}$ are the unit tangent and normal vectors. In

strong form the problem reads

$$(u_t^{(i)} \cdot \nu^{(i)})\nu^{(i)} = (1 + \varepsilon|u_x^{(i)}|)H^{(i)},$$

$$(u_t^{(i)} \cdot \tau^{(i)})\tau^{(i)} = \frac{1}{|u_x^{(i)}|^2}(\tau^{(i)} \cdot u_{xx})\tau^{(i)},$$

$$0 = \sum_{i=1}^{3} \tau^{(i)} + \varepsilon u_x^{(i)},$$

where H is the curvature. The terms with ε are the deviations from the problem that we want to solve.

The weak formulation is suitable to linear finite elements, and we have the following results for the solution to the semi-discrete problem:

Theorem 1 (*h*-**convergence** (ε **fixed**)). *Assume that there is a unique (sufficiently regular) solution* $\Gamma = (u^{(1)}, u^{(2)}, u^{(3)})$ *with*

$$0 < c_0 \leq |u_x^{(i)}| \leq 1/c_0.$$

For all h small enough the semi-discrete problem has a unique solution $\Gamma_h = (u_h^{(1)}, u_h^{(2)}, u_h^{(3)})$ *satisfying*

$$\int_0^T \|u_t^{(i)} - u_{ht}^{(i)}\|_{L^2((0,1))}^2 dt + \sup_{t \in [0,T]} \|u_x^{(i)}(t) - u_{hx}^{(i)}(t)\|_{L^2((0,1))}^2 \leq Ch^2, \quad i = 1, 2, 3.$$

The constant $C > 0$ *depends on* c_0, T, *norms of the* $u^{(i)}$, *and scales with* ε^{-1}.

The proof follows the lines of [1] and uses a fixed-point argument. For further details we refer to [4]. The latter work also contains numerical examples that support the theoretical findings.

Case 2: Elastic flow with tangential mesh movement. When studying the elastic flow of curves, often, the length functional (multiplied with some penalty parameter $\lambda > 0$) is added to the elastic energy to ensure that curves do not expand to infinity. The L^2 gradient flow then still is geometric as the energy only changes when varying the curve in the normal direction.

Our idea has been to replace the length functional with the Dirichlet energy and to consider the L^2 gradient flow of

$$\mathcal{D}_\lambda(u) = \frac{1}{2}\int_0^1 |\kappa|^2 dx + \frac{1}{2}\lambda\int_0^1 |u_x|^2 dx,$$

where $\kappa = \partial_{ss}u$ is the curvature vector (second arc-length derivative of the parametrisation $u : [0, 1] \to \mathbb{R}^n$). Critical points of the two energies are the same modulo rescaling the penalty parameter λ. Thanks to the Dirichlet energy, tangential mesh movement is ensured to enable long-term computations. In turn, the resulting flow is not geometric due to these tangential contributions.

The weak formulation is based on [2] and uses second order splitting:

$$\int_0^1 (u_t \cdot \phi)|u_x| - \int_0^1 \frac{P\kappa_x \cdot \phi_x}{|u_x|} - \frac{1}{2}\int_0^1 |\kappa|^2(\tau \cdot \phi_x) + \lambda\int_0^1 u_x \cdot \phi_x = 0,$$

$$\int_0^1 (\kappa \cdot \psi)|u_x| + \int_0^1 (\tau \cdot \psi_u) = 0,$$

where $P = I - \tau \otimes \tau$ is the projection to the normal space. We assume that there is a unique smooth, periodic (in space) solution, $u : (0, T) \times (0, 1) \to \mathbb{R}^n$ which is regular:

$$c_0 \le |u_x| \le C_0, \qquad\qquad |\kappa| \le C_0.$$

Using linear finite elements and denoting the interpolation operator with I_h the semi-discrete problem is:

$$\int_0^1 I_h(u_{ht} \cdot \phi_h)|u_{hx}| - \int_0^1 \frac{P_h \kappa_{hx} \cdot \phi_{hx}}{|u_{hx}|} - \frac{1}{2}\int_0^1 I_h(|\kappa_h|^2)(\tau_h \cdot \phi_{hx})$$

$$+ \lambda\int_0^1 u_{hx} \cdot \phi_{hx} = 0,$$

$$\int_0^1 I_h(\kappa_h \cdot \psi_h)|u_{hx}| + \int_0^1 (\tau_h \cdot \psi_{hx}) = 0,$$

where $P_h = I - \tau_h \otimes \tau_h$. As the continuous problem, it satisfies a natural energy (dissipation) identity:

$$\int_0^1 I_h(|u_{ht}|^2)|u_{hx}| + \frac{d}{dt}\left\{ \frac{1}{2}\int_0^1 I_h(|\kappa_h|^2)|u_{hx}| + \frac{\lambda}{2}\int_0^1 |u_{hx}|^2 \right\} = 0.$$

Theorem 2 (Convergence and error estimate). *For all h small enough the semi-discrete problem has a unique solution and is such that*

$$\sup_{t\in[0,T]} \|u(t,\cdot) - u_h(t,\cdot)\|_{H^1}^2 + \int_0^T \|u_t(t,\cdot) - u_{ht}(t,\cdot)\|_{L^2}^2 dt \le Ch^2,$$

$$\sup_{t\in[0,T]} \|\kappa(t,\cdot) - \kappa_h(t,\cdot)\|_{L^2}^2 + \int_0^T \|\kappa_u(t,\cdot) - \kappa_{hu}(t,\cdot)\|_{L^2}^2 dt \le Ch^2.$$

The proof is based on [2]. Some technical estimates are simplified thanks to using the Dirichlet energy rather than the length functional, which makes controlling the length element $|u_x|$ easier. The publication [5] contains the details of the proof. It also presents simulation results that support the theory and illustrates the behaviour of evolution.

REFERENCES

[1] K. Deckelnick, G. Dziuk, *On the Approximation of the Curve Shortening Flow*, in Calculus of Variations, Applications and Computations: Pont-à-Mousson, 1994, Pitman Research Notes in Mathematics Series (1994), 100–108.

[2] K. Deckelnick, G. Dziuk, *Error analysis for the elastic ow of parametrized curves*, Math. Comp. **78,266** (2009), 645–671.

[3] G. Dziuk, *Convergence of a Semi-Discrete Scheme for the Curve Shortening Flow*, Math. Models Methods Appl. Sci. **4**,4 (1994), 589–606.

[4] P. Pozzi, B. Stinner, *On motion by curvature of a network with a triple junction*, SMAI J Comput. Math. **7** (2021), 27–55.

[5] P. Pozzi, B. Stinner, *Convergence of a scheme for an elastic flow with tangential mesh movement*, ESAIM: Mathematical Modelling and Numerical Analysis, **57**,2 (2023), 445–466.

Analysis of a quasi-variational contact problem arising in thermoelasticity

AMAL ALPHONSE

(joint work with Carlos N. Rautenberg and Jose Francisco Rodrigues)

We discuss a model of a thermoforming process involving a system of PDEs with an implicit obstacle constraint that describes the thermoelastic behaviour of materials in the process. The obstacle is *a priori* unknown and it depends on the other unknown variables in the system leading to a *quasi-variational* problem. Thermoforming is an industrial process that aims to manufacture precision parts and it involves forcing a sheet/membrane u onto a mould $\Phi_0 \equiv 0$ (we can assume it is zero without much loss of generality) by means of air pressure (or other mechanisms). The sheet is heated (with temperature denoted by θ_1) in order to enter the shape-acquiring phase and to reduce brittleness of the material, while the mould (temperature denoted by θ_2) is not; in fact, the mould might be cooled. The temperature difference triggers a complex heat transfer process during contact, and this is coupled with changes of shape of the mould (whose resulting position is denoted by Φ) and sheet due to the thermal linear expansion phenomenon. Lastly, the membrane takes on the shape of the mould via a cooling down phase. The full model as described is evolutionary; we focus in the talk on the following associated stationary counterpart: with

$$A_\theta u := -\nabla \cdot (a(\theta_1)\nabla u),$$

for $i = 1, 2$,

$$
\begin{align}
\text{(1a)} \quad & -\kappa_i \Delta \theta_i + c_i \theta_i = h_i + (-1)^i b_i(\theta_1 - \theta_2)\chi_{\{u=\Phi\}} && \text{in } \Omega, \\
\text{(1b)} \quad & \partial_n \theta_i = 0 && \text{on } \partial\Omega, \\
\text{(1c)} \quad & -\Delta\Phi = \alpha(\theta_1 - \theta_2)\chi_{\{u=\Phi\}} + g && \text{in } \Omega, \\
\text{(1d)} \quad & \Phi = 0 && \text{on } \partial\Omega, \\
\text{(1e)} \quad & u \leq \Phi, \quad A_\theta u \leq f, \quad (A_\theta u - f)(u - \Phi) = 0 && \text{in } \Omega, \\
\text{(1f)} \quad & u = 0 && \text{on } \partial\Omega.
\end{align}
$$

Here, $\kappa_i > 0$, $c_i > 0$, $f, g, h_i \colon \Omega \to \mathbb{R}$, $b_i \geq 0$ and $\alpha > 0$ for $i = 1, 2$ are given data, $\chi_{\{u=\Phi\}}$ is the characteristic function of the contact set and $\partial_n \theta$ denotes the normal derivative at the boundary $\partial\Omega$ of a bounded Lipschitz domain Ω. We

assume throughout that

(2) $a \in C^1(\mathbb{R})$ with $0 < \lambda_1 \leq a \leq \lambda_2$,   and a' is bounded.

Let us briefly discuss the assumptions and explain the role of the unknown quantities that appear in (1). We assume that displacements of the membrane and the mould occur only in one spatial direction and denote those displacements as u and Φ, respectively. The initial or undeformed membrane and mould are denoted respectively by $u_0 \equiv 0$ and Φ_0; hence the deformed structures are given by u and $\Phi + \Phi_0$, and the former is assumed to be below the latter. Additionally, we do not allow for displacement in the boundary $\partial\Omega$ and we assume that mechanical contact has a negligible effect on the deformation of the mould. We take for granted that heat transfer between the membrane and mould is present only when contact occurs and that boundaries are insulated; as mentioned θ_1 and θ_2 denote the temperatures of the membrane and the mould, respectively. Furthermore, the linear thermal expansion effect on the mould appears in the displacement equation as a term proportional to the temperature difference $\theta_1 - \theta_2$ and is active only when contact is present. Additionally, we do not assume thermal expansion of the membrane due to the fact that this term is significantly smaller than the force pushing the membrane. Without loss of generality, when Φ_0 is smooth, we can assume $\Phi_0 \equiv 0$. The problem described above is a highly complex type of *contact problem in thermoelasticity* as it couples elastic with heat transfer phenomena and at the same time the constraint associated to the non-penetration condition between the membrane and the mould holds. In particular, the static conduction of heat across the two thermoelastic materials depends on the extent of the contact area which in turn depends on the thermoelastic displacement.

Observe that (1) is a free boundary problem since the boundary of the contact set $\{u = \Phi\}$ is not known *a priori*.

In the talk, we prove the following results. We first look at existence of a notion of solution which is slightly weaker than the natural one. Define the graph

$$J(s) = \begin{cases} 1 & : s < 0 \\ [0,1] & : s = 0 \\ 0 & : s > 0. \end{cases}$$

We say $(\theta_1, \theta_2, u, \Phi) \in H^1(\Omega)^2 \times H_0^1(\Omega)^2$ is a **weak solution** if

$$\int_\Omega \kappa_1 \nabla\theta_1 \cdot \nabla\eta + c_1\theta_1\eta = \int_\Omega (h_1 - b_1(\theta_1 - \theta_2)\chi)\eta \quad \forall \eta \in H^1(\Omega),$$

$$\int_\Omega \kappa_2 \nabla\theta_2 \cdot \nabla\zeta + c_2\theta_2\zeta = \int_\Omega (h_2 + b_2(\theta_1 - \theta_2)\chi)\zeta \quad \forall \zeta \in H^1(\Omega),$$

$$\int_\Omega \nabla\Phi \cdot \nabla\xi = \alpha \int_\Omega ((\theta_1 - \theta_2)\chi + g)\xi \quad \forall \xi \in H_0^1(\Omega),$$

$$u \in \mathbb{K}(\Phi) : \int_\Omega a(\theta_1)\nabla u \cdot \nabla(u - v) \leq \int_\Omega f(u - v) \qquad \forall v \in \mathbb{K}(\Phi)$$

holds, where

$$\chi \in J(\Phi - u).$$

Theorem 1 (**Weak solutions**). *If*

$$c_0 := \min \left\{ c_1 - (b_2 - b_1)^+/4, c_2 - (b_1 - b_2)^+/4 \right\} > 0,$$

(1) *has a weak solution.*

We say $(\theta_1, \theta_2, u, \Phi) \in (H^2_{\mathrm{loc}}(\Omega))^4 \cap (H^1(\Omega)^2 \times H^1_0(\Omega)^2)$ is a **regular solution** if the above weak formulation holds and

$$\chi = \chi_{\{\Phi = u\}}.$$

Theorem 2 (**Regular solutions**). *If additionally*

$$c_2/\kappa_2 \geq c_1/\kappa_1 \qquad and \qquad h_1/\kappa_1 \geq h_2/\kappa_2 \geq 0,$$
$$f + \nabla \cdot (a(\theta_1)\nabla\Phi) > 0 \quad a.e. \ in \ \Omega,$$

we have $\chi = \chi_{\{u=\Phi\}}$ and (1) *has a regular solution.*

Notice that we needed additional assumptions to ensure existence of regular solutions; this can be roughly thought of as 'strong forces lead to regular solutions'.

REFERENCES

[1] A. Alphonse, C. N. Rautenberg, J.F. Rodrigues, *Analysis of a quasi-variational contact problem arising in thermoelasticity*, Nonlinear Analysis 217, 112728, (2022).

Understanding microswimmer locomotion with Cosserat rods

THOMAS RANNER

(joint work with Netta Cohen, Lukas Deutz, Thomas P. Ilett,
and Yongxing Wang)

1. INTRODUCTION

The nematode *Caenorhabditis elegans* has been used for over 50 years as a genetic model for understanding developmental biology and neurobiology. It has approximately 1000 cells in total, of which 302 are neurons. Despite this *C. elegans* manages to live freely: for example, it moves around, reproduces, eats, avoids predators. For almost all of the last 50 years, *C. elegans* and especially its locomotion has been studied on a two-dimensional plate under a microscope, see Figure 1 (left). Its 2D locomotion is very well characterised consisting of periods of sinosoidal forward undulations interrupted by turning and reversal manoeuvres [4].
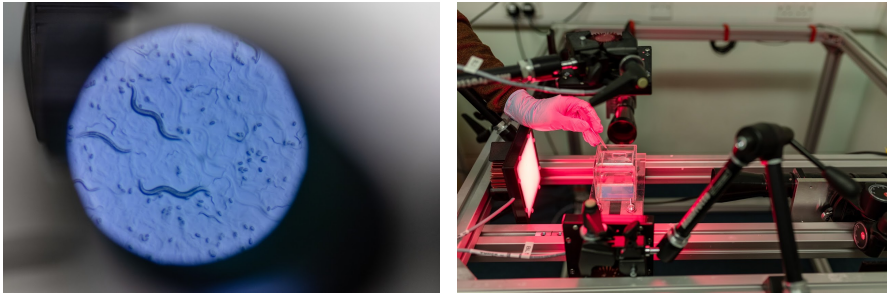
FIGURE 1. (Left): *C. elegans* on a 2D plate. (Right): 3D experimental set up.

Recent years have seen several groups (including ours, Figure 1, right) interested in capturing three-dimensional locomotion of *C. elegans*. Our previous study [5] has produced a large dataset of over 4 hours of fully reconstructed three-dimensional postures (midlines only). We find that in fact postures in these recordings are typically nonplanar with new manoeuvres such as a torsion roll [2] and a 3D coiling gait [7] identified.

2. The computational model

For full details of the model and its derivation are given in [6] based on ideas by [3] and [1]. We give a brief summary here.

(A) Schematic of Cosserat rod

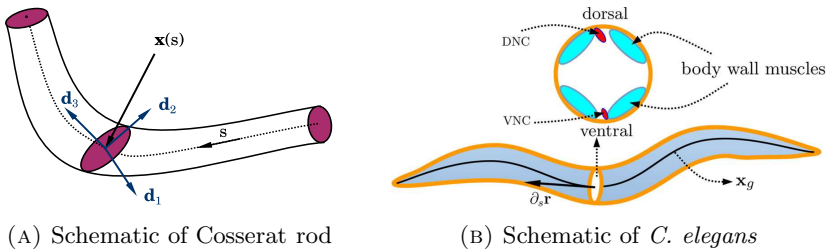(B) Schematic of *C. elegans*

FIGURE 2. Schematics for geometry and anatomy of model.

To describe the geometry of *C. elegans* body, we use a Cosserat rod. A Cosserat rod describes the geometry of a long thin body that can undergo bending, twisting, stretching and shearing. We describe the rod using a parametrisation of the midline $\vec{x} \colon [a, b] \to \mathbb{R}^3$ and an orthonormal frame $\{\vec{d_1}, \vec{d_2}, \vec{d_3}\} \colon [a, b] \to SO^3$, see Figure 2a for an example. The orthonormal frame allows us to parametrise the (small) thickness by describing the orientation of a set of discs akin to a set of salami slices from a sausage. We note that for a Cosserat rod we expect $\vec{d_3}$ to be close to, but not equal to, the tangent to the midline $\partial_s \vec{x}$. The orientation of the thickness of the rod is important in modelling *C. elegans* anatomy as the muscles,

and especially their neural connectivity, are not symmetric about the midline, see Figure 2b. In particular, the rod formulation allows us to distinguish between bending (and shearing) in different directions.

Rather than working with the frame $\{\vec{d_1}, \vec{d_2}, \vec{d_3}\}$ directly, we parametrise the frame using three rotation (Euler) angles $\vec{\theta} = [\alpha, \beta, \gamma] \colon [a, b] \to \mathbb{R}^3$. The rotations describe how a global coordinate system, often called the lab reference frame, $\vec{e_1}, \vec{e_2}, \vec{e_3}$ can be rotated onto $\vec{d_1}, \vec{d_2}, \vec{d_3}$. This gives us a convenient way to describe the geometry without having to impose any external constraints.

The conservation of linear and angular momentum of a Cosserat rod is given in the classical textbook by [1]. We adopt constitutive laws assuming a linear relationship between internal force and strain and between internal torque and (generalised) curvature. Combining the balance of linear and angular momentum with our constitutive relation gives the continuous model.

The finite element formulation is based on the formulation of the continuous problem in the reference configuration, also known as the total Lagrangian formulation. We approximate solution variables as vector-valued piecewise linear functions.

3. Using the model to augment the dataset

The dataset we work with consists of a sequence of midlines but to understand the locomotion of *C. elegans* we must also be able to determine the frame. To attempt to do this, we pose the inverse problem: can we determine the forces and torques which best match the midlines in the dataset by using our forwards model? Since our forwards model maps forces and torques to midlines *and frames*, the inverse problem automatically gives a sequence of candidate frames which match the midline and are consistent with the model.

We formulate the inverse problem in an optimal control framework where we seek to minimise an objective function which depends on input forces and torques which move the solution of the model from one time point to the next - so called piecewise-in-time control. We includes an L^2 data mismatch term and regularisation terms both on the input forces and torques as well as on the output frame: We penalise deviations of the $\vec{d_3}$ director from the tangent direction, high (generalised) curvatures and high angular velocity of the frame. The regularisation terms on the frame are required for well-posedness since the model has a rotational degree of freedom.

Results show that we can accurately capture the dynamics of the data set using our control framework. We accurately capture synthetic and real data sets. Unfortunately the quantitative results depend on the regularisation parameters, which makes it difficult to answer questions about the underlying biological mechanisms.

References

[1] S S Antman. Problems in nonlinear elasticity. *Nonlinear Problems of Elasticity*, pages 513–584, 2005.

[2] A Bilbao, A K Patel, M Rahman, S A Vanapalli, and J Blawzdziewicz. Roll maneuvers are essential for active reorientation of Caenorhabditis elegans in 3d media. *Proceedings of the National Academy of Sciences*, 115(16):E3616–E3625, 2018.

[3] D Q Cao and R W Tucker. Nonlinear dynamics of elastic rods using the cosserat theory: Modelling and simulation. *International Journal of Solids and Structures*, 45(2):460–477, January 2008.

[4] N Cohen and J H Boyle. Swimming at low reynolds number: a beginners guide to undulatory locomotion. *Contemporary Physics*, 51(2):103–123, 2010.

[5] T P Ilett, O Yuval, T Ranner, N Cohen, and D C Hogg. 3d shape reconstruction of semi-transparent worms. In *Proceedings of the IEEE/CVF Conference on Computer Vision and Pattern Recognition (CVPR)*, pages 12565–12575, 2023.

[6] Y Wang, T Ranner, T P Ilett, Y Xia, and N Cohen. A monolithic optimal control method for displacement tracking of cosserat rod with application to reconstruction of *C. elegans* locomotion. *Computational Mechanics*, 71(3):409–432, 2022.

[7] O Yuval. *The neuromechanical control of Caenorhabditis elegans head motor behavior in a 3D environment*. PhD thesis, University of Leeds, 2022.

SFEM for Penalty and Lagrange formulations of surface Stokes

Achilleas Mavrakis

We will consider two different discrete formulations of the surface Stokes problem using a surface finite element approximation. These formulations have been derived and proven to be well-posed in the continuous case [1], involving the tangential surface Stokes equation. More precisely, we use Taylor-Hood finite elements, and thus our discrete velocity vector belongs to $H^1(\Gamma_h)$. We need to enforce a tangential constraint. The first formulation uses a penalty term in order to enforce a tangential condition on the discrete velocity (see also [1]), while the second one enforces the tangential condition via an extra Lagrange multiplier. We analyze well-posedness and convergence results for these two different discrete formulations using, as mentioned, $\mathcal{P}_{k_u}/\mathcal{P}_{k_p}$ Taylor-Hood elements for the penalty and $\mathcal{P}_{k_u}/\mathcal{P}_{k_p}/\mathcal{P}_{k_\lambda}$ Taylor-Hood finite elements for the Lagrange multiplier formulation.

So let us define our discrete formulations. Considering parametric finite element space [3], $S_{h,k_g}^{k_u} := \{u_h \in C^0(\Gamma_h) : u_h|_T = \tilde{u}_h \circ F_T^{-1} \text{ for some } \tilde{u}_h \in S_{h,1}^{k_u}, \text{ for all } T \in \mathcal{T}_h\}$, for mapping $F_T : \{\Gamma_h^{(1)}, \tilde{\mathcal{T}}_h\} \to \{\Gamma_h, \mathcal{T}_h\}$, $\tilde{\mathcal{T}}_h$ the linear triangulation on the planar triangulated surface $\Gamma_h^{(1)}$, we have the spaces

$$\mathbf{V}_h = (S_{h,k_g}^{k_u})^3 \subset (H^1(\Gamma_h))^3, \quad Q_h = S_{h,k_g}^{k_{pr}} \cap L_0^2(\Gamma_h), \quad \Lambda_h = S_{h,k_g}^{k_\lambda} \subset H^1(\Gamma_h).$$

So, since our finite element spaces are subspaces of $H^1(\Gamma_h)$ we have

- **Penalty method :** Find $(\mathbf{u}_h, p_h) \in \mathbf{V}_h \times Q_h$ such that,

(PhP)
$$\begin{cases} \alpha_h^\tau(\mathbf{u}_h, \mathbf{v}_h) + b_h(\mathbf{v}_h, p_h) = (\mathbf{f}, \mathbf{P}_h \mathbf{v}_h)_{L^2(\Gamma_h)} & \text{for all } \mathbf{v}_h \in \mathbf{V}_h, \\ \qquad\qquad\qquad b_h(\mathbf{u}_h, q_h) = (-g_h, q_h)_{L^2(\Gamma_h)} & \text{for all } q_h \in Q_h, \end{cases}$$

- $\alpha_h^\tau(\mathbf{u}_h, \mathbf{v}_h) := a_{T,h}(\mathbf{u}_h, \mathbf{v}_h) + \tau(\mathbf{u}_h \cdot \tilde{\mathbf{n}}_h, \mathbf{v}_h \cdot \tilde{\mathbf{n}}_h)$
- $a_{T,h}(\mathbf{u}_h, \mathbf{v}_h) = \int_{\Gamma_h} E_{T,h}(\mathbf{u}_h) : E_{T,h}(\mathbf{v}_h) + \mathbf{P}_h \mathbf{u}_h \cdot \mathbf{P}_h \mathbf{v}_h \, d\sigma_h$

$$- E_{T,h}(\mathbf{u}_h) = E_h(\mathbf{u}_h) - (\mathbf{u}_h \cdot \mathbf{n}_h)\mathbf{H}_h$$

$$- b_h(\mathbf{u}_h, q_h) := \int_{\Gamma_h} \mathbf{u}_h \cdot \nabla_{\Gamma_h} q_h \, d\sigma,$$

where $\mathbf{n}_h, \mathbf{H}_h$ are the known geometric approximations (see [3]). On the other hand $\tilde{\mathbf{n}}_h$ is a different higher order approximation of the normal, which is needed for optimal convergence $\|\mathbf{n} - \tilde{\mathbf{n}}_h\|_{L^\infty(\Gamma_h)} \leq ch^{k_p}$, $k_p \geq k_g$, k_g the geometric order of approximation. Lastly, one may wonder what about the penalty parameter τ? Our stability and convergence analysis will determine it.

- **Lagrange multiplier method :** Determine $(\mathbf{u}_h, \{p_h, \lambda_h\}) \in \mathbf{V}_h \times Q_h \times \Lambda_h$ such that

(LhP) $\quad \begin{cases} \alpha_h^\lambda(\mathbf{u}_h, \mathbf{v}_h) + \tilde{b}_h(\mathbf{v}_h, \{p_h, \lambda_h\}) & = (\mathbf{f}_h, \mathbf{v}_h) \ \text{ for all } \mathbf{v}_h \in \mathbf{V}_h, \\ \tilde{b}_h(\mathbf{u}_h, \{q_h, \xi_h\}) & = 0 \qquad \text{for all } \{q_h, \xi_h\} \in Q_h \times \Lambda_h, \end{cases}$

$$- \alpha_h^\lambda(\mathbf{u}_h, \mathbf{v}_h) := \int_{\Gamma_h} E_h(\mathbf{u}_h) : E_h(\mathbf{v}_h) d\sigma_h + \int_{\Gamma_h} \mathbf{u}_h \cdot \mathbf{v}_h d\sigma_h, = a_h(\mathbf{u}_h, \mathbf{v}_h)$$

$$- \tilde{b}_h(\mathbf{v}_h, \{p_h, \lambda_h\}) := \int_{\Gamma_h} \mathbf{v}_h \cdot \nabla_{\Gamma_h} p_h \, d\sigma_h + \int_{\Gamma_h} \lambda_h \mathbf{v}_h \cdot \mathbf{n}_h \, d\sigma_h.$$

For the well-posedness we use the $\|\cdot\|_{L^2(\Gamma_h)}$ for the pressure p and Lagrange multiplier λ, while the norm of the velocity is dictated by the *discrete surface Korn's inequality*. That is, since our finite element vector functions are not tangential we may only have the following approximation

$$\|\mathbf{v}_h\|_{H^1(\Gamma_h)} \leq c(\|E_{T,h}(\mathbf{v}_h)\|_{L^2(\Gamma_h)} + \|\mathbf{P}_h \mathbf{v}_h\|_{L^2(\Gamma_h)} + h^{-1}\|\mathbf{v}_h \cdot \tilde{\mathbf{n}}_h\|_{L^2(\Gamma_h)}),$$

$\mathbf{v}_h \in H^1(\Gamma_h)^3$. Thus, for both formulations one uses their respective energy norms $\|\cdot\|_{\alpha_h^\tau}$ and $\|\cdot\|_{\alpha_h^\lambda}$. Notice for $\tau = ch^{-2}$ we have $\|\cdot\|_{H^1(\Gamma_h)} \leq c\|\cdot\|_{\alpha_h^\tau}$ while $\|\cdot\|_{H^1(\Gamma_h)} \leq ch^{-1}\|\cdot\|_{\alpha_h^\lambda}$ holds for the Lagrange formulation. The difficult part of proving well-posedness is proving that the discrete *inf-sup* condition holds,

$$\beta\|r_h\|_{L^2(\Gamma_h)} \leq \sup_{\mathbf{v}_h \in \mathbf{V}_h} \frac{|b_h(\mathbf{v}_h, r_h)|}{\|\mathbf{v}_{h\alpha}\|} \quad \forall r_h \in R_h,$$

where $\alpha = \alpha_h^\tau$, $r_h = q_h$ and $R_h = Q_h$ for the penalty formulation, and $\alpha = \alpha_h^\lambda$, $r_h = \{q_h, \lambda_h\}$, $R_h = Q_h \times \Lambda_h$ for the Lagrange multiplier method. This is done by using the "Verfürth's trick", i.e. choosing with the help of Scott-Zhang interpolant $\widetilde{I_h^z}$ [4] (we need its super-approximation property) a correct velocity (e.g. $\mathbf{v}_h = \widetilde{I_h^z}(\mathbf{v}_*) = \widetilde{I_h^z}(\mathbf{v}_T + \lambda_h^\ell \mathbf{n}_\Gamma)$ for the Lagrange approach), using the inf-sup condition of the continuous problem (see [1]) and calculating

(1) $\quad \sup_{\mathbf{v}_h \in \mathbf{V}_h} \frac{|\tilde{b}_h(\mathbf{v}_h, \{q_h, \lambda_h\})|}{\|\mathbf{v}_h\|_{\alpha_h^\lambda}} \geq \|\{q_h, \lambda_h\}\|_{L^2(\Gamma_h)} - ch\|\nabla_{\Gamma_h} q_h\|_{L^2(\Gamma_h)}.$

One then needs to control the last gradient term. We need to map back to the planar triangulation $\Gamma_h^{(1)}$ where the geometry is more suitable. Again choosing a tangent velocity $\tilde{\mathbf{v}}_h = \sum_{E \in \mathcal{E}_h} h_E^2 \varphi_E |\mathbf{s}_h^{(1)} \cdot \nabla_{\Gamma_h^{(1)}} \tilde{q}_h| \mathbf{s}_h^{(1)} \in \mathbf{V}_h$, where $\mathcal{E}_h$ the interior edges, $\mathbf{s}_h^{(1)} = \mathbf{n}_h^{(1),+} \times \mathbf{m}_h^{(1),+} = \mathbf{n}_h^{(1),-} \times \mathbf{m}_h^{(1),-}$ the cross product of the normal and conormal (it is therefore tangent across the edges), and φ_E a piecewise nodal surface finite element function which is zero everywhere apart the midpoint of

the edges, after heavy calculations one may control that term and thus prove the inf-sup condition.

So having proved the well-posedness for aforementioned norms, one then can calculate the following error bounds.

Theorem 1 (Penalty Method Error bounds). *Let $(\mathbf{u}_h, p_h) \in \mathbf{V}_h \times Q_h$ be the solution to the penalty discrete scheme* (PhP). *For $k_u \geq 1$, $k_{pr} = k_u - 1 \geq 0$, the geometric variables $k_p \geq k_g \geq 1$ and τ at most of order $\mathcal{O}(h^{-2})$ we have the following error estimates*

$$\|\mathbf{u} \; - \; \mathbf{u}_h^\ell\|_{L^2(\Gamma)} + h\|\mathbf{u}^{-\ell} - \mathbf{u}_h\|_{\alpha_h^\tau} + h\|p^{-\ell} - p_h\|_{L^2(\Gamma_h)}$$
$$\leq c(h^{m+1} + \tau^{-1/2}h^m + \tau^{1/2}h^{m+2})(\|\mathbf{u}\|_{H^{k_u+1}(\Gamma)} + \|p\|_{H^{k_{pr}+1}(\Gamma)} + \|\mathbf{f}\|_{L^2(\Gamma)}),$$

where $m = \min\{h^{k_u}, h^{k_{pr}+1}, h^{k_g-1}\tau^{-1/2}, h^{k_g}, h^{k_p}\tau^{1/2}\}$.

Theorem 2 (Lagrange Multiplier Error bounds). *Let $(\mathbf{u}_h, \{p_h, \lambda_h\}) \in \mathbf{V}_h \times Q_h \times \Lambda_h$ be the solution to the discrete scheme* (LhP). *Then for k_u, $k_{pr} = k_u - 1$, $k_\lambda = k_u - 1$, we have the following error estimates*

$$\|\mathbf{P}_\Gamma(\mathbf{u} - \mathbf{u}_h^\ell)\|_{L^2(\Gamma)} + h\|\mathbf{u}^{-\ell} - \mathbf{u}_h\|_{\alpha_h^\lambda} + h\|p^{-\ell} - p_h\|_{L^2(\Gamma_h)} + \|\lambda^{-\ell} - \lambda_h\|_{L^2(\Gamma_h)}$$
$$\leq c(h^{m+1})\mathbb{D},$$

where $m = \min\{h^{k_u}, h^{k_{pr}+1}, h^{k_\lambda+1}, h^{k_g-1}\}$ and $\mathbb{D} = \|\mathbf{u}\|_{H^{k_u+1}(\Gamma)} + \|p\|_{H^{k_{pr}+1}(\Gamma)} + \|\lambda\|_{H^{k_\lambda+1}(\Gamma)} + \|\mathbf{f}\|_{L^2(\Gamma)}$.

For the penalty method we get optimal convergence for $\tau = \mathcal{O}(h^{-2})$, $k_p = k_g + 1$ and also we gain one order $\mathcal{O}(h)$ for the full velocity in L^2-norm. On the other hand for the Lagrange multiplier method we need a higher approximation of the surface s.t. $k_g = k_u + 1$ to get optimal convergence. Also, notice that we only gain one order $\mathcal{O}(h)$ for the tangential velocity in L^2-norm.

These results have also been observed numerically. For example let us consider the surface with level set : $\phi(x) = \frac{1}{4}x_1^2 + x_2^2 + \frac{4x_3^2}{(1 + \frac{1}{2}\sin(\pi x_1))^2} - 1$, with solution $\mathbf{u} = \mathbf{curl}_\Gamma(\frac{1}{2\pi}\cos(2\pi x_1)\cos(2\pi x_2)\cos(2\pi x_3))$, $p = \sin(\pi x_1)\sin(2\pi x_2)\sin(2\pi x_3)$. The solution is both tangent and divergence free. For the above mentioned choices we have for $\mathcal{P}_2/\mathcal{P}_1(/\mathcal{P}_1)$ *Taylor-Hood* finite elements the following graphs:

REFERENCES

[1] A. Reusken, *Analysis of the taylor-hood surface finite element method for the surface stokes equation.*, arXiv preprint arXiv:2401.03561 (2024).

[2] T. Jankuhn, M. A. Olshanskii *Incompressible fluid problems on embedded surfaces: modeling and variational formulations*, Interfaces and Free Boundaries **20** (2018), no.3, 353–377.

[3] C. M. Elliott, T. Ranner *A unified theory for continuous-in-time evolving finite element space approximations to partial differential equations in evolving domains*, IMA Journal of Numerical Analysis **41** (2021), 1696–1845.

[4] P. Hansbo, M. G. Larson, K. Larsson *Analysis of finite element methods for vector Laplacians on surfaces*, IMA Journal of Numerical Analysis **40** (2020), no. 3, 1652–1701.
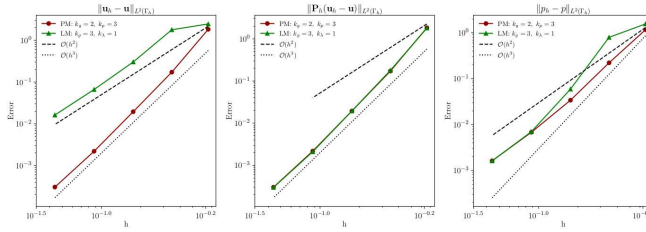
FIGURE 1. Dziuk-Elliott Surface — Velocity-pressure L^2-Errors
— P.M.: $\{k_g = 2, k_u = 2, k_{pr} = 1, k_p = 3\}$,
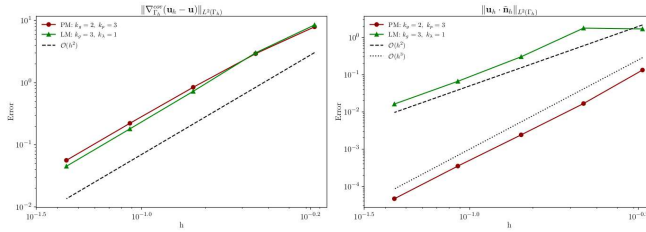L.M.: $\{k_g = 3, k_u = 2, k_{pr} = 1, k_\lambda = 1\}$.

FIGURE 2. Dziuk-Elliott surface — Velocity (a) $\nabla_{\Gamma_h}^{cov}$-Errors, (b)
Normal-Errors (P.M. : $\|\mathbf{u}_h \cdot \tilde{\mathbf{n}}_h\|_{L^2(\Gamma_h)}$, L.M. : $\|\mathbf{u}_h \cdot \mathbf{n}_h\|_{L^2(\Gamma_h)}$)
— P.M: $\{k_g = 2, k_u = 2, k_{pr} = 1, k_p = 3\}$, L.M.: $\{k_g = 3, k_u = 2, k_{pr} = 1, k_\lambda = 1\}$.

Mathematics of phase separation on evolving surfaces

ANDREA POIATTI

(joint work with Helmut Abels, Diogo Caetano, Charles M. Elliott,
Harald Garcke, and Maurizio Grasselli)

I am presenting some recent results about the mathematical analysis of phase-field models on evolving surfaces. In particular, in [5] we propose the study of the Cahn-Hilliard equation on an evolving two-dimensional surface, whose evolution is assumed to be given *a priori*. Given a finite time horizon $T > 0$, we study the following system of equations: in $\bigcup_{t \in [0,T]} \{t\} \times \Gamma(t)$, find φ, i.e., the relative concentration variable, such that

(1) $$\begin{cases} \partial^\bullet \varphi + \varphi \operatorname{div}_{\Gamma(t)} \mathbf{V} - \operatorname{div}_{\Gamma(t)}(\varphi \mathbf{V}_a^\tau) - \Delta_{\Gamma(t)} \mu = 0, \\ \mu = -\Delta_{\Gamma(t)} \varphi + \Psi'(\varphi), \\ \varphi(0) = \varphi_0, \end{cases}$$

where we assume that $\{\Gamma(t)\}_{t \in [0,T]}$ is a family of closed, connected, oriented surfaces in $\mathbb{R}^3$ and that its evolution is given *a priori* as a flow determined by the (sufficiently smooth) velocity field $\mathbf{V}$. The additional (prescribed) velocity term

$\mathbf{V}_a^\tau$ corresponds to the difference between the tangential surface velocity $\mathbf{V}_\tau$ and a tangential advection $\mathbf{V}_a$ on the surface, given for instance by some tangential fluid flow. Furthermore, $\partial^\bullet$ denotes the material time derivative, and Ψ is the Flory-Huggins free energy defined as follows

$$(2) \qquad \Psi(r) = \frac{\theta}{2}\left((1+r)\ln(1+r) + (1-r)\ln(1-r)\right) - \frac{\theta_0}{2}r^2, \quad r \in (-1,1),$$

where θ, θ_0 are absolute temperatures and satisfy $0 < \theta < \theta_0$. This ensures that Ψ has a double-well shape, but also allows the solution φ to attain values only in the physical interval $[-1,1]$. After introducing a suitable functional framework following [3, 4], under some regularity assumptions on the initial datum φ_0, we prove the instantaneous regularization of weak solutions and show the validity of the instantaneous strict separation property. This means that for any $\tau > 0$ there exists $\delta = \delta(\tau) > 0$ such that

$$\sup_{t \in [\tau,T]} \|\varphi(t)\|_{L^\infty(\Gamma(t))} \leq 1 - \delta.$$

The proof of this result is made possible by the use of a suitable approximation scheme, as well as of a Moser-Trudinger-type inequality for two-dimensional compact Riemannian manifolds (see [6]). Applications of models similar to (1) can be found, for instance, in cell membrane phase separation phenomena leading to lipid rafts formation. In such models it is interesting to introduce the effects of a tangential fluid flow $\mathbf{V}_a$ (from now on denoted by $\mathbf{u}$) which is not *a priori* prescribed. Indeed, it has been observed that the membrane fluidity within the lipid rafts can be lower than that in the liquid disordered surrounding phase ([9]). In order to allow more accurate predictions on membrane phase behavior taking into account the membrane viscosity differences between liquid ordered and disordered phases, an incompressible Cahn-Hilliard-Navier-Stokes model appears naturally as a valid alternative ([10]). Following some ideas from [1], and assuming an inextensible material surface, in [2] we thus derive a model taking into account two incompressible fluids with unmatched densities and viscosities, leading to the following system of equations: given a prescribed normal surface velocity $\mathbf{V_n} = (\mathbf{V} \cdot \mathbf{n})\mathbf{n}$ such that $\int_{\Gamma(\cdot)} v_{\mathbf{n}}H d\sigma \equiv 0$ (where $v_{\mathbf{n}} = \mathbf{V_n} \cdot \mathbf{n}$ and H is the double mean curvature), find $(\mathbf{u}, p, \varphi)$, where $\mathbf{u}$ is the tangential fluid velocity and p is the fluid pressure, such that, for any $(t,x) \in \bigcup_{t \in [0,T]} \{t\} \times \Gamma(t)$,

$$\begin{cases} \rho\mathbf{P}\partial^\circ\mathbf{u} + ((\rho\mathbf{u} + \mathbf{J}_\rho) \cdot \nabla_{\Gamma(t)})\mathbf{u} + \rho v_{\mathbf{n}}H\mathbf{u} + v_{\mathbf{n}}H\mathbf{J}_\rho - 2\mathbf{P}\mathrm{div}_{\Gamma(t)}(\nu(\varphi)\mathcal{E}_S(\mathbf{u})) \\ \quad + \nabla_{\Gamma(t)}p = -\mathbf{P}\mathrm{div}_{\Gamma(t)}(\nabla_{\Gamma(t)}\varphi \otimes \nabla_{\Gamma(t)}\varphi) + 2\mathbf{P}\mathrm{div}_{\Gamma(t)}(\nu(\varphi)v_{\mathbf{n}}H) + \frac{\rho}{2}\nabla_{\Gamma(t)}(v_{\mathbf{n}})^2, \\ \mathrm{div}_{\Gamma(t)}\mathbf{u} = -Hv_{\mathbf{n}}, \\ \partial^\circ\varphi + \mathbf{u} \cdot \nabla_{\Gamma(t)}\varphi - \Delta_{\Gamma(t)}\mu = 0, \\ \mu = -\Delta_{\Gamma(t)}\varphi + \Psi'(\varphi), \\ \mathbf{u}(0) = \mathbf{u}_0, \quad \varphi(0) = \varphi_0, \end{cases}$$

where $\mathbf{P}(x,t)$ is the normal projector on the tangent space at $x \in \Gamma(t)$, ∂° is the normal material time derivative, $\mathbf{H} := \nabla_{\Gamma(t)}\mathbf{n}$, and $\mathcal{E}_S(\mathbf{u}) := \frac{1}{2}(\nabla_{\Gamma(t)}\mathbf{u} + \nabla_{\Gamma(t)}^T\mathbf{u})$

is the symmetric (tangential) strain rate tensor. Moreover, $\nu(\cdot)$ is the viscosity function, whereas

$$\rho(\varphi) := \rho_1 \frac{1+\varphi}{2} + \rho_2 \frac{1-\varphi}{2}$$

is the density function, with $\rho_1, \rho_2 > 0$ and $\rho_1 \neq \rho_2$, leading to the presence of an additional tangential flux term

$$\mathbf{J}_\rho := -\frac{\rho_1 - \rho_2}{2} \nabla_{\Gamma(t)} \mu,$$

which generates issues in the analysis due to its higher-order nonlinearity.

Given the model above, by extending the recent results in [8] to the evolving surface setting, we prove the existence of a unique local strong solution. Furthermore, by means of some careful higher-order energy estimates, we prove the well-posedness of *global* strong solutions, as well as the validity of the strict separation property from pure phases. In this case, we prove this property by means of a different approach from the Moser-Trudinger inequality, i.e., exploiting a De Giorgi iteration scheme adapted from [7] to the evolving surface setting. This allows to consider much more general singular potentials than (2).

REFERENCES

[1] H. Abels, H. Garcke, G. Grün, *Thermodynamically consistent, frame indifferent diffuse interface models for incompressible two-phase flows with different densities*, Math. Models Methods Appl. Sci. **22** (2012), 1150013.

[2] H. Abels, H. Garcke, A. Poiatti, *Well-posedness of a diffuse interface model for binary incompressible viscous fluids with different densities on evolving surfaces* (2024), in preparation.

[3] A. Alphonse, C.M. Elliott, B. Stinner, *An abstract framework for parabolic PDEs on evolving spaces*, Port. Math. **72** (2015), 1–46.

[4] D. Caetano, C.M. Elliott, *Cahn-Hilliard equations on an evolving surface*, European J. Appl. Math. **32** (2021), 937–1000.

[5] D. Caetano, C.M. Elliott, M. Grasselli, A. Poiatti, *Regularisation and separation for evolving surface Cahn-Hilliard equations*, SIAM J. Math. Anal. **55** (2023), 6625–6675.

[6] L. Fontana, *Sharp borderline Sobolev inequalities on compact Riemannian manifolds*, Comment. Math. Helv. **68** (1993), 415–454.

[7] C.G. Gal, A. Poiatti, *Unified framework for the separation property in binary phase-segregation processes with singular entropy densities* (2023), ResearchGate preprint 10.13140/RG.2.2.35972.30089/1.

[8] J. Prüss, G. Simonett, M. Wilke, *On the Navier-Stokes equations on surfaces*, J. Evol. Equ. **21** (2021), 3153–3179.

[9] E. Sezgin, I. Leventhal, M. Grzybek, G. Schwarzmann, V. Mueller, A. Honigmann, V.N. Belov, C. Eggeling, Ü. Coskun, K. Simons, P. Schwille, *Partitioning, diffusion, and ligand binding of raft lipid analogs in model and cellular plasma membranes*, Biochim. Biophys. Acta Biomembr. **1818** (2012), 1777–1784.

[10] Y. Wang, Y. Palzhanov, A. Quaini, M. Olshanskii, S. Majd, *Lipid domain coarsening and fluidity in multicomponent lipid vesicles: A continuum based model and its experimental validation*, Biochim. Biophys. Acta Biomembr. **1864** (2022), 183898.

A phase-field model for a binary mixture with surfactants

Clemens Ullrich

(joint work with Günther Grün and Stefan Metzger)

Surfactants (= 'surface active agents') are chemical compounds that, by adsorbing onto a fluid interface, reduce its surface tension. Thus, when modelling a two-phase system with surfactants, the concentration of adsorbed surfactant has to enter the surface energy in a suitable way. Based on a sharp-interface model for two-phase flow with surfactants in [3], a first phase-field formulation was introduced in [4], where a weighted Cahn–Hilliard energy density $e(\phi, c) = \gamma(c)(\frac{\varepsilon}{2}|\nabla\phi|^2 + \frac{1}{\varepsilon}W(\phi))$ is assigned to an order parameter ϕ and a surfactant density c.

A modified energy density of the form $\widetilde{e}(\phi, c) = \frac{\varepsilon}{2}|\nabla\phi|^2 + \frac{\widetilde{d}(c)}{\varepsilon}W(\phi)$ is considered in [1, 2], which brings advantages for mathematical analysis since the leading-order term does not depend on c. The two models are connected by a common sharp-interface limit.

We want to follow a different approach that builds on the original energy density $e(\phi, c)$. In order to capture phenomena such as the evolution of bridges between originally separated portions of the same phase (network formation, cf. [5]), it is advisable to allow for negative surface tensions induced by the concentration of adsorbed surfactant on the fluid interface and to balance the weighted Cahn–Hilliard energy against a higher-order bending energy.

The state variables of this system are a velocity field $\boldsymbol{v}$, a phase field ϕ, an interfacial surfactant density c^Γ, and a bulk surfactant density c^b. Dimensionwise, c^b is a volume density while c^Γ is a surface density. Assuming that both fluids are incompressible with matched densities, we consider a total energy of the form

$$E(\boldsymbol{v}, \phi, c^\Gamma, c^b) = E_{kin} + E_{CH} + E_{bend} + E_{chem}$$

$$= \frac{1}{2}\int_\Omega |\boldsymbol{v}|^2\, dx + \int_\Omega \gamma(c^\Gamma)\left(\frac{\varepsilon}{2}|\nabla\phi|^2 + \frac{1}{\varepsilon}W(\phi) + \delta\right) dx$$

$$+ \frac{A}{2}\int_\Omega \left(\varepsilon\Delta\phi - \frac{1}{\varepsilon}W'(\phi)\right)^2 dx + \sum_{i=1}^2 \int_\Omega \xi_i(\phi)G_i(c^b)\, dx,$$

where W is the polynomial double-well potential, $\delta > 0$ is a small positive shift, and ξ_i are smooth cutoffs of the phases $i \in \{1, 2\}$ such that $\xi_1 + \xi_2 \equiv 1$.

Regarding the free energy densities γ and G_i, we make the choices

$$\gamma(c^\Gamma) = c^\Gamma(\ln c^\Gamma - 1), \qquad G_i(c^b) = \frac{1}{N_i}c^b\left(\ln(A_i^{N_i}c^b) - 1\right),$$

which are motivated by Freundlich's adsorption isotherm (cf. [4]). Furthermore, via the Legendre transform $\gamma^* : \mathbb{R} \to \mathbb{R}$ of γ, we define

$$\sigma(c^\Gamma) := -\gamma^*(\gamma'(c^\Gamma)) = \gamma(c^\Gamma) - c^\Gamma\gamma'(c^\Gamma) = \sigma_0 - c^\Gamma.$$

The function $\sigma(c^\Gamma)$ will play the role of a surface tension for the fluid interface.

Starting from general evolution equations and invoking Onsager's principle of least dissipation of energy as well as Fick's law of diffusion, we arrive at a system

of the form

(1a)
$$\partial_t^\bullet \boldsymbol{v} = \mathrm{div}\, (-p\mathbb{I} + 2\eta(\phi)D\boldsymbol{v}) + \mu\nabla\phi$$
$$+ f(\phi, \nabla\phi)\nabla\sigma(c^\Gamma) \qquad\qquad \text{in } (0,T)\times\Omega,$$

(1b) $\qquad \mathrm{div}\, \boldsymbol{v} = 0 \qquad\qquad\qquad\qquad\qquad\qquad\qquad \text{in } (0,T)\times\Omega,$

(1c) $\qquad \partial_t^\bullet \phi = \mathrm{div}\, (m(\phi)\nabla\mu) \qquad\qquad\qquad\qquad \text{in } (0,T)\times\Omega,$

(1d)
$$\mu = \frac{1}{\varepsilon}\sigma(c^\Gamma)W'(\phi) - \varepsilon\mathrm{div}\, (\sigma(c^\Gamma)\nabla\phi)$$
$$+ A\varepsilon^2\Delta^2\phi - 2A\Delta\phi W''(\phi)$$
$$- AW'''(\phi)|\nabla\phi|^2 + \frac{A}{\varepsilon^2}W'(\phi)W''(\phi)$$
$$+ \sum_{i=1}^{2}\xi_i'(\phi)G_i(c^b) \qquad\qquad \text{in } (0,T)\times\Omega,$$

(1e)
$$\partial_t^\bullet \left(f(\phi,\nabla\phi)c^\Gamma \right) = \mathrm{div}\, (\widetilde{f}\nabla c^\Gamma)$$
$$+ \beta f(\phi,\nabla\phi)\left(\sum_{i=1}^{2}\xi_i(\phi)G_i'(c^b) - \gamma'(c^\Gamma) \right) \qquad \text{in } (0,T)\times\Omega,$$

(1f)
$$\partial_t^\bullet c^b = \sum_{i=1}^{2}\mathrm{div}\, \left(M(c^b,\phi)\nabla\left(\xi_i(\phi)G_i'(c^b) \right) \right)$$
$$- \beta f(\phi,\nabla\phi)\left(\sum_{i=1}^{2}\xi_i(\phi)G_i'(c^b) - \gamma'(c^\Gamma) \right) \qquad \text{in } (0,T)\times\Omega,$$

(1g) $\qquad \boldsymbol{v} = \partial_{\boldsymbol{\nu}}\phi = \partial_{\boldsymbol{\nu}}\Delta\phi = \partial_{\boldsymbol{\nu}}\mu = \partial_{\boldsymbol{\nu}}c^\Gamma = \partial_{\boldsymbol{\nu}}c^b = 0 \qquad \text{on } (0,T)\times\partial\Omega,$

(1h) $\quad \boldsymbol{v}(0,\cdot) = \boldsymbol{v}_0, \quad \phi(0,\cdot) = \phi_0, \quad c^\Gamma(0,\cdot) = c_0^\Gamma, \quad c^b(0,\cdot) = c_0^b \quad \text{in } \Omega,$

where $\partial_t^\bullet$ denotes the material time derivative, $f(\phi,\nabla\phi) := \frac{\varepsilon}{2}|\nabla\phi|^2 + \frac{1}{\varepsilon}W(\phi) + \delta$ is the characteristic function of the diffuse interface as used in E_{CH}, and $\widetilde{f}$ is a smooth, strictly positive approximation of the interface.

The momentum equations (1a)–(1b) involve two force terms, one due to the spatial structure of the phase field, the other a Marangoni-type force due to surface tension gradients. The order parameter ϕ obeys a sixth-order Cahn–Hilliard–Willmore type equation (1c)–(1d), whereas (1e) and (1f) are advection-reaction-diffusion equations for the interfacial and bulk surfactant. This evolution conserves both phases, $\int_\Omega \phi(t,x)dx = const$, as well as the total mass of bulk and interfacial surfactant, $\int_\Omega (c^b + f(\phi,\nabla\phi)c^\Gamma)(t,x)dx = const$. However, since the system allows for dynamical adsorption/desorption at a rate

$$R_{ad} = \beta f(\phi,\nabla\phi)\left(\sum_{i=1}^{2}\xi_i(\phi)G_i'(c^b) - \gamma'(c^\Gamma) \right),$$

the solute (bulk) and adsorbed (interfacial) surfactant are not conserved individually. Formally testing (1a) by $\boldsymbol{v}$, (1c) by μ, (1d) by $\partial_t\phi$, (1e) by $\gamma'(c^\Gamma)$, and (1f) by $\xi_1 G_1'(c^b) + \xi_2 G_2'(c^b)$ yields the energy dissipation inequality

$$
\frac{d}{dt} E(\boldsymbol{v}, \phi, c^\Gamma, c^b) = -2 \int_\Omega \eta(\phi)|D\boldsymbol{v}|^2 dx - \int_\Omega m(\phi)|\nabla\mu|^2 dx
$$

$$
(2) \qquad\qquad -4 \int_\Omega \widetilde{f}|\nabla\sqrt{c^\Gamma}|^2 dx - \int_\Omega M(c^b, \phi) \left| \sum_{i=1}^2 \nabla(\xi_i(\phi)G_i'(c^b)) \right|^2 dx
$$

$$
-\beta \int_\Omega f(\phi, \nabla\phi) \left| \sum_{i=1}^2 \xi_i(\phi)G_i'(c^b) - \gamma'(c^\Gamma) \right|^2 dx.
$$

The (ϕ, c^Γ)-subsystem consisting of (1c)–(1e) without the advection, bulk surfactant, and adsorption/desorption terms describes phase separation in a binary mixture with an *insoluble* surfactant adsorbed onto the fluid interface. If Neumann boundary conditions as in (1g) are prescribed on the boundary of a smooth bounded connected open set $\Omega \subset \mathbb{R}^d$, $d \in \{2, 3\}$, then the existence of weak solutions can be shown for arbitrary time intervals and general initial data (ϕ_0, c_0^Γ) of finite energy.

REFERENCES

[1] H. Abels, H. Garcke, K. F. Lam, and J. Weber, *Two-Phase Flow with Surfactants: Diffuse Interface Models and Their Analysis*, In: Transport Processes at Fluidic Interfaces (eds.: D. Bothe and A. Reusken), 255–270, Advances in Mathematical Fluid Mechanics, Birkhäuser 2017.

[2] H. Abels, H. Garcke, and J. Weber, *Existence of Weak Solutions for a Diffuse Interface Model for Two-Phase Flow with Surfactants*, Comm. Pure Appl. Anal. **18** (2019), 195–225.

[3] D. Bothe, J. Prüss, and G. Simonett, *Well-Posedness of a Two-Phase Flow with Soluble Surfactant*, In: Nonlinear Elliptic and Parabolic Problems. A Special Tribute to the Work of Herbert Amann (eds.: M. Chipot and J. Escher), 37–61, Progress in Nonlinear Differential Equations and Their Applications **66**, Birkhäuser 2005.

[4] H. Garcke, K. F. Lam, and B. Stinner, *Diffuse Interface Modelling of Soluble Surfactants in Two-Phase Flow*, Commun. Math. Sci. **12** (2014), 1475–1522.

[5] N. Gavish, G. Hayrapetyan, K. Promislow, L. Yang, *Curvature Driven Flow of Bi-layer Interfaces*, Physica D **240** (2011), 675–693.

Sharp-Interface Modeling and VOF-Simulation of Dynamic Contact Lines

DIETER BOTHE

(joint work with Mathis Fricke, Tomas Fullana, Yash Kulkarni, Shahriar Afkhami, Stéphane Popinet, and Stéphane Zaleski)

We revisit the sharp-interface modeling of two-phase flows with moving contact lines on a planar solid boundary. From an analysis of the kinematics of the flow, it can be shown that regular solutions of the two-phase incompressible Navier-Stokes equations with a contact angle relation of type $\theta = f(V_\Gamma)$ are unphysical if the

standard Navier slip boundary condition is used [3], [6]. Motivated by phase field models going back to work by Qian et al. [11],[12],[13], we derive a hybrid sharp-interface / contact region model [7], which employs a generalized Navier boundary condition of the form (see Fig. 1 for notation)

$$-\beta \mathbf{v}_\| = (\mathbf{S}\mathbf{n}_{\partial\Omega})_\| + \sigma \left(\cos\theta - \cos\theta_0\right) \mathbf{n}_\Gamma \delta_\Gamma^\varepsilon. \tag{1}$$

Here $\mathbf{S} = \eta(\nabla\mathbf{v} + \nabla\mathbf{v}^\mathsf{T})$ is the viscous stress tensor, $\beta > 0$ is the sliding friction coefficient, $\sigma > 0$ is the surface tension coefficient and θ_0 is the equilibrium contact angle. Furthermore, the term $\delta_\Gamma^\varepsilon$ denotes a smoothed version of the contact line Dirac distribution, where $\varepsilon > 0$ is considered as a physical parameter describing the width of the contact line zone. One can show that the boundary condition (1) leads to a generalized dynamic contact angle relation of the type $V_\Gamma = f(\theta, \dot\theta)$, where $\dot\theta$ denotes the co-moving derivative of θ (see [7] for more details). To be more specific, this relation reads as

$$V_\Gamma = 2L\,\dot\theta + \frac{1}{\beta\varepsilon}\sigma \left(\cos\theta - \cos\theta_0\right), \tag{2}$$

where $L := \eta/\beta > 0$ is the Navier slip length. Notably, equation (2) simplifies for quasi-stationary states (i.e. for $\dot\theta = 0$) to

$$-(\beta\varepsilon)V_\Gamma = \sigma \left(\cos\theta_0 - \cos\theta\right). \tag{3}$$

Equation (2) is well-known in the literature as a linear contact angle model. This indicates that there exists a deep relation between the present model in quasi-stationary states and other modeling approaches such as the molecular kinetic theory (MKT) (see, e.g., [1] and [2]). In particular, the so-called contact line friction parameter can be identified as $\zeta = \beta\varepsilon$.
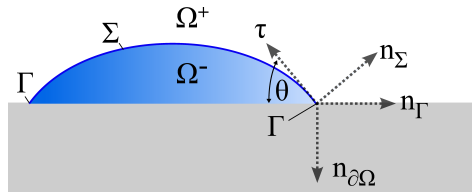

FIGURE 1. Notation for contact line modeling.

It is important to note that within the present model, the parameter $L = \eta/\beta$ decouples from the "apparent slip length" defined as the distance to the wall, where the tangential velocity component extrapolates to zero (see Fig. 2). In particular, we show that the viscous stress component (1) vanishes at the contact line in quasi-stationary states. This is a consequence of the kinematics of the flow and leads to equation (3). In other words, we can show that there is apparent free slip at the contact line for quasi-stationary states. This result is consistent to observations from molecular dynamics, where a similar conclusion is drawn (see, e.g., [14]).
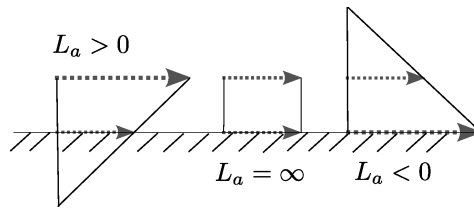
FIGURE 2. Apparent slip length (positive, infinite and negative).

We have implemented this generalized Navier boundary condition into the geometrical Volume-of-Fluid code *Basilisk* [9], [10]. To make the method consistent with the kinematics of the contact line, the contact angle is not prescribed during the advection of the interface but is reconstructed from the volume fraction field (see also [5]) and used to evaluate the right-hand side of (1). Notably, numerical simulations of the withdrawing plate experiment show that the logarithmic pressure singularity at the contact line, known for the standard Navier boundary condition [8], is not present for the GNBC model with finite contact line zone, i.e. for $\varepsilon > 0$ (see [7]). Finally, we introduce a more general non-linear closure relation which leads to non-linear variants of (1). This class of models is relevant for high velocities of the contact line (relative to the solid surface) and will be studied in more detail in the future.

REFERENCES

[1] T.D. Blake and J.M. Haynes, *Kinetics of liquid-liquid displacement*, Journal of Colloid and Interface Science **30**(3) (1969), 421–423.

[2] T.D. Blake and J. De Coninck, *The influence of pore wettability on the dynamics of imbibition and drainage*, Colloids and Surfaces A: Physicochemical and Engineering Aspects **250** (2004), 395–402, December.

[3] M. Fricke and M. Köhne and D. Bothe, *A kinematic evolution equation for the dynamic contact angle and some consequences*, Physica D: Nonlinear Phenomena **394** (2019), 26–43.

[4] M. Fricke and D. Bothe, *Boundary conditions for dynamic wetting - A mathematical analysis*, The European Physical Journal Special Topics **229**(10) (2020), 1849–1865.

[5] M. Fricke, T. Marić, and D. Bothe, *Contact Line Advection using the geometrical Volume of Fluid Method*, Journal of Computational Physics **407** (2020), 109221.

[6] M. Fricke, *Mathematical Modeling and Volume-of-Fluid based simulation of dynamic wetting*, PhD thesis, TU Darmstadt, 2021.

[7] T. Fullana and Y. Kulkarni and M. Fricke and S. Popinet and S. Afkhami and D. Bothe and S. Zaleski, *A consistent treatment of dynamic contact angles in the sharp-interface framework with the generalized Navier boundary condition*, Preprint (2023), DOI:10.5281/zenodo.10142047.

[8] C. Huh and S. G. Mason, *The steady movement of a liquid meniscus in a capillary tube*, Journal of Fluid Mechanics **81**(3) (1977), 401–419.

[9] S. Popinet, *An accurate adaptive solver for surface-tension-driven interfacial flows*, Journal of Computational Physics **228**(16) (2009), 5838–5866.

[10] S. Popinet, *Numerical Models of Surface Tension*, Annual Review of Fluid Mechanics **50**(1) (2018), 49–75.

[11] T. Qian and X.-P. Wang and P. Sheng, *Molecular scale contact line hydrodynamics of immiscible flows*, Physical Review E **68** (2003), 016306.

[12] T. Qian and X.-P. Wang and P. Sheng, *A variational approach to moving contact line hydrodynamics*, Journal of Fluid Mechanics **564** (2006), 333.

[13] T. Qian and X.-P. Wang and P. Sheng, *Molecular Hydrodynamics of the Moving Contact Line in Two-Phase Immiscible Flows*, Commun. Comput. Phys. **1**(1) (2006), 1–52.

[14] P. A. Thompson and M. O. Robbins, *Simulations of contact-line motion: Slip and the dynamic contact angle*, Physical Review Letters **63**(7) (1989), 766–769.

Convergence to the planar interface for the Mullins-Sekerka evolution

RICHARD SCHUBERT

(joint work with Felix Otto and Maria G. Westdickenberg)

The Mullins-Sekerka interfacial evolution is a nonlocal free boundary evolution: The normal velocity of the interface is a nonlocal function of the interface and, in particular, its mean curvature. More precisely, the evolution describes the coarsening of two phases, each occupying their respective mutually disjoint domains Ω_+ and Ω_-. The normal velocity of the interface $\Gamma = \overline{\Omega_+} \cap \overline{\Omega_-}$ is given as the jump of the normal derivative of the chemical potential f,

$$V = -[\nabla f \cdot n],$$

which in turn solves the Dirichlet problem

$$-\Delta f = 0 \quad \text{in } \Omega_+ \cup \Omega_-$$
$$f = H \quad \text{on } \Gamma,$$

with mean curvature H of Γ.

Essential features of Mullins-Sekerka are the preservation of mass and the reduction of surface area. In addition, there is a scale invariance: The solution space is invariant under a rescaling of length by a factor of λ and time by a factor of λ^3. Hence Mullins-Sekerka is a geometric version of a third-order parabolic equation.

As the evolution is driven towards (local) energy minimizers, large connected components of one phase grow at the expense of smaller ones, which eventually vanish, a behaviour known as Ostwald ripening. The relaxation behaviour towards energy minimizing configurations has been analyzed in a perturbative setting in [1, 3] for spheres, and in [2] for the plane. In [4] exponential convergence to a collection of equally sized discs is proved on the torus of dimension $d + 1 = 2$ starting from non-perturbative initial data.

Exponential convergence is expected for compact surfaces while the problem in the whole space admits no spectral gap and thus only algebraic relaxation of the energy towards the ground state can be expected. In [5] we prove convergence towards the plane in three ambient dimensions for very general initial data and with optimal rates. Starting with initial data that have finite excess mass and excess energy with respect to the two-dimensional plane, but without assuming graph-structure or even connectedness of the phases, we prove that graph-structure is generated in a quantified time scale and that the energy gap eventually relaxes

as expected from the linearization:

$$E(t) \leq C \min \left\{ E(0), \frac{V(0)^2 + E(0)^3}{t^{4/3}} \right\}.$$

In particular this result includes the Ostwald-ripening regime. Optimality of the decay rate can be read off from the properties of the linearization

$$-\Delta f = 0 \quad \text{in } \mathbb{R}^{d+1}_+,$$
$$f = \Delta' h \quad \text{on } \mathbb{R}^d,$$
$$h_t = -2f_z \quad \text{on } \mathbb{R}^d,$$
$$h(0) = h_0 \quad \text{on } \mathbb{R}^d,$$

where z is the variable orthogonal to the plane. The kernel is in (tangential) Fourier space given by $G(k,t) = \exp -2|k|^3 t$ which leads to decay of the energy

$$\|\nabla h\|_{L^2} \leq t^{-(d+2)/3}\|h(0)\|_{L^1},$$

and of the amplitude as well as the Lipschitz constant

$$\|h\|_{L^\infty} + t^{1/3}\|\nabla h\|_{L^\infty} \leq t^{-d/3}\|h(0)\|_{L^1}.$$

Core to the analysis is the monitoring of the three quantities excess mass, excess energy, and dissipation, given as

$$V = \int_{\mathbb{R}^3} |\chi_+ - \chi_0|, \qquad E = \int_\Gamma 1 - n \cdot n_0, \qquad D = \int_{\mathbb{R}^3} |\nabla f|^2,$$

where χ_+, χ_0 are the characteristic functions of the positive phase and the positive half-space, respectively, n is the normal of Γ, and n_0 is the normal of the plane. Assuming that Γ is the graph of a Lipschitz function, the Nash-type inequality

$$(1) \qquad\qquad E \leq CV^{6/7}D^{4/7}$$

delivers the optimal decay rate for E by using (1) as a lower bound for the dissipation in the gradient flow inequality $\frac{d}{dt}E \leq -D$, and employing that $V(t) \leq C(V(0) + E(0)^{3/2})$. This bound in turn is proved in a buckling argument together with the decay of the energy by testing with the solution of the linearized dual equation, and thus extracting the nonlinear behaviour.

The generation of graph-structure relies on the observation that the scale-invariant quantity ED^2, if small enough, already prevents by Allard's theorem more than one connected component and overhangs, and in this case also controls the Lipschitz constant of the thus apparent graph. The quantity ED^2 must become small during times of order $E(0)^{3/2}$ due to the fact that $-(ED^2)^{1/2} = -E^{1/2}D$ is up to constants the derivative of $E^{3/2}$ which is strictly decreasing.

References

[1] X. Chen, *The Hele-Shaw problem and area-preserving curve-shortening motions*, Arch. Rational Mech. Anal. **123** (1993), 117–151.

[2] O. Chugreeva, F. Otto, and M. G. Westdickenberg, *Relaxation to a planar interface in the Mullins-Sekerka problem*, Interfaces Free Bound., **21** (2019), 21–40.

[3] J. Escher, and G. Simonett, *A center manifold analysis for the Mullins-Sekerka model*, J. Differential Equations, **143** (1998), 267-292.

[4] V. Julin, M. Morini, M. Ponsiglione, and E. Spadaro, *The asymptotics of the area-preserving mean curvature and the Mullins–Sekerka flow in two dimensions*, Mathematische Annalen, **387** (2023), 1969–1999.

[5] F. Otto, R. Schubert, and M. G. Westdickenberg, *Convergence to the planar interface for a nonlocal free-boundary evolution*, Preprint (2023).

Phase separation on varying surfaces and convergence of diffuse interface approximations

MATTHIAS RÖGER

(joint work with Heiner Olbermann)

Variational models for multiphase membranes depend on both the shape of the membrane and the internal composition. Typical ingredients are a bending energy with phase-dependent parameters and a line tension energy between phases. In the two-phase case an extension of the classical one-phase shape energies of Canham and Helfrich has been proposed by Jülicher–Lipowsky [6]. Defined on tuples (S, S_1, S_2), where $S \subset \mathbb{R}^3$ is a closed surface decomposed into a disjoint union of open subsets S_1, S_2 of S representing the phases and their common boundary Γ, the energy consists of a phase-dependent bending and a line tension contribution.

In many models and numerical simulations a diffuse description of the phases and the line tension energy is used. Our interest is on the connection between such diffuse and sharp interface description in the spirit of Modica–Mortola type results. A corresponding result for the Jülicher–Lipowsky energy has been given by Helmers [4] in rotational symmetry. We aim for a corresponding result for a reduced Jülicher–Lipowsky energy but without restriction to special symmetries. Mathematical results on multi-phase membrane energies are rather sparse, see [3, 5, 4] for the rotationally symmetric and [2] for the general case.

Since the relevant shape energies do not guarantee good compactness properties in classes of differentiable surfaces we need to consider classes of generalized surfaces and a suitable generalization of functions of bounded variations and sets of finite perimeter.

We first consider an approximation result for a generalized perimeter energy of phase interfaces. The class of underlying surfaces is chosen as reduced boundaries $\partial_* E$ of finite perimeter sets $E \subset \mathbb{R}^n$, $n \geq 2$. We associate to E its characteristic function $\chi_E \in BV(\mathbb{R}^n, \{0, 1\})$, the generalized inner unit normal field $\nu_E : \partial_* E \to \mathbb{S}^{n-1}$, and the associated unit density current $S = [\![\partial_* E, *\nu_E, 1]\!] \in \mathbf{I}_{n-1}(\mathbb{R}^n)$. We follow the work of Anzellotti, Delladio, Scianna [1] and define functions of bounded variation over S. Consider an $\mathcal{H}^{n-1}$-measurable function $u : \partial_* E \to [0, \infty]$ and the subgraph

$$E_{u,S} = \left\{ (x, y) \in \partial_* E \times \mathbb{R}_y \: : \: 0 < y < u(x) \right\} \subset \mathbb{R}^{n+1} .$$

We associate to $E_{u,S}$ the *induced current*

$$\Sigma_{u,S} := [\![E_{u,S}, -\vec{e}_{n+1} \wedge *\nu_E(x), 1]\!] \in \mathcal{D}_n(\mathbb{R}^{n+1}) \,.$$

The *generalized graph* $T_{u,S} \in \mathcal{D}_{n-1}(\mathbb{R}^{n+1})$ of u over S is defined as

$$T_{u,S} = -\partial \Sigma_{u,S}(\omega) + S \,.$$

We say that u is a function of bounded variation over S and write $u \in BV(S)$ if the total mass $\mathsf{M}(T_{u,S})$ is finite.

A more general concept of BV functions over currents was considered in [1] and a number of good properties of this notions have been derived, in particular a co-area formula and a closure theorem.

We justify a suitable notion of jump set.

Proposition 1. *Let $E \subset \mathbb{R}^n$ and $S = [\![\partial_* E, *\nu_E, 1]\!]$ be as above and consider $u \in BV(S)$ with $u : \partial_* E \to \{0, b\}$, $b > 0$. Then the generalized jump set*

$$J_u := \operatorname{supp}\big(\partial [\![u^{-1}(b), *\nu_E, 1]\!]\big)$$

is $(n-2)$-rectifiable with $\mathsf{M}(T_{u,S}) - \mathsf{M}(S) = b\mathcal{H}^{n-2}(J_u)$.

We next define the diffuse approximation of the generalized area of phase interface. Fix the standard double-well potential $W : \mathbb{R} \to \mathbb{R}_0^+$, $W = \frac{1}{4}t^2(1-t)^2$ and let $k = \int_0^1 \sqrt{W(t)}\,\mathrm{d}t$.

For $\varepsilon > 0$ and $(E_\varepsilon, u_\varepsilon)$ with $E_\varepsilon \subset\subset \mathbb{R}^n$ a set of finite perimeter and $u_\varepsilon \in C_c^1(\mathbb{R}^n)$ we define the *generalized Modica–Mortola functional*

$$I_\varepsilon(u_\varepsilon, E_\varepsilon) = \int_{\partial_* E_\varepsilon} \big(\varepsilon |P_\varepsilon \nabla u_\varepsilon|^2 + \varepsilon^{-1} W(u_\varepsilon)\big)\,\mathrm{d}\mathcal{H}^2\,, \quad P_\varepsilon = \mathrm{id} - \nu_{E_\varepsilon} \otimes \nu_{E_\varepsilon}\,.$$

Our first main result is the following compactness and lower bound statement.

Theorem 2. *Let a family $(E_\varepsilon, u_\varepsilon)_\varepsilon$ as above be given with $\sup_{\varepsilon>0} I_\varepsilon(u_\varepsilon, E_\varepsilon) < \Lambda$. Assume $\chi_{E_\varepsilon} \to \chi_E$ strictly in $BV(\mathbb{R}^n)$ for some set E, and let $S = [\![\partial_* E, *\nu_E, 1]\!]$. Then there exist $u \in BV(S, \{0,1\})$ and a subsequence $\varepsilon \to 0$ such that*

$$\big(|\nabla \chi_{E_\varepsilon}|, u_\varepsilon\big) \to \big(|\nabla \chi_E|, u\big) \quad \text{as measure-function pairs in } L^2\,,$$
$$\liminf_{\varepsilon \to 0} I_\varepsilon(u_\varepsilon, E_\varepsilon) \geq 2k\mathcal{H}^{n-2}\,(J_u)\,.$$

The measure-function pair convergence means

$$\lim_{\varepsilon \to 0} \int_{\mathbb{R}^n} \varphi(x, u_\varepsilon(x))\,\mathrm{d}|\nabla \chi_{E_\varepsilon}|(x) = \int_{\mathbb{R}^n} \varphi(x, u(x))\,\mathrm{d}|\nabla \chi_E|(x) \quad \forall \varphi \in C_c^0(\mathbb{R}^{n+1})$$

$$\text{and } \lim_{R \to \infty} \sup_{\varepsilon > 0} \int_{\{|u_\varepsilon| > R\}} |u_\varepsilon|^2\,\mathrm{d}|\nabla \chi_{E_\varepsilon}| = 0\,.$$

Our second main result concerns a reduction of the Jülicher–Lipowsky energy in a generalized diffuse- and sharp-interface formulation. Consider a finite perimeter set $E \subset \mathbb{R}^3$ as above, $S = [\![\partial_* E, *\nu, 1]\!] \in \mathbf{I}_2(\mathbb{R}^3)$, $u \in BV(S, \{0,1\})$. Assume that $\partial_* E$ has weak mean curvature $H \in L^2(|\nabla \chi_E|, \mathbb{R}^3)$, in the sense of

$$\int_{\partial_* E} (\mathrm{id} - \nu_E \otimes \nu_E) : D\eta + H \cdot \eta\,\mathrm{d}\mathcal{H}^2 = 0 \quad \text{for all } \eta \in C_c^1(\mathbb{R}^3, \mathbb{R}^3)\,.$$

For given constants $a_1, a_2, k > 0$ define the sharp interface energy

$$\mathcal{E}(u, E) := \int_{\partial_* E} \left(a_1 u + a_2(1 - u) \right) |H|^2 \, \mathrm{d}\mathcal{H}^2 + 2k\mathcal{H}^1(J_u) \, .$$

For E_ε, S_ε as above, $u_\varepsilon \in C^1(\mathbb{R}^3)$ and $a(r) = (1 - r)a_2 + ra_1$ we define the diffuse interface energy

$$\mathcal{E}_\varepsilon(u_\varepsilon, E_\varepsilon) = \int_{\partial_* E_\varepsilon} a \circ u_\varepsilon |H_\varepsilon|^2 \, \mathrm{d}\mathcal{H}^2 + \int_{\partial E_\varepsilon} \left(\varepsilon |\nabla_{\tan} u_\varepsilon|^2 + \varepsilon^{-1} W(u_\varepsilon) \right) \mathrm{d}\mathcal{H}^2 \, .$$

Theorem 3. *Consider $(E_\varepsilon, u_\varepsilon)_\varepsilon$ as above and assume*

$$\sup_{\varepsilon > 0} \left(\mathcal{H}^{n-1}(\partial_* E_\varepsilon) + \mathcal{E}_\varepsilon(u_\varepsilon, V_\varepsilon) \right) < \infty \, ,$$

$$\int_{\partial_* E_\varepsilon} a \circ u_\varepsilon |H_\varepsilon|^2 \, \mathrm{d}\mathcal{H}^2 < 8\pi \min\{a_1, a_2\} - \delta \, .$$

Then there exists a subsequence $\varepsilon \to 0$, a finite perimeter set $E \subset \mathbb{R}^3$ such that $\chi_{E_\varepsilon} \to \chi_E$ strictly in $BV(\mathbb{R}^3)$, and $u \in BV(S, \{0, 1\})$ such that

$$\partial_* E \text{ has weak mean curvature } H \in L^2(|\nabla \chi_E|, \mathbb{R}^3) \, ,$$

$$(|\nabla \chi_{E_\varepsilon}|, u_\varepsilon) \to (|\nabla \chi_E|, u) \quad \text{as measure-function pairs in } L^2 \, ,$$

$$\liminf_{\varepsilon \to 0} \mathcal{E}_\varepsilon(u_\varepsilon, V_\varepsilon) \geq \mathcal{E}(u, V) \, .$$

In both theorems a key point is that the functionals are considered of *pairs* of surfaces and phase partitioning. We can extend the result to the case $u_\varepsilon \in H^1_{|\nabla u_\varepsilon|}(\mathbb{R}^n)$, where $H^1_{|\nabla u_\varepsilon|}(\mathbb{R}^n)$ is a suitably defined generalized Sobolev space. A crucial assumption in Theorem 2 is the strict BV-convergence of the χ_{E_ε}. This is related to a corresponding condition in the closure theorem in [1]. In Theorem 3 the assumption of small (phase-dependent) Willlmore energy allows to apply the Li–Yau inequality and to deduce the strict BV-convergence of χ_{E_ε}. Finally, we also obtain existence of minimizer for the diffuse perimeter functional I_ε and for the reduced diffuse Jülicher–Lipowsky energy $\mathcal{E}_\varepsilon$ under constraints on the mass of the two phases.

See [7] for the proofs and more details.

References

[1] Gabriele Anzellotti, Silvano Delladio, and Giuseppe Scianna, *BV functions over rectifiable currents*, *Annali di Matematica Pura ed Applicata* **170** (1996).

[2] Katharina Brazda, Luca Lussardi, and Ulisse Stefanelli, Existence of varifold minimizers for the multiphase Canham–Helfrich functional, *Calc. Var. Partial Dif.* **59** (2020).

[3] Rustum Choksi, Marco Morandotti, and Marco Veneroni, Global minimizers for axisymmetric multiphase membranes, *ESAIM: Control, Optimisation and Calculus of Variations*, **19** (2013).

[4] M. Helmers, Convergence of an approximation for rotationally symmetric two-phase lipid bilayer membranes, *Q. J. Math.* **66** (2014).

[5] Michael Helmers, Kinks in two-phase lipid bilayer membranes, *Calc. Var. Partial Dif.* **48** (2012).

[6] Frank Jülicher and Reinhard Lipowsky, Shape transformations of vesicles with intramembrane domains, *Phys. Rev. E* **53** (1996).

[7] Heiner Olbermann and Matthias Röger, Phase separation on varying surfaces and convergence of diffuse interface approximations, *Calc. Var. Partial Differ. Equ.* **62** (2023).

Finite element approximation with tangential motion for fourth order geometric curve evolutions

Klaus Deckelnick

(joint work with Robert Nürnberg)

Let Γ be a closed curve in $\mathbb{R}^d$ ($d \geq 2$). Two of the most frequently studied geometric energies associated with Γ are the length functional and the elastic energy, given by

$$L(\Gamma) := \int_\Gamma 1 ds \qquad \text{and} \qquad E(\Gamma) := \frac{1}{2} \int_\Gamma |\vec{\kappa}|^2 ds + \lambda L(\Gamma).$$

In the above, s denotes arclength, while τ and $\vec{\kappa} = \tau_s$ are the unit tangent and the curvature vector of Γ, respectively. In what follows, we focus on two gradient flows for these energies which give rise to fourth order parabolic PDEs, namely curve diffusion as the H^{-1}-gradient flow of L and elastic flow as the L^2-gradient flow of E. Using a parametric approach in order to describe the evolving curves, i.e. $\Gamma(t) = x(I, t)$ for some mapping $x : I \times [0, T] \to \mathbb{R}^d$ ($I = \mathbb{R}/\mathbb{Z}$), one is led to the following equations, see [6]:

(1) $\qquad P x_t = -\nabla_s^2 \vec{\kappa};$ $\qquad\qquad\qquad$ (curve diffusion)

(2) $\qquad P x_t = -\nabla_s^2 \vec{\kappa} - \frac{1}{2}|\vec{\kappa}|^2 \vec{\kappa} + \lambda \vec{\kappa}.$ $\qquad$ (elastic flow)

In the above, $P = I_d - \tau \otimes \tau$ is the projection onto the part normal to Γ and $\nabla_s \eta = P \eta_s$ for a vector field η. Note that the laws (1) and (2) only prescribe the motion in normal direction.

Finite element schemes that approximate the systems $x_t = -\nabla_s^2 \vec{\kappa}$ and $x_t = -\nabla_s^2 \vec{\kappa} - \frac{1}{2}|\vec{\kappa}|^2 \vec{\kappa} + \lambda \vec{\kappa}$, respectively, have been proposed in [6, 4], with [4] also presenting a corresponding error analysis. In these approaches the curves move in normal direction, which may lead to clustering of grid points and a potential breakdown of the simulation. A possible remedy for this issue is the introduction of a suitable tangential motion. The BGN–schemes in [1, 2, 3] have the property that mesh points are distributed almost uniformly along the discrete curve, but so far there are no error bounds for these schemes. The paper [7] examines a modified elastic flow, which arises as the L^2–gradient flow for the energy that is obtained by replacing the length in the definition of E above by the Dirichlet energy $\int_I |x_\rho|^2 d\rho$. The resulting flow is no longer geometric but is still related to the elastic flow (2) in that it has the same stationary points. For a semidiscrete finite element approximation, error estimates are shown while the scheme also exhibits good properties with respect to the distribution of grid points.

Concentrating first on curve diffusion, our aim is to introduce a suitable tangential component $x_t \cdot \tau$ such that the resulting system of PDEs

- is strictly parabolic,
- is amenable to discretization by continuous, piecewise linear finite elements,
- exhibits good behaviour with respect to the distribution of grid points.

To do so, we follow the common approach of splitting the fourth order problem into two second order problems via the introduction of a second variable, which we choose to be $y = \frac{x_{\rho\rho}}{|x_\rho|^2}$. By expressing the operator $\nabla_s^2 \vec{\kappa}$ in terms of x and y, one finds that solutions of the system

$$x_t = \frac{1}{|x_\rho|^2}\left(-y_{\rho\rho} + 2(y_\rho \cdot x_\rho)y + 2(y \cdot x_\rho)y_\rho - 2(y \cdot x_\rho)^2 y + |x_\rho|^2|y|^2 y\right) + \alpha\frac{x_\rho}{|x_\rho|^2},$$

satisfy (1), so that $\frac{d}{dt}\int_I |x_\rho| d\rho \le 0$. The scalar function α multiplying the tangential term is then chosen in such a way that the solution of the above system satisfies in addition $\frac{d}{dt}\int_I |x_\rho|^2 d\rho \le 0$. This leads to the choice

$$\alpha = 2y \cdot x_\rho |y|^2 - 2y_\rho \cdot y,$$

and the resulting system takes the form

$$|x_\rho|^2 x_t + y_{\rho\rho} = F_{cd}(x_\rho, y, y_\rho)y, \tag{3}$$

$$|x_\rho|^2 y - x_{\rho\rho} = 0, \tag{4}$$

where $F_{cd}(a, b, c) \in \mathbb{R}^{d\times d}$ is given by $F_{cd} = F_1 + F_2$ with

$$F_1(a, b, c) = \left(2a \cdot c + |a|^2|b|^2\right)I_d,$$
$$F_2(a, b, c) = 2\left(c \otimes a - a \otimes c\right) + 2a \cdot b\left(a \otimes b - b \otimes a\right),$$

see [5] for details. A similar system, with F_{cd} replaced by a suitable matrix–valued function F_{el}, can be derived for the elastic flow, although the inequality $\frac{d}{dt}\int_I |x_\rho|^2 d\rho \le 0$ will in general no longer hold in this case. In order to discretize (3), (4) in space we denote by V_h the set of continuous, piecewise linear finite elements which are periodic on $[0, 1]$ and look for a pair $x_h, y_h : I \times [0, T] \to \mathbb{R}^d$ such that $x_h(\cdot, t), y_h(\cdot, t) \in V_h^d$ and

$$\int_I x_{h,t} \cdot \chi |x_{h,\rho}|^2 d\rho - \int_I y_{h,\rho} \cdot \chi_\rho d\rho = \int_I F(x_{h,\rho}, y_h, y_{h,\rho})y_h \cdot \chi d\rho \quad \forall \, \chi \in V_h^d, \tag{5}$$

$$\int_I y_h \cdot \eta |x_{h,\rho}|^2 d\rho + \int_I x_{h,\rho} \cdot \eta_\rho d\rho = 0 \qquad \forall \, \eta \in V_h^d, \tag{6}$$

(7) $x_h(\cdot, 0) = x_h^0$.

Here, $F = F_{cd}$ or $F = F_{el}$ and the initial function $x_h^0 \in V_h^d$ is given by

$$\int_I x_{h,\rho}^0 \cdot \eta_\rho d\rho + \int_I x_h^0 \cdot \eta d\rho = \int_I \pi^h x_0 \cdot \eta d\rho - \int_I \pi^h\left[\frac{x_{0,\rho\rho}}{|x_{0,\rho}|^2}\right] \cdot \eta\, |(\pi^h x_0)_\rho|^2 d\rho$$

for all $\eta \in V_h^d$. Our main result then reads:

Theorem. *If* (3), (4) *has a smooth solution* (x, y), *then there exists* $h_0 > 0$ *such that for* $0 < h \leq h_0$ *the semidiscrete problem* (5)–(7) *has a unique solution* (x_h, y_h) *and the following error bounds hold:*

$$\max_{t \in [0,T]} [\|x(\cdot, t) - x_h(\cdot, t)\|_{L^2} + \|y(\cdot, t) - y_h(\cdot, t)\|_{L^2}] \leq Ch^2,$$

$$\max_{t \in [0,T]} [\|x_\rho(\cdot, t) - x_{h,\rho}(\cdot, t)\|_{L^2} + \|y_\rho(\cdot, t) - y_{h,\rho}(\cdot, t)\|_{L^2}] \leq Ch,$$

$$\left(\int_0^T \|x_t - x_{h,t}\|_{L^2}^2 dt \right)^{\frac{1}{2}} \leq Ch^2.$$

The proof is carried out in §4 of [5]. Furthermore, numerical experiments show that the schemes behave very well with respect to the distribution of mesh points along the curves. In the case of curve diffusion, heuristic arguments show that one obtains parametrizations that are almost proportional to arclength as t increases.

REFERENCES

[1] J. W. Barrett, H. Garcke and R. Nürnberg, *A parametric finite element method for fourth order geometric evolution equations*, J. Comput. Phys. **222** (2007) 441–462.

[2] J. W. Barrett, H. Garcke and R. Nürnberg, *Numerical approximation of gradient flows for closed curves in* $\mathbb{R}^d$, IMA J. Numer. Anal. **30** (2010) 4–60.

[3] J. W. Barrett, H. Garcke and R. Nürnberg, *Parametric approximation of isotropic and anisotropic elastic flow for closed and open curves*, Numer. Math. **120** (2012) 489–542.

[4] K. Deckelnick and G. Dziuk, *Error analysis for the elastic flow of parametrized curves*, Math. Comp. **78** (2009) 645–671.

[5] K. Deckelnick and R. Nürnberg, *Finite element schemes with tangential motion for fourth order geometric evolutions equations in arbitrary codimension*, arXiv:2402.16799, 2024.

[6] G. Dziuk, E. Kuwert and R. Schätzle, *Evolution of elastic curves in* $\mathbb{R}^n$: *Existence and computation*, SIAM J. Math. Anal. **33** (2002) 1228–1245.

[7] P. Pozzi and B. Stinner, *Convergence of a scheme for an elastic flow with tangential mesh movement*, ESAIM Math. Model. Numer. Anal. **57** (2023) 445–466.

Reporters: Thomas Sales, Clemens Ullrich

Participants

Prof. Dr. Helmut Abels
Fakultät für Mathematik
Universität Regensburg
93040 Regensburg
GERMANY

Dr. Amal Alphonse
Weierstraß-Institut für Angewandte
Analysis und Stochastik
Mohrenstraße 39
10117 Berlin
GERMANY

Prof. Dr. Weizhu Bao
Department of Mathematics
National University of Singapore
Lower Kent Ridge Road
Singapore 119 076
SINGAPORE

Prof. Dr. Sören Bartels
Abteilung für Angewandte Mathematik
Universität Freiburg
Hermann-Herder-Straße 10
79104 Freiburg i. Br.
GERMANY

Prof. Dr. Dieter Bothe
Mathematische Modellierung und
Analysis
Fachbereich Mathematik
Technische Universität Darmstadt
Peter-Grünberg-Straße 10
64287 Darmstadt
GERMANY

Prof. Dr. Lia Bronsard
Dept. of Mathematics
Mc Master University
1280 Main st West
Hamilton, ON L8S 4K1
CANADA

Prof. Dr. Antonin Chambolle
CEREMADE, CNRS, Université
Paris-Dauphine,
PSL Research University
Place de Lattre de Tassigny
75775 Paris Cedex 16
FRANCE

Prof. Dr. Klaus Deckelnick
Institut für Analysis und Numerik
Otto-von-Guericke-Universität
Magdeburg
Universitätsplatz 2
39106 Magdeburg
GERMANY

Prof. Dr. Ana Djurdjevac
Institut für Mathematik
Freie Universität Berlin
Arnimallee 6
14195 Berlin
GERMANY

Prof. Dr. Charles M. Elliott
Mathematics Institute
University of Warwick
Gibbet Hill Road
Coventry CV4 7AL
UNITED KINGDOM

Prof. Dr. Julian Fischer
Institute of Science and Technology
Austria
(IST Austria)
Am Campus 1
3400 Klosterneuburg
AUSTRIA

Prof. Dr. Harald Garcke
Fakultät für Mathematik
Universität Regensburg
93040 Regensburg
GERMANY

Dr. Mi-Ho Giga
Graduate School of Mathematical
Sciences
The University of Tokyo
3-8-1 Komaba, Meguro-ku
Tokyo 153-8914
JAPAN

Prof. Dr. Yoshikazu Giga
Graduate School of Mathematical
Sciences
The University of Tokyo
3-8-1 Komaba, Meguro-ku
Tokyo 153-8914
JAPAN

Prof. Dr. Maurizio Grasselli
Dipartimento di Matematica
Politecnico di Milano
Via E. Bonardi, 9
20133 Milano
ITALY

Prof. Dr. Günther Grün
Department Mathematik
Universität Erlangen-Nürnberg
Cauerstraße 11
91058 Erlangen
GERMANY

Prof. Dr. Matthias Hieber
Fachbereich Mathematik
Technische Universität Darmstadt
Schloßgartenstraße 7
64289 Darmstadt
GERMANY

Prof. Dr. Michael Hintermüller
Weierstraß-Institut für
Angewandte Analysis und Stochastik
Mohrenstraße 39
10117 Berlin
GERMANY

Prof. Dr. Michael Hinze
Mathematisches Institut
Universität Koblenz
Universitätsstraße 1
56070 Koblenz
GERMANY

Prof. Dr. John R. King
School of Mathematical Sciences
The University of Nottingham
University Park
Nottingham NG7 2RD
UNITED KINGDOM

Dr. Patrik Knopf
Fakultät für Mathematik
Universität Regensburg
Universitätsstraße 31
93053 Regensburg
GERMANY

Prof. Dr. Ralf Kornhuber
Institut für Mathematik
Freie Universität Berlin
Arnimallee 6
14195 Berlin
GERMANY

Dr. Balázs Kovács
Institut für Mathematik
Universität Paderborn
Warburger Str. 100
33098 Paderborn
GERMANY

Prof. Dr. Tim Laux
Fakultät für Mathematik
Universität Regensburg
Universitätsstr. 31
93053 Regensburg
GERMANY

Prof. Dr. Chun Liu
Department of Applied Mathematics
Illinois Institute of Technology
Chicago, Il 60616
UNITED STATES

Dr. Alice Marveggio
Hausdorff Center for Mathematics
University of Bonn
Endenicher Allee 60
53115 Bonn
GERMANY

Achilleas Mavrakis
Mathematics Institute
University of Warwick
Gibbet Hill Road
Coventry CV4 7AL
UNITED KINGDOM

Prof. Dr. Barbara Niethammer
Institut für Angewandte Mathematik
Universität Bonn
Endenicher Allee 60
53115 Bonn
GERMANY

Prof. Dr. Ricardo H. Nochetto
Department of Mathematics
Institute for Physical Science and
Technology
University of Maryland
College Park, MD 20742-2431
UNITED STATES

Prof. Dr. Matteo Novaga
Dipartimento di Matematica
Università di Pisa
Largo Bruno Pontecorvo 5
56127 Pisa
ITALY

Prof. Dr. Robert Nürnberg
Dipartimento di Mathematica
Università di Trento
38123 Trento
ITALY

Prof. Dr. Maxim A. Olshanskii
Department of Mathematics
University of Houston
Houston, TX 77204-3476
UNITED STATES

Dr. Alessandra Pluda
Dipartimento di Matematica
Università di Pisa
Largo Bruno Pontecorvo, 5
56127 Pisa
ITALY

Andrea Poiatti
Dipartimento di Matematica
Politecnico di Milano
Piazza Leonardo da Vinci, 32
20133 Milano
ITALY

Prof. Dr. Paola Pozzi
Fachbereich Mathematik
Universität Duisburg-Essen
Thea-Leymann-Straße 9
45127 Essen
GERMANY

Dr. Tom Ranner
School of Computing
University of Leeds
Leeds LS2 9JT
UNITED KINGDOM

Prof. Dr. Arnold Reusken
Institut für Geometrie und
Praktische Mathematik
RWTH Aachen
Templergraben 55
52062 Aachen
GERMANY

Prof. Dr. Matthias Röger
Fakultät für Mathematik
Technische Universität Dortmund
Vogelpothsweg 87
44227 Dortmund
GERMANY

Tom Sales
Mathematics Institute
University of Warwick
Gibbet Hill Road
Coventry CV4 7AL
UNITED KINGDOM

Dr. Richard Schubert
Mathematisches Institut
Universität Bonn
Endenicher Allee 60
53115 Bonn
GERMANY

Prof. Dr. James A. Sethian
Department of Mathematics
University of California
Berkeley, CA 94720-3840
UNITED STATES

Prof. Dr. Gieri Simonett
Department of Mathematics
Vanderbilt University
1326 Stevenson Center
Nashville, TN 37240
UNITED STATES

Dr. Björn Stinner
Mathematics Institute
University of Warwick
Coventry CV4 7AL
UNITED KINGDOM

Prof. Dr. Vanessa Styles
Department of Mathematics
University of Sussex
Falmer
Brighton BN1 9QH
UNITED KINGDOM

Dennis Trautwein
Fakultät für Mathematik
Universität Regensburg
Universitätsstr. 31
93053 Regensburg
GERMANY

Clemens Ullrich
Department Mathematik
Friedrich-Alexander-Universität
Erlangen-Nürnberg
Cauerstr. 11
91058 Erlangen
GERMANY

Dr. Chandrasekhar Venkataraman
School of Mathematics and Physical
Sciences
University of Sussex
Falmer
Brighton BN1 9QH
UNITED KINGDOM

Prof. Dr. Axel Voigt
Abteilung Mathematik
Technische Universität Dresden
Mommsenstraße 13
01069 Dresden
GERMANY

Prof. Dr. Barbara A. Wagner
Weierstraß-Institut für
Angewandte Analysis und Stochastik
Mohrenstraße 39
10117 Berlin
GERMANY

Prof. Dr. Changyou Wang
Department of Mathematics
Purdue University
150 N. University Street
West Lafayette, IN 47907-1395
UNITED STATES

Prof. Dr. Mathias Wilke
Martin-Luther-Universität
Halle-Wittenberg
Naturwissenschaftliche Fakultät II
Institut für Mathematik
06099 Halle / Saale
GERMANY

Julia Wittmann
Fakultät für Mathematik
Universität Regensburg
Universitätsstr. 31
93053 Regensburg
GERMANY

Prof. Dr. Sara Zahedi
Department of Mathematics
KTH Royal Institute of Technology
10044 Stockholm
SWEDEN